



An updated digital model of plate boundaries

Peter Bird

*Department of Earth and Space Sciences, University of California, Los Angeles, California 90095, USA
(pbird@ess.ucla.edu)*

[1] A global set of present plate boundaries on the Earth is presented in digital form. Most come from sources in the literature. A few boundaries are newly interpreted from topography, volcanism, and/or seismicity, taking into account relative plate velocities from magnetic anomalies, moment tensor solutions, and/or geodesy. In addition to the 14 large plates whose motion was described by the NUVEL-1A poles (Africa, Antarctica, Arabia, Australia, Caribbean, Cocos, Eurasia, India, Juan de Fuca, Nazca, North America, Pacific, Philippine Sea, South America), model PB2002 includes 38 small plates (Okhotsk, Amur, Yangtze, Okinawa, Sunda, Burma, Molucca Sea, Banda Sea, Timor, Birds Head, Maoke, Caroline, Mariana, North Bismarck, Manus, South Bismarck, Solomon Sea, Woodlark, New Hebrides, Conway Reef, Balmoral Reef, Futuna, Niuafo'ou, Tonga, Kermadec, Rivera, Galapagos, Easter, Juan Fernandez, Panama, North Andes, Altiplano, Shetland, Scotia, Sandwich, Aegean Sea, Anatolia, Somalia), for a total of 52 plates. No attempt is made to divide the Alps-Persia-Tibet mountain belt, the Philippine Islands, the Peruvian Andes, the Sierras Pampeanas, or the California-Nevada zone of dextral transtension into plates; instead, they are designated as “orogens” in which this plate model is not expected to be accurate. The cumulative-number/area distribution for this model follows a power law for plates with areas between 0.002 and 1 steradian. Departure from this scaling at the small-plate end suggests that future work is very likely to define more very small plates within the orogens. The model is presented in four digital files: a set of plate boundary segments; a set of plate outlines; a set of outlines of the orogens; and a table of characteristics of each digitization step along plate boundaries, including estimated relative velocity vector and classification into one of 7 types (continental convergence zone, continental transform fault, continental rift, oceanic spreading ridge, oceanic transform fault, oceanic convergent boundary, subduction zone). Total length, mean velocity, and total rate of area production/destruction are computed for each class; the global rate of area production and destruction is 0.108 m²/s, which is higher than in previous models because of the incorporation of back-arc spreading.

Components: 28,925 words, 19 figures, 3 tables, 4 datasets.

Keywords: Plate tectonics; Euler pole.

Index Terms: 3040 Marine Geology and Geophysics: Plate tectonics (8150, 8155, 8157, 8158); 5475 Planetology: Solid Surface Planets: Tectonics (8149); 8150 Tectonophysics: Evolution of the Earth: Plate boundary—general (3040); 8158 Tectonophysics: Evolution of the Earth: Plate motions—present and recent (3040).

Received 12 October 2001; **Revised** 23 July 2002; **Accepted** 3 December 2002; **Published** 14 March 2003.

Bird, P., An updated digital model of plate boundaries, *Geochem. Geophys. Geosyst.*, 4(3), 1027, doi:10.1029/2001GC000252, 2003.

1. Definitions of Plates and Orogens

[2] An idealized plate of lithosphere is a region which rotates (with respect to some other specified plate) without internal deformation about an imaginary axis through the center of the planet [Morgan, 1968]. This axis intersects the surface of the idealized spherical planet at two points known as Euler poles. One variant of this definition describes plates as features of the neotectonic velocity field (on timescales of 10^0 to 10^6 years), in which case the rotation may be described by an Euler vector from the center of the planet toward the Euler pole, with magnitude measured in degrees per million years (or other rotation-rate units). A second variant describes plates as features in a finite-displacement field (on timescales of 10^6 to 10^9 years) in which case the rotation is described by an Euler vector with magnitude in degrees or radians. This paper concerns neotectonics, and begins from the former definition.

[3] On the real Earth, it is understood that any plate model is only an approximation. First, elastic strain accumulation around temporarily-locked faults is always discounted, although it may not always be clear in practice which strain rates are elastic and which are anelastic. Second, it has been conventional to overlook small amounts of anelastic deformation within one “plate” provided that (1) the “plate” is surrounded by boundary zones in which anelastic strain rates are an order of magnitude higher than they are in the interior; and (2) the velocity anomalies with respect to the best-fitting ideal-plate model are near, or below, the threshold of current measurement technologies. This approach, in which the plate model is treated as a useful approximation rather than literal truth, is continued here. I overlook measured or suspected internal velocity variations of as much as 2 to 8 mm/a; the lower thresholds apply in regions of slow relative plate motion (e.g., North America, Atlantic Ocean, Mediterranean, Africa) and the higher thresholds apply to regions of rapid relative plate motion (e.g., Indian and Pacific oceans and their margins).

[4] Even with such a relaxed definition, there are clearly regions (such as the Alpine-Himalayan

mountain belt) in which it is very difficult to define plates, because there is so much seismic, geologic, and geodetic evidence for distributed anelastic deformation [Gordon, 1995]. One approach is to define a large number of very small plates, as in the Bird and Rosenstock [1984] model of 22 very small plates in southern California alone. This is data-intensive and time-consuming, and not yet practical on a global basis. It may also fail in the case of true viscous deformation, which would be so evenly distributed as to fail criterion 1 stated above. A second reasonable approach would be to conduct local kinematic modeling using the continuum approaches of Holt *et al.* [1991, 2000], Haines and Holt [1993], Jackson *et al.* [1995], Bird [1998], Lamb [2000], or Kreemer *et al.* [2000]. This is also too difficult to attempt in one global survey paper. Alternatively, certain regions can simply be labeled as zones of unmodeled complexity, where more data are needed (either to define very small plates, or to rule out their existence). In this paper, I take this easy third approach; I will refer to these complex regions (which may include regions of truly distributed deformation) as “orogens” (i.e., regions of mountain-formation, or at least topographic roughening). Thirteen of these zones are identified in Figure 1. Perhaps it should be emphasized that the designation of an “orogen” is not purely a statement about the nature of the kinematics in that region; it is a culturally-relative statement that the velocity field in that region has more degrees of freedom than present data can constrain.

[5] For some applications of a plate model, it may be more important to have global coverage than high precision. One such application is the spherical-harmonic expansion of plate velocities to examine torroidal versus poloidal components. Another is use of plate velocities as a boundary condition in modeling of mantle convection. A third example is the computation of element and isotope cycling by creation and subduction of crust. To accommodate such applications, I have treated the set of orogens as an overlay layer (giving warning of unmodeled complexity) rather than as a set of polygons competing with the plates for planetary surface area. By simply ignoring the

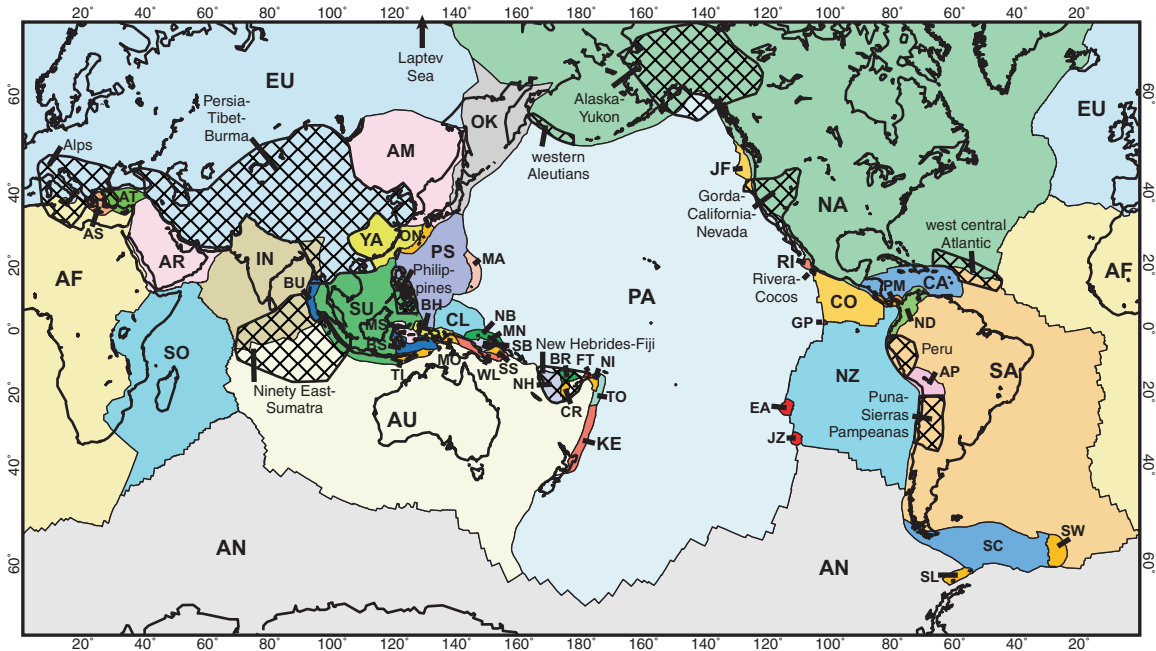


Figure 1. The 52 plates of model PB2002 are shown with contrasting colors. Two-letter plate identifiers are explained in Table 1. The 13 cross-hatched areas with are “orogens” in which an Eulerian plate model is not expected to be accurate. Labels of small plates and orogens are offset (with leader lines) for clarity. Mercator projection.

overlay layer, the reader will find a finite globe-covering set of plates for applications which require one. Plates in this set will always obey criterion 1, but may locally fail to satisfy criterion 2. Another advantage of this “overlay” format is that there is less chance that unsophisticated users will (incorrectly) infer elevated seismic hazard at the boundaries of the orogens (where no velocity discontinuity is implied). A third advantage is that it maximizes continuity with previous usage of plate terminology, so that the shapes of the familiar large plates are not arbitrarily modified without compelling reasons.

2. Previous Plate-Boundary Models

[6] Considering the lengthy and successful development of plate tectonic models, it is surprising that there are no generally-accepted standard references on plate boundary locations worldwide. The list of published resources is short. Authors of global inverse solutions for Euler poles of large plates [Minster and Jordan, 1978 (RM2); DeMets *et al.*, 1990 (NUVEL-1)] provided boundaries of

the largest plates in the form of small-scale maps, plus lists of locations of discrete plate-boundary data used in the inversion. Stoddard [1992] digitized transform faults worldwide from an assortment of maps, but did not address spreading and subduction zones. Zoback [1992] published boundaries for large plates as part of the World Stress Map. Gordon [1995] distinguished plates (85% of Earth) from deforming zones (15%), and roughly sketched the shapes of 5 small plates in eastern Asia, plus a Somalia plate, a Capricorn plate, a Caroline plate, a Rivera plate, and a Scotia Sea plate (totalling 24). The Paleo-Oceanographic Mapping Project (POMP) at the University of Texas created a rough set of plate boundaries which emphasized major mid-ocean spreading ridges and large plates; their boundaries and gridded digital model of oceanic lithosphere age were published by Mueller *et al.* [1997]. More recently, the PLATES project at the University of Texas Institute of Geophysics (led by Lawrence Lawver and Ian Dalziel) maintains a site (<http://www.ig.utexas.edu/research/projects/plates/plates.htm>) which offers an incomplete working set of

plate boundaries, some of which are highly detailed.

3. Assembly of Plate Boundaries

[7] Probably the lack of a standard reference results from a combination of logistics and professional caution: few groups had the resources to assemble the necessary maps, and no person or group felt prepared to claim adequate knowledge of the whole Earth. However, the task has become much easier in recent years due to the publication of global digital data sets on topography, seismicity, seafloor age, and geodetic velocity. Using these aids, I undertook to assemble a set of plate boundaries because it is required for a project to estimate global seismic hazard based on plate tectonic theory. This present version of the plate boundaries, called PB2002, is a major refinement of the preliminary model PB1999 that was used in *Bird et al.* [2002]. The principal change is the inclusion of 38 small plates (Figure 1) in addition to the 14 large plates that were mapped in the previous version. Most of these boundaries were proposed (and many also mapped in detail) in published sources, so they do not represent new research results; their assembly and digitization was editorial work involving occasional applications of editorial judgment.

[8] The single most important basis for model PB2002 was the set of digitized boundaries created by POMP, and published by *Mueller et al.* [1997]. In areas of seafloor spreading with magnetic anomaly bands, my editorial changes were very minor: I edited out boundaries that are only relevant to paleotectonics, ensured that the active plate boundaries meet at triple-junction points that are common to all digitized boundary segments, and replaced non-transform offsets on spreading ridges with idealized transforms. (Boundaries from the PLATES model under development at the University of Texas Institute of Geophysics were not used in PB2002, but some boundaries may be the same because of common inheritance from *Mueller et al.* [1997].)

[9] Most boundaries other than mid-ocean spreading ridges (e.g., continental, subduction, and back-

arc boundaries) were selected manually, using graphical software which permits me to overlay: (1) gridded seafloor ages from POMP with 6' resolution; (2) gridded topography/bathymetry from ETOPO5 [*Anonymous*, 1988] with 5' resolution; (3) 1,511 subaerial volcano locations from the Smithsonian Institution's Global Volcanism Program [*Simkin and Siebert*, 1995]; (4) moment tensors of shallow earthquakes from the Harvard Centroid Moment Tensor (CMT) catalog and epicenters from the International Seismological Centre (ISC) catalog; and (5) previous boundary selections digitized from figures in the literature. These were combined by giving highest priority to seafloor ages, second priority to topographic lineaments, and third priority to the principle that volcanism highlights extensional boundaries, but consistently lies 200–250 km to one side of subduction boundaries. Seismicity was used as the primary basis for plate boundaries in a few difficult cases (North America-South America boundary, India-Australia boundary, Okhotsk-North America boundary, inland boundaries of Amur and Yangtze plates, southern part of Africa-Somalia boundary). Generally, these are places where new plate boundaries are developing in former plate interiors, or where small plates are nearly surrounded by orogens.

[10] In the complex southwest Pacific region, a valuable resource was the Plate-Tectonic Map of the Circum-Pacific Region, which was published in 6 sheets and is available in at least two editions [*Circum-Pacific Mapping Project*, 1981, 1986]. A few boundaries were digitized directly from this map set (e.g., western parts of the Solomon Sea plate, west boundary of the Kermadec plate). In other cases, it served as a valuable source of informed opinion (as of the publication date) about which arcs and topographic lineaments represent active boundaries.

[11] Among the small oceanic plates lying east of the Sunda plate, convergence is dominant, and Quaternary magnetic anomaly lineations are unknown. In this area, Global Positioning System (GPS) geodesy gives the best estimate of the relative velocities of those plates which include islands within their interiors. The interpretation of project GEODYSSSEA results by *Rangin et al.*

[1999] was a primary resource in this area. Unfortunately, geodesy does not precisely delimit plate boundaries, and gives only the minimum extent of any plate. There may be additional regions of very low anelastic strain rate which cannot be surveyed because of a lack of islands. Also, episodic fault locking and unlocking (seismic coupling) causes temporary elastic strain changes around many plate edges, which typically modifying the benchmark velocity component in the direction of the velocity of a neighboring plate. Therefore, I have used geodetic velocities as a rough guide to plate shapes and Euler poles, but have not felt obliged to fit any single divergent velocity vector observation by introducing a new plate, except where there is supporting evidence such as topographic and/or seismic lineaments. The Australia-Pacific (AU-PA) plate boundary south of New Zealand was taken directly from *Massell et al.* [2000].

4. Euler Poles

[12] It is necessary to estimate poles jointly with plate boundaries because (1) the expression of any plate boundary in topography and seismicity depends on its sense of relative velocity, and (2) it is often by attempting to quantitatively fit velocity and azimuth data that discrepancies indicating additional plates or orogens are discovered. For each small plate in model PB2002, an Euler vector is estimated with respect to a large neighboring plate. Then, relative rotation rates of large plates from a published “framework” model are used to express these Euler vectors in the Pacific plate reference frame in Table 1. The many new poles for small plates in this paper are mostly approximate and not the results of formal inversions (unless performed by the authors cited). Many are likely to be revised in the future based on new geodetic results.

[13] The “framework” set of Euler poles for the 14 large plates in this paper is the model known as NUVEL-1A. *DeMets et al.* [1990] performed a global inversion to determine the relative rotation rates of the 12 largest plates (the NUVEL-1 model), and noted that published information also

constrains the relative motions of the Philippine Sea and Juan de Fuca plates. *Seno et al.* [1993] then updated the pole for the Philippine Sea plate. Although their result was questioned on procedural grounds by *Heki et al.* [1999], it has been geodetically confirmed [*Kato et al.*, 1998; *Rangin et al.*, 1999]. Finally, *DeMets et al.* [1994] adjusted the rates of all the vectors by a constant factor to give the NUVEL-1A solution.

5. Small Plates

[14] As a majority of the small plates on Earth are located along the western margin of the Pacific Ocean, this presentation will progress counterclockwise around that margin, and then eastward around the world. The naming of plates generally follows precedents in the literature. Since a plate is a geologic structure, I follow the geologic convention that the word “plate” is not capitalized, and that the type locality of the plate is never modified to form an adjective. (For example, “North American Plate” is non-standard, and the preferred term is “North America plate”.) I continue another long-standing tradition by using a two-letter abbreviation as a short form for each plate name; to avoid duplication, a few of these abbreviations are necessarily different from abbreviations used by previous authors.

5.1. Okhotsk Plate (OK) and Amur Plate (AM)

[15] In early 14-plate models of the Earth such as RM2 and NUVEL-1, the North America plate (NA) was considered [*Chapman and Solomon*, 1976] to extend across the Bering Sea and include the Kamchatka Peninsula, the Sea of Okhotsk, and northern Honshu. This proposed slender projection of NA would be subject to compressional tractions on its western boundary with the Eurasia or Amur plate (EU or AM) in the vicinity of Sakhalin Island, and a mixture of topographic relative tension and tectonic compression on its eastern boundary with the Pacific plate (PA) in the Kuril Trench. Unless these tractions are very well-balanced, high deviatoric stresses and faulting would be expected near the narrow neck of the projection, in the northern Sea of Okhotsk (Shelikov Bay) and northern Kamchatka.

Table 1. Plate Identifiers, Areas, and Euler Poles^a

Identifier	Plate Name	Area, Steradian	Pole Latitude, deg. N.	Pole Longitude, deg. E	Rotation Rate, deg./Ma	Reference
AF	Africa	1.44065	59.160	-73.174	0.9270	<i>DeMets et al.</i> [1994]
AM	Amur	0.13066	57.645	-83.736	0.9309	<i>Heki et al.</i> [1999]
AN	Antarctica	1.43268	64.315	-83.984	0.8695	<i>DeMets et al.</i> [1994]
AP	Altiplano	0.02050	33.639	-81.177	0.9160	<i>Lamb</i> [2000]
AR	Arabia	0.12082	59.658	-33.193	1.1616	<i>DeMets et al.</i> [1994]
AS	Aegean Sea	0.00793	74.275	-87.237	0.6497	<i>McClusky et al.</i> [2000]
AT	Anatolia	0.01418	56.283	8.932	1.6400	<i>McClusky et al.</i> [2000]
AU	Australia	1.13294	60.080	1.742	1.0744	<i>DeMets et al.</i> [1994]
BH	Birds Head	0.01295	12.559	87.957	0.3029	this paper
BR	Balmoral Reef	0.00481	45.900	-111.000	0.2000	this paper
BS	Banda Sea	0.01715	16.007	122.442	2.1250	<i>Rangin et al.</i> [1999]
BU	Burma	0.01270	8.894	-75.511	2.6670	<i>Circum-Pacific Map Project</i> [1986]
CA	Caribbean	0.07304	54.313	-79.431	0.9040	<i>Weber et al.</i> [2001]
CL	Caroline	0.03765	10.130	-45.570	0.3090	<i>Seno et al.</i> [1993]
CO	Cocos	0.07223	36.823	-108.629	1.9975	<i>DeMets et al.</i> [1994]
CR	Conway Reef	0.00356	-12.628	175.127	3.6050	this paper
EA	Easter	0.00411	28.300	66.400	11.4000	<i>Engeln and Stein</i> [1984]
EU	Eurasia	1.19630	61.066	-85.819	0.8591	<i>DeMets et al.</i> [1994]
FT	Futuna	0.00079	-10.158	-178.305	4.8480	this paper
GP	Galapagos	0.00036	9.399	79.690	5.2750	<i>Lonsdale</i> [1988]
IN	India	0.30637	60.494	-30.403	1.1034	<i>DeMets et al.</i> [1994]
JF	Juan de Fuca	0.00632	35.000	26.000	0.5068	<i>Wilson</i> [1988]
JZ	Juan Fernandez	0.00241	35.910	70.166	22.5200	<i>Anderson-Fontana et al.</i> [1986]
KE	Kermadec	0.01245	47.521	-3.115	2.8310	this paper
MA	Mariana	0.01037	43.777	149.205	1.2780	this paper
MN	Manus	0.00020	-3.037	150.456	51.3000	<i>Martinez and Taylor</i> [1996]
MO	Maoke	0.00284	59.589	78.880	0.8927	this paper
MS	Molucca Sea	0.01030	11.103	-56.746	4.0700	<i>Rangin et al.</i> [1999]
NA	North America	1.36559	48.709	-78.167	0.7486	<i>DeMets et al.</i> [1994]
NB	North Bismarck	0.00956	-4.000	139.000	0.3300	<i>Tregoning et al.</i> [1998]
ND	North Andes	0.02394	58.664	-89.003	0.7009	<i>Trenkamp et al.</i> [1996]
NH	New Hebrides	0.01585	13.000	-12.000	2.7000	this paper
NI	Niuafu'ou	0.00306	6.868	-168.868	3.2550	<i>Zellmer and Taylor</i> [2001]
NZ	Nazca	0.39669	55.578	-90.096	1.3599	<i>DeMets et al.</i> [1994]
OK	Okhotsk	0.07482	55.421	-82.859	0.8450	<i>Cook et al.</i> [1986]
ON	Okinawa	0.00802	48.351	142.415	2.8530	this paper
PA	Pacific	2.57685	0.000	0.000	0.0000	(arbitrary choice of reference frame)
PM	Panama	0.00674	54.058	-90.247	0.9069	<i>Kellogg et al.</i> [1995]
PS	Philippine Sea	0.13409	-1.200	-45.800	1.0000	<i>Seno et al.</i> [1993]; <i>Kato et al.</i> [1998]
RI	Rivera	0.00249	26.700	-105.200	4.6923	<i>DeMets and Traylen</i> [2000]
SA	South America	1.03045	54.999	-85.752	0.6365	<i>DeMets et al.</i> [1994]
SB	South Bismarck	0.00762	10.610	-32.990	8.4400	<i>Tregoning et al.</i> [1999]
SC	Scotia	0.04190	48.625	-81.454	0.6516	<i>Pelayo and Wiens</i> [1989]
SL	Shetland	0.00178	63.121	-97.084	0.8558	(hypothetical; see text)
SO	Somalia	0.47192	58.789	-81.637	0.9783	<i>Chu and Gordon</i> [1999]
SS	Solomon Sea	0.00317	19.529	135.017	1.4780	this paper
SU	Sunda	0.21967	55.442	-72.955	1.1030	<i>Rangin et al.</i> [1999]
SW	Sandwich	0.00454	-19.019	-39.640	1.8400	<i>Pelayo and Wiens</i> [1989]
TI	Timor	0.00870	19.524	112.175	1.5140	this paper
TO	Tonga	0.00625	28.807	2.263	9.3000	<i>Zellmer and Taylor</i> [2001]
WL	Woodlark	0.01116	22.134	132.330	1.5460	<i>Tregoning et al.</i> [1998]
YA	Yangtze	0.05425	69.067	-97.718	0.9983	<i>Heki et al.</i> [1999]

^a All poles are expressed in the Pacific-plate reference frame. Rotation about each pole is counterclockwise when seen from outside the Earth. All Euler vectors are stated with high precision to avoid round-off error in differencing, but accuracy is much less.

[16] *Savostin et al.* [1982, 1983] were possibly the first to use the name “Okhotsk plate” for the region lying south of a chain of small sedimentary basins in the Cherskii Mountains, which they interpreted as active grabens in an extensional OK-NA boundary. *Cook et al.* [1986] studied a chain of moderate ($5 < m_b < 6$) earthquakes in this region, and found focal mechanisms along the proposed OK-NA boundary to be sinistral-transpressive, rejecting the previous interpretation that the small sedimentary basins are active grabens. They used slip vectors to estimate an OK-NA pole position at (72.4°N , 169.8°E) in the East Siberian Sea, but could not address the rate of relative movement. *DeMets* [1992] used 256 slip vectors from the highly seismic Kuril Trench to test for the significance of proposed OK-NA motion in a three-plate study, and concluded that if there is such motion it is no faster than 5 mm/a. *Seno et al.* [1996] added slip vectors of earthquakes in the Sakhalin Island-Japan Sea lineament to the data base, solved for OK-EU and OK-NA poles, and found that the improvement to the fit by adding a separate OK plate was statistically significant. Their estimate of the OK-NA velocity was 8 mm/a. Based on slip vectors of local earthquakes, they defined the OK plate as extending south to central Honshu, so that major earthquakes in the eastern Japan Sea are occurring on the EU-OK boundary (or Amur-OK boundary; see below).

[17] Thrusting events along the eastern coast of northern Kamchatka also provide evidence that the North America plate does not extend into the Sea of Okhotsk, but converges with a separate Okhotsk plate. This belt of seismicity was first discussed by *Lander et al.* [1996], who used it as the basis for a proposed “Beringia” plate; however, I consider it to be a part of the OK/NA boundary (Figure 2), sharing the same northern Euler pole quoted above.

[18] The name “Amur microplate” was also proposed by *Savostin et al.* [1982, 1983] for the parts of eastern Mongolia, north China, and southeastern Russia which lie southeast of the Lake Baikal extensional province. Their proposal was that this block moves southeast with respect to EU between a sinistral transform system in the Stanovoy Mountains on the northeast and a second transform

system on the southwest (possibly at the Qinling fault, but more likely further north in the Yellow Sea). The southeastern boundary of the plate would include the seismically active fold-and-thrust belt in the eastern Japan Sea offshore northern Honshu, then cut across central Honshu, and continue as the Nankai Trough subduction zone boundary with the Philippine Sea plate. *Miyazaki et al.* [1996] combined GPS velocities from Japan and Korea with seismic slip vectors from Baikal and the Stanovoy Mountains to confirm that this motion occurs at several millimeters per year. *Wei and Seno* [1998] performed a six-plate analysis (PA, NA, EU, OK, PS, AM) of earthquake slip vectors and NUVEL-1 data, including an Amur plate distinct from EU, and still concluded that OK is distinct from NA. Their AM-OK and EU-OK poles are both located in northern Sakhalin Island, near the AM-OK-EU triple junction, so that all relative plate velocities decrease to small values in this complex region. They derived a slow AM-EU velocity of only 0.4–0.7 mm/a. This is questionable because it conflicts with geodetic results which they did not use in their inversion: both the previous results of *Miyazaki et al.* [1996], and newer results of *Calais et al.* [1998] which showed extension around the Baikal Rift to be at 4.5 ± 1.2 mm/a.

[19] Additional GPS geodetic results of *Takahashi et al.* [1999] were interpreted as confirming the *Miyazaki et al.* [1996] model for AM-EU motion, but again showing that the AM-EU motion predicted by the *Wei and Seno* [1998] model is too slow by a factor of 5. Also, they point out that a station in south Sakhalin Island moves with the Amur plate, requiring the AM-OK boundary to lie east of this point. (However, elastic strain accumulation could also explain this vector, especially if the AM-OK boundary in Sakhalin is an east-dipping thrust.) Unfortunately, the only remaining stations on the OK plate were one in north Sakhalin (which only confirms the proximity of the EU-OK pole) and two in Kamchatka (which were not useful due to elastic strain accumulation in the adjacent subduction zone).

[20] The most recent geodetic study on Amur plate motion is *Heki et al.* [1999]. Using 15 GPS stations, they find that AM separates from EU at

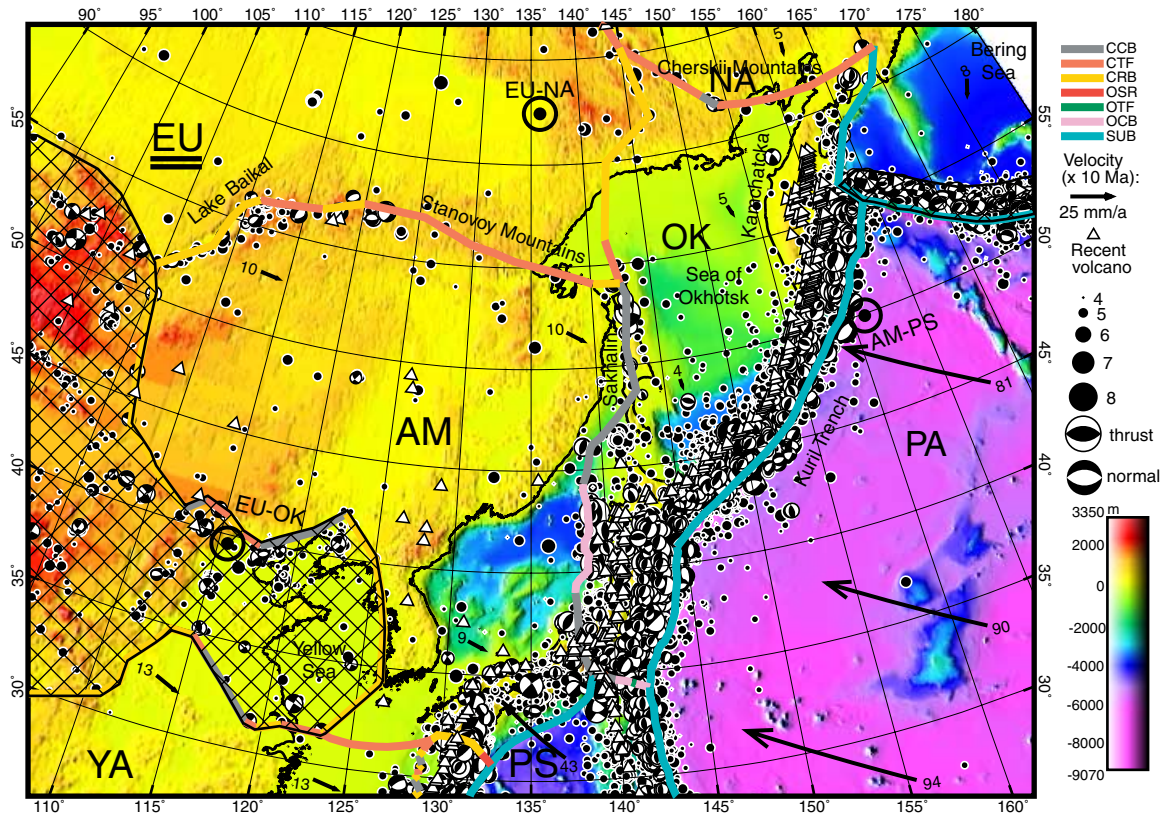


Figure 2. Boundaries of the Okhotsk (OK) and Amur (AM) plates. Surrounding plates include Eurasia (EU), North America (NA), Pacific (PA), Philippine Sea (PS), and Yangtze (YA). Boundary types are: CCB continental convergent boundary, CTF continental transform fault, CRB continental rift boundary, OSR oceanic spreading ridge, OTF oceanic transform fault, OCB oceanic convergent boundary, SUB subduction zone. Cross-hatched regions are orogens. Color shows topography from ETOPO5. Solid dots are shallow (<70 km) hypocenters from ISC catalog, 1964–1991; beachballs are lower-hemisphere projections of double-couple parts of moment tensors of shallow centroids from Harvard CMT catalog, 1977–1998. White triangles are subaerial Recent volcanoes from *Simkin and Siebert* [1995]. Black vectors give model velocities (with numbers in mm/a) relative to plate whose identifier is underlined. Black circles are locations of Euler poles, about which the first-named plate rotates counterclockwise relative to the second. Oblique Mercator projection with great circle passing E-W through (135°E, 48°N).

9–10 mm/a, and compute its Euler pole. Their direction of relative velocity at Baikal is nearly E-W, which conflicts with seismic slip vectors pointing SE-NW; this is an unresolved problem. An important implication of their results is that seismic slip vectors and convergence in the Japan Sea and offshore Sakhalin Island are largely explained by AM-NA motion, and do not require the invocation of an OK plate separate from NA.

[21] My interpretation is that the seismic evidence for an OK-NA boundary [*Cook et al.*, 1986; *Lander et al.*, 1996] still stands, as does the constraint of *DeMets* [1992] that relative velocity on this boundary be less than 5 mm/a. However, the poles and

rates determined by *Seno et al.* [1996] and *Wei and Seno* [1998] are in doubt because of their neglect, or underestimation, of EU-AM relative motion. Therefore, for an Euler pole I adopt the OK-NA pole position of *Cook et al.* [1986] and rather arbitrarily assign a relative velocity of 3 mm/a to this boundary (0.14°/Ma at the OK-NA pole). I compute AM plate motion from the latest geodetic result, that of *Heki et al.* [1999]. My plate boundary locations are generally based on the map of *Wei and Seno* [1998], since geodesy is not yet able to define plate boundaries with the resolution that topography and seismicity provide. However, I have modified the OK-NA boundary to more closely follow seismicity recorded in the ISC and CMT

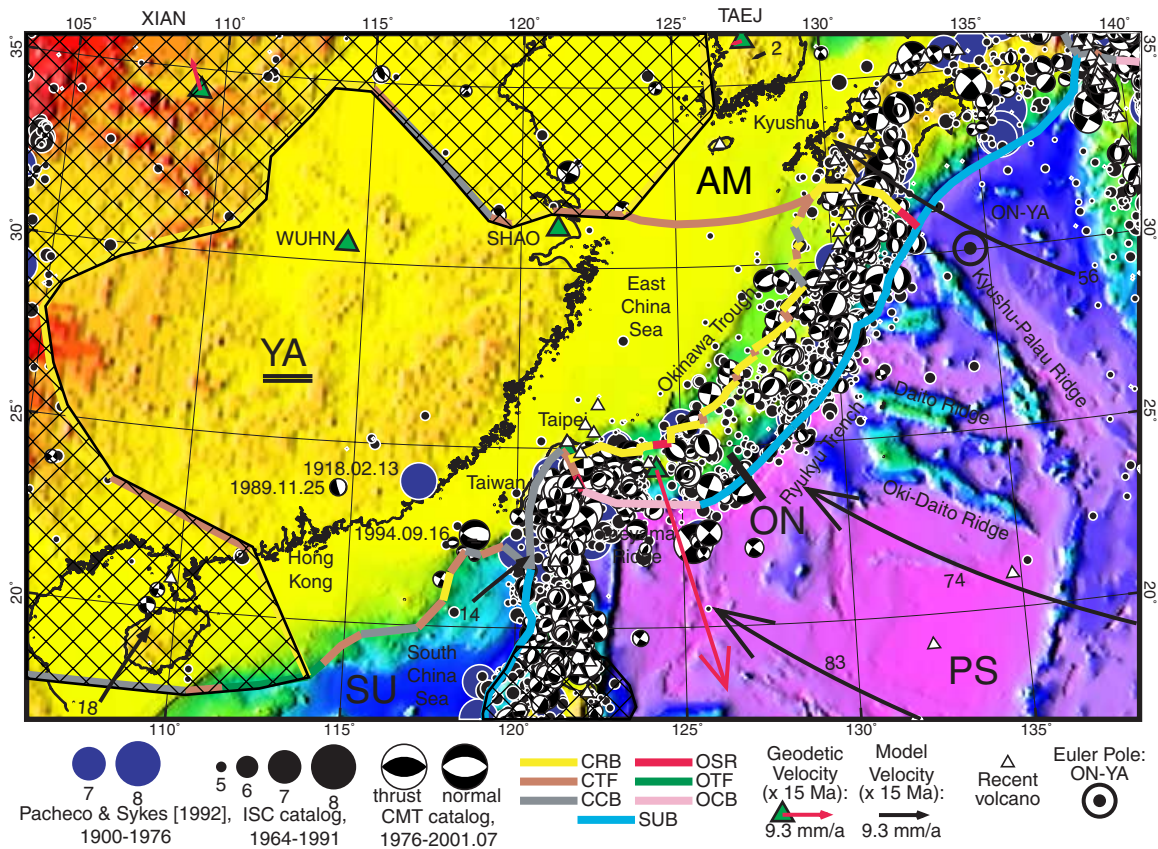


Figure 3. Boundaries (heavy colored lines) of the Yangtze (YA) and Okinawa (ON) plates. Surrounding plates include Sunda (SU), Philippine Sea (PS), and Amur (AM). Conventions as in Figure 2. Additional epicenters in blue ($m_w > 7$, 1900–1976) are from Pacheco and Sykes [1992]. Geodetic velocity of Ishigaki Island from Kato *et al.* [1998] is plotted relative to YA. Oblique Mercator projection with great circle passing E-W through (127°E, 27°N).

catalogs (Figure 2). Also, along the southwestern parts of the AM-EU boundary, I have placed the boundary north of the highly seismic Tanlu fault and other NE-trending faults around Bo Hai. These regions of complex distributed seismicity are assigned to an eastern extension of the Persia-Tibet-Burma orogen. Heki *et al.* [1999] have shown that GPS stations southwest of AM move ESE with respect to stable (northern European and Siberian) Eurasia. Several of these appear to define a distinct Yangtze plate.

5.2. Yangtze Plate (YA)

[22] There is an aseismic region in southeastern China [Giardini *et al.*, 1999] which seems to be unaffected by the Himalayan continental collision (Figure 3). GPS geodesy [Heki *et al.*, 1999] has shown that the region contains at least 3 stations

whose velocity is consistent with the hypothesis that they belong to a rigid plate: WUHN (Wuhan), SHAO (Shanghai), and Taipei. Their common motion is different from that of Eurasia by about 13 mm/a to the ESE (Euler pole 61.2°N, 142°E, 0.206°/Ma), well in excess of measurement errors.

[23] Geodesists have sometimes referred to this region as the “South China” plate, but that name was already established in the literature to describe the (larger) Paleozoic plate which collided with the Sino-Korean plate to form the Dabie Shan and adjacent Hercynian ranges [e.g., Benpei *et al.*, 1998]. For the neotectonic (and possibly Tertiary) plate, I prefer the name “Yangtze” [Gordon, 1995] for one of its most prominent Tertiary-Quaternary features.

[24] The only distinct boundary of the Yangtze plate (YA) is in the east, where it collides with the

Philippine Sea plate (PS) in Taiwan, and separates from the Okinawa plate (discussed below) in the Okinawa Trough. If both AM and YA are rigid plates, there should be a short, slow-moving boundary between them, where velocities would be determined by the differential YA-AM Euler pole, here computed to be (39.9°N, 125.8°E, 0.23°/Ma) by differencing the two geodetic poles with respect to stable EU cited above. As there are only a few strike-slip earthquakes and no obvious bathymetric lineament in the relevant area of the East China Sea, I suggest a possible sinistral transform boundary (Figure 3) which would have slip rates of only about 4 mm/a.

[25] Southwest of Taiwan, a boundary should occur between YA and the Sunda plate (SU; discussed below). Since the YA-SU pole is computed (using poles of *Heki et al.* [1999] and *Rangin et al.* [1999]) to be near (4°N, 133°E), motion along this boundary should be sinistral-transpressive, with rates on the order of 15 mm/a. Largely on the basis of the 1994.09.16 $m_w = 6.7$ thrust event, I have assumed that this boundary follows the ocean-continent boundary along the northern margin of the South China Sea, becoming a compressive boundary in each of the right steps. However, if the geodetic velocity of Taipei had not been available, it would also have been reasonable to draw a YA-SU plate boundary along one of the SW-trending sinistral faults which occur on land in the provinces between Shanghai and Hong Kong. Seismicity here is low and ambiguous (Figure 3): a large ($m_w \cong 7.3$) event on 1918.02.13 was located somewhere near (24°N, 117°E) by *Pacheco and Sykes* [1992] but its mechanism is unknown. A more recent and smaller earthquake was located by the CMT catalog (1989.11.25; $m_w = 5.6$) but it had a dip-slip solution with NW-striking nodal planes, inconsistent with any SW-NE-trending boundary. Six small ($m_b < 5$) events are also found in the ISC catalog. The ambiguity of this data suggests that additional geodetic stations are needed to determine the reality and location of the expected YA-SU boundary, and place it either near the continental margin, or alternatively onshore.

[26] Most of the remaining southwest, northwest, and northeast boundaries of stable YA are treated

as nominal boundaries with with EU, but these parts of EU are deforming within the Persia-Tibet-Burma orogen. These boundaries are rather subjectively drawn to outline only the region of low seismicity as the YA plate. Like other proposed boundaries of orogens, these lines are not necessarily faults, and there is no implication of special seismic hazard there. See the preceding section on the Amur plate for a discussion of their short mutual boundary.

5.3. Okinawa Plate (ON)

[27] The Ryukyu trench and arc is the site of rapid subduction of Philippine Sea plate. The Ryukyu forearc is separating from Asia by NW-SE extension in the Okinawa Trough, which has been inferred from marine geology and seismic reflection [*Sibuet et al.*, 1987; *Park et al.*, 1998], island geology and normal-faulting earthquakes [*Fabbri and Fournier*, 1999], paleomagnetism [*Miki*, 1995], and geodesy [*Kato et al.*, 1998; *Hu et al.*, 2001]. Therefore, the forearc is a small plate (Figure 3), which was called the “Okinawa platelet” by *Sibuet et al.* [1987].

[28] The southwest end of the Okinawa plate (ON) is in or near the north end of Taiwan, where there is a sharp reversal in subduction polarity [*Lallemant et al.*, 1997a]. Its southeast boundary with PS is the Ryukyu trench. Its southwestern boundary, also with PS, appears to be a former subduction zone which is now highly oblique. Based on swath bathymetry of *Lallemant et al.* [1997b] and seismic refraction results [*Liu et al.*, 1997], I interpret that the dextral Yaeyama Ridge fault zone within the Ryukyu forearc has become the primary plate boundary between 122° and 123°E. The northwestern boundary of the Okinawa plate in the Okinawa Trough is primarily with the Yangtze plate discussed previously. I have digitized this YA-ON boundary by connecting linear zones of localized extension mapped by *Letouzey and Kimura* [1985] and/or *Sibuet et al.* [1987]; the implied transform faults linking these zones are hypothetical, although the CMT seismic catalog shows 5 events in the Trough with appropriately-oriented strike-slip mechanisms. The suggested northeastward termination of ON (and boundary

with AM) in southern Kyushu is based on two features: a strong gradient in geodetic velocities observed by the GEONET array of the Geographical Survey Institute (<http://mekira.gsi.go.jp>), and a transverse belt of ISC epicenters and Harvard CMT centroids with diverse mechanisms (Figure 3). Admittedly, a clear topographic lineament and master fault are not evident.

[29] The Okinawa Trough does not contain linear magnetic anomalies of seafloor-spreading origin to constrain its Euler pole and spreading rate. *Sibuet et al.* [1995] attempted to determine ON-EU (or ON-YA?) poles based primarily on azimuths of normal faults, and calculated that these poles lie southwest of the Trough. However, spreading may be oblique, in which case normal fault azimuths yield inaccurate poles, and transform azimuths or rate data must be used. In the Okinawa Trough, transform faults are obscure or nonexistent, and the geologic and gravity evidence suggests decreasing total extension to the northeast, inconsistent with a southwestern pole position. *Sibuet et al.* [1995] estimated net extensions between 80 and 25 km on different profiles, decreasing northeastward. *Park et al.* [1998] used Quaternary normal faults visible in seismic reflection sections to measure spreading rates of 11 and 20 mm/a, respectively, on two adjacent transects. (They acknowledge that these rates are minima because additional extension by distributed pure shear and/or dike intrusion would probably not be visible with seismic reflection.)

[30] The data most useful for determining the neotectonic ON-YA pole are geodetic results from the Ryukyu arc, although any single velocity or local group of velocities observed there may be strongly affected by transient locking and unlocking of the subduction zone. A GPS geodetic station on Ishigaki Island (central ON plate) moved 55 ± 2.2 mm/a toward $150 \pm 2^\circ$ azimuth with respect to stable EU [*Kato et al.*, 1998], which means that it moved about 47 mm/a toward 163° with respect to adjacent YA. Voluminous data (from 36 continuous GPS stations) collected by the GEONET array of the Geographical Survey Institute and made available electronically (<http://mekira.gsi.go.jp>) show similar velocities at Ishigaki Island, and a consistent decrease of southeastward velocities

(with respect to either YA or EU) toward the northeast, all the way to central Kyushu. I fit this dataset by maximum-likelihood (allowing 10% chance of contamination of each velocity by other processes) and estimated the ON-YA pole to be (29.8°N , 133.9°E , $2.42^\circ/\text{Ma}$). The implied rates of back-arc spreading are greater in the southwest, where the Philippine Seafloor is deep and smooth, than they are in the northeast, where the Kyushu-Palau, Daito and Oki-Daito Ridges are entering the Ryukyu Trench.

5.4. Sunda Plate (SU)

[31] The Sunda plate (Figure 4) includes most of southeast Asia, the South China Sea, the Malay Peninsula, most of Sumatra, Java, Borneo, and the intervening shallow seas [*Rangin et al.*, 1999]. The very low rate of shallow earthquakes is evidence of its low anelastic strain rates.

[32] In early 14-plate models of the Earth like RM2 and NUVEL-1, this region was considered part of the Eurasia plate (EU). However, the history of the India-Eurasia continental collision in the Himalaya has involved large relative movements of south China and southeast Asia with respect to the European-Siberian core of Eurasia [e.g., *Peltzer and Tapponnier*, 1988]. So, any previous connection to Eurasia was broken early in the Tertiary. Kinematic connections to other adjacent plates can only be attempted through interpretation of seismic slip vectors, since SU is separated from the Australia (AU) and Philippine Sea (PS) plates by subduction zones. However, slip vectors may be misleading if there is slip partitioning in an oblique subduction zone. Therefore, it was necessary to use space geodesy to determine its motion.

[33] *Genrich et al.* [1996] used GPS to define a "Sunda shelf block" which was indistinguishable from a rigid body, but they lacked the network breadth to precisely fix its rotation with respect to Eurasia. The GEODYSSSEA geodetic campaigns of 1994 and 1996 in and around "Sundaland" resulted in a consensus solution which has the SU-EU pole of (33.2°S , 129.8°E , $-0.286^\circ/\text{Ma}$) [*Chamote-Rooke and Le Pichon*, 1999; *Rangin et al.*, 1999]. This has been confirmed

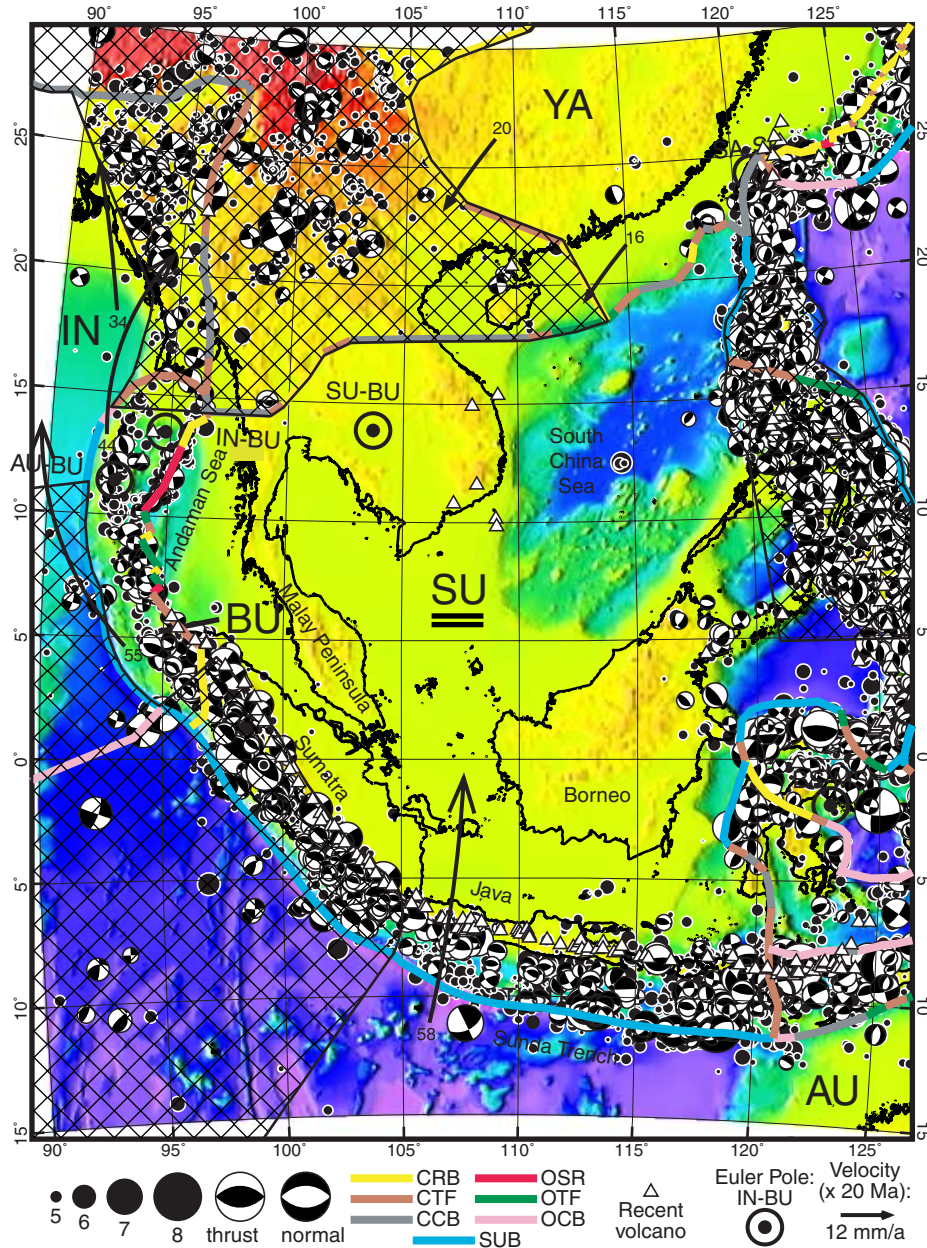


Figure 4. Boundaries (heavy colored lines) of the Sunda (SU) and Burma (BU) plates; surrounding plates include India (IN), Australia (AU), and Yangtze (YA). An orogen and several small plates east of SU are better represented in Figures 5 and 6, respectively. The southeastern prong of Eurasia (EU) is not stable but is part of the Persia-Tibet-Burma orogen. Cross-hatching in southwest shows Ninety East-Sumatra orogen. Conventions as in Figure 2. Transverse Mercator projection on meridian 108°E.

by seismic slip vectors in the Sunda and Philippine Trenches [Chamote-Rooke and Le Pichon, 1999]. This pole implies SU-EU relative velocities of 17–28 mm/a in directions from NE to ENE. For Table 1, I convert this motion to a SU-PA pole by adding the EU-PA rotation of DeMets *et al.* [1994].

[34] The inland boundary of the Sunda plate must lie north of GPS stations NONN in Vietnam and CHON in Thailand [Rangin *et al.*, 1999]. But the SU plate apparently does not extend as far north as 30°N, where Heki *et al.* [1999] found that several stations to the south of the Amur plate have a coherent velocity which is ESE with respect to

Eurasia, and thus different from (convergent with) the velocity of SU. Station CAMP in northern Vietnam also has a slightly anomalous, convergent velocity. Within these loose constraints, I have drawn a northern boundary of SU that is guided by the northern extent of the aseismic region and of smooth topography in southeast Asia, and then follows the continental/oceanic lithosphere boundary along the northern margin of the South China Sea. A similar northern boundary for the Sunda plate was shown (at a very small scale) by *Kreemer et al.* [2000]. It is important to note that the western part of this north boundary of SU is not a boundary with stable EU, but instead is a boundary with deforming parts of EU within the Persia-Tibet-Burma orogen (Figure 1). Therefore, this line is not predicted to be a zone of particular seismic hazard, and any calculation of relative velocity across this line using the Euler poles for SU and EU would be inappropriate. The eastern part of the north boundary should be a boundary with stable YA, and its very low seismicity is perplexing. (See the section on YA for further discussion.)

5.5. Burma Plate (BU)

[35] *Fitch* [1972] first proposed that the Burma-Andaman-Sunda subduction zone is the site of partitioned slip, which is driven by the oblique convergence of the India and Australia plates (IN and AU) on the west with the Eurasia and Sunda plates (EU and SU) on the east. Dextral strike-slip faulting occurs on the Sagaing fault of Burma, and also on the Great Sumatra fault which runs the entire length of that island. *Curry et al.* [1979, 1982] defined the narrow sliver between western thrusts and the eastern dextral faults as the “Burma plate”. They also showed how N-S seafloor spreading in the Andaman Sea links these two dextral faults and provides rate information for the entire system: the average rate has been 460 km/13 Ma = 35 mm/a, and the Quaternary rate has been 37 mm/a. Although *Curry et al.* [1982] did not discuss seismicity, the main features of their model are supported by the seismicity study of *Mukhopadhyay* [1984], which shows that the Burmese-Andaman subduction zone, the back-arc spreading system of the Andaman Sea, and Saga-

ing fault are all active. He also revised the location of the Andaman Sea spreading center slightly eastward. This geometry is shown on the Tectonic Map of the Circum-Pacific Region [*Circum-Pacific Mapping Project*, 1986].

[36] One complication is that *Mukhopadhyay* [1984] also identified active faults within this proposed Burma plate, but lying west of the Andaman Sea spreading center, in the latitude range 8°N to 15°N. Focal mechanisms for earthquakes with epicenters near these faults include a mixture of normal, strike-slip, and thrust, but the nodal planes of the strike-slip solutions are not well aligned with adjacent mapped faults. Because of hypocentral depth uncertainty, many of these events may have occurred within the subducting India plate. Therefore, I do not consider this sufficient evidence to divide the Burma plate into multiple plates (nor did he propose to). *Maung* [1987] more explicitly proposed that the Burma plate has, at times, been divided into two plates by a dextral fault system including the West Andaman fault and the Kabaw fault of Burma. The proposed fault system runs along the old geologic boundary between accretionary prism and stable forearc basin, where dip-slip faulting has certainly occurred. However, the focus of his paper is on finite strain, rather than neotectonics, and it is not clear that the West Andaman-Kabaw system is presently active or dextral. (There is an alignment of earthquakes with this fault trace in Burma, but the events are deeper than 70 km and therefore occur within the India plate.) *Maung* [1987] also presented evidence for 425 km dextral offset of the Irrawaddy-Chindwin river system by the Sagaing dextral fault, confirming its dominant role in regional tectonics. *Mukhopadhyay and Dasgupta* [1988] confirm that upper-plate earthquakes in Burma are mostly associated with the Sagaing fault or nearby Shan Scarp fault.

[37] A different modification to the *Curry et al.* [1979, 1982] concept of the Burma plate is required by results of *McCaffrey* [1991, 1992, 1996a], who studied the variation of seismic slip vector trends in the Sunda Trench, and used them to infer changes in forearc velocity as a function of latitude. He finds that northwestward velocity with respect to the Sunda plate (his “Southeast Asia”) increases grad-

ually along the length of Sumatra, from zero at the Sunda Strait to 45–60 mm/a. This implies an orogen in the southern part of the “Burma plate” of Curry et al. and a variable rate of dextral slip on the Great Sumatra dextral fault. The strain within the forearc is believed to occur primarily by strike-slip faulting, rather than normal faulting.

[38] For PB2002, I digitized the shape of the central part (1°N–14.4°N) of the “Burma plate” as given by the Tectonic Map of the Circum-Pacific Region [*Circum-Pacific Mapping Project*, 1986], but I terminated the plate to the south at Pulau Simuelue (Figure 4). The deforming Sumatran forearc is included in the large “Ninety East-Sumatra orogen”. Since any possible northern extension of the Burma plate past 14.4°N would abut the Persia-Tibet orogen, only information from latitudes 4.6°N to 14.4°N (the Andaman-Nicobar Islands region) can be used for estimation of an Euler pole. From information on the Tectonic Map [*Circum-Pacific Mapping Project*, 1986] I estimate the SU-BU Euler vector to be (103.7°E, 13.9°N, 2.1°/Ma). Then, using the SU-PA rotation estimated in the previous section, the BU-PA pole shown in Table 1 is computed. It also follows (using the IN-PA pole of *DeMets et al.* [1994]), that the IN-BU pole is at (94.8°E, 13.5°N). This pole only implies convergence and subduction of IN under BU for latitudes south of the pole. To the north of the pole it, it predicts sinistral strike-slip (if the IN-BU boundary turns east), or rapid spreading (if the IN-BU boundary continues to the north). I chose the former alternative as more consistent with topography and focal mechanisms. Apparently the northern part of the nation of Burma is not in the BU plate (as redefined here) and does not participate in the rapid clockwise rotation of the Andaman-Nicobar Islands region; instead it is part of the great Persia-Tibet-Burma orogen. The best possible approximation to a single plate boundary in this area is probably to identify the Sagaing fault and Shan Scarp fault as the primary faults in a transpressive IN-EU boundary embedded in this orogen.

5.6. Luzon Plate and Visayas Plate?

[39] The Philippine Islands lie in a zone of convergence (at about 90–100 mm/a toward 290°)

between the Philippine Sea plate (PS) on the east and the Sunda plate (SU) on the west (Figure 5). There is a switch in the dominant polarity of subduction, from the east-dipping Luzon (or Manila) trench (consuming SU) in the north to the west-dipping Philippine trench (consuming PS) in the south. (The east-dipping Negros-Sulu trench system also continues south from the Manila trench along the west side of the Philippine Islands group, but is less seismically active and topographically discontinuous.) These map relations require that there is at least one additional plate or an orogen in the Philippine Islands region.

[40] *Rangin et al.* [1999] presented a neotectonic model for the region based on information from the GEODYSSSEA geodetic campaigns, interpreted in light of seismicity, topography, and geology. They proposed two small plates in the Philippine Islands: a Luzon plate in the north, and a Visayas plate in the southwest. Specific Euler vectors were computed for these plates, based on two and three geodetic stations, respectively. They also identified an “East Philippine Sliver” which contains only one station, and which may be stable in its northern part, but which is cross-cut by numerous normal faults in the south, which collectively reduce the slip rate on the Philippine fault along its border with the proposed Visayas plate from 35 to 22 mm/a.

[41] *Rangin et al.* [1999] also note additional distributed deformation, both within the two named plates and southwest of them. They cite geodetic evidence for 20 mm/a sinistral slip on the Infanta segment of the Philippine fault, yet consider both sides of this fault to be parts of the Luzon plate. They acknowledge that two control points in the Visayas block which should have equal velocity actually differ by 18 mm/a, and that the Euler rotation best-fit to three velocity vectors leaves residuals up to 13 mm/a. Also, they propose subduction at the aseismic Sulu Trench and the seismically active Cotabato Trench, but show these trenches as terminating in a plate interior, which therefore cannot be rigid.

[42] Because of this evidence for high strain rates and differential velocities in each of the proposed small plates (and East Philippine Sliver) at the level

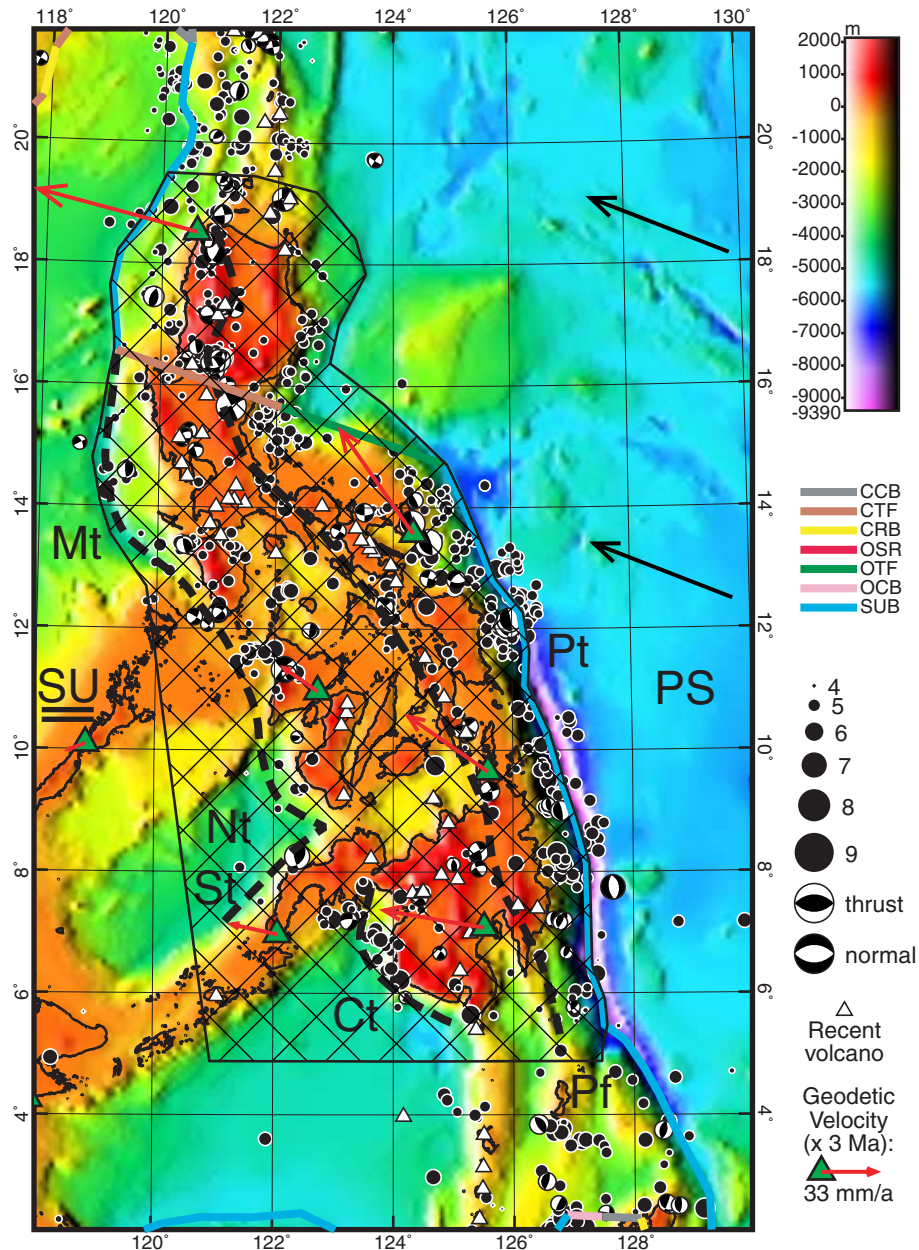


Figure 5. The Philippines orogen (black outline with cross-hatching) surrounds the Philippine Sea (PS) - Sunda (SU) convergent plate boundary (heavy colored lines). Important active faults plotted with heavy dashed lines: Philippine trench Pt, Manila trench Mt, Negros trench Nt, Sulu trench St, Cotabato trench Ct, Philippine fault Pf. Geodetic velocities from *Rangin et al.* [1999] are plotted relative to SU. Other conventions as in Figure 2. Transverse Mercator projection on meridian 124°E.

of 13–20 mm/a, it would inconsistent with the definitions in the rest of this compilation to accept them as part of the global set. I have instead indicated the entire Philippine Islands region as an orogen (Figure 5). This orogen also extends southwest to include the GEODYSSSEA station at Zamboanga (28 mm/a with respect to SU) and the single

active volcanic center (Bud Dajo) in the Sulu arc. This orogen designation is overlaid on an oversimplified first-order SU-PS boundary which includes the Luzon trench and a strike-slip connection to the Philippine trench. This plate model cannot make predictions of fault slip rates or seismic hazard in the Philippines with reasonable

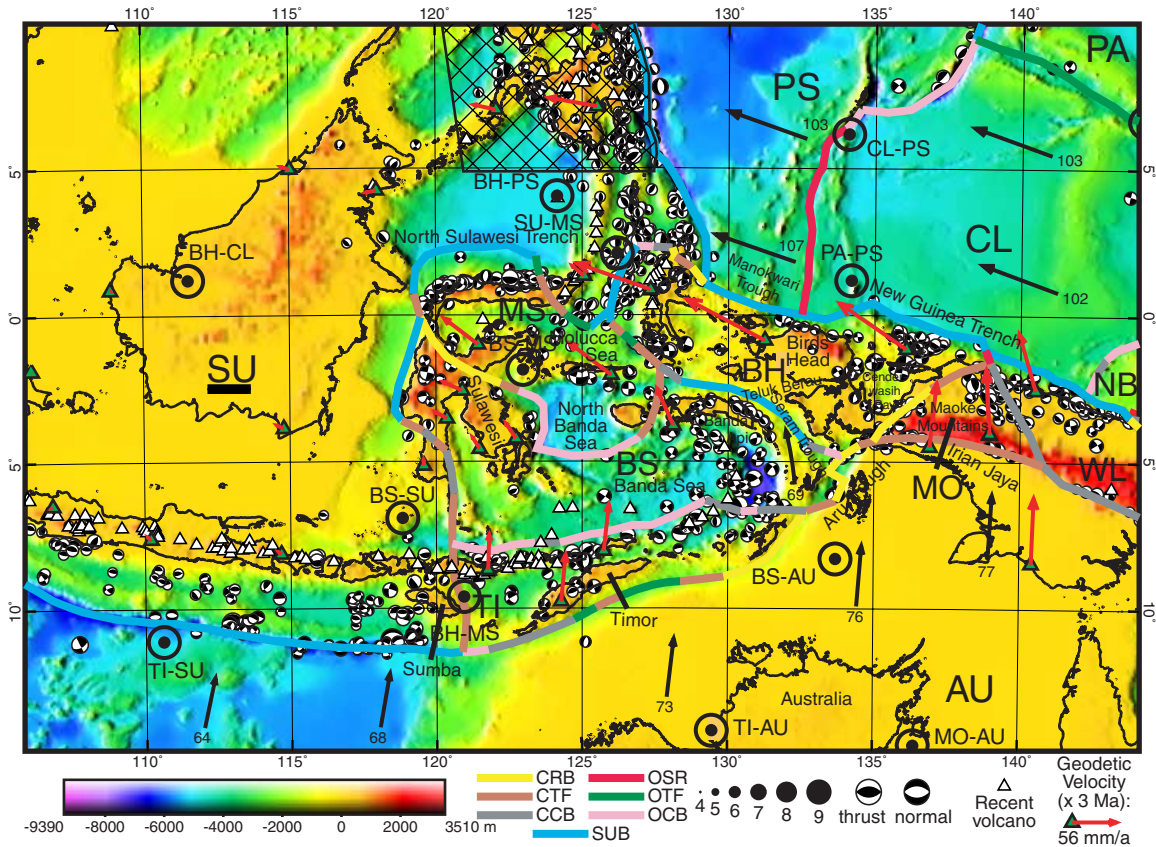


Figure 6. Boundaries (heavy colored lines) of the Molucca Sea (MS), Banda Sea (BS), Timor (TI), Birds Head (BH), and Maoke (MO) plates. Surrounding plates include Sunda (SU), Australia (AU), Woodlark (WL), North Bismarck (NB), Caroline (CL), and Philippine Sea (PS). Conventions as in Figure 2, except ISC epicenters are omitted for clarity. Geodetic velocities from *Puntodewo et al.* [1994] and *Rangin et al.* [1999] are plotted relative to SU. Oblique Mercator projection with great circle passing E-W through (125°E, 2.5°S).

precision, and continuum modeling methods should be applied instead.

5.7. Molucca Sea (MS), Banda Sea (BS), Timor (TI), Birds Head (BH), and Maoke (MO) Plates

[43] The region of the Molucca Sea, the Banda Sea, and Irian Jaya lies between four large plates (SU, PS, PA, and AU), and has the most complex neotectonics on Earth. *Rangin et al.* [1999] presented a neotectonic model emphasizing 4 small plates in addition to the 4 large bounding plates. I closely follow Rangin et al. in their definition of the 3 central plates: Molucca Sea (their “Sulu block”), Banda Sea, and Timor, because each of these has both a geodetic and a seismological expression. I simplify the Java Sea region to the west (combining their “Deformed Sundaland”

with SU) because I prefer not to define additional plates based only on small differences in geodetic velocity where there are no seismicity lineaments. In the eastern region, I also interpret a Birds Head plate, but with slightly different boundaries (Figure 6). I will also present arguments for a small Maoke plate between the Birds Head and Australia plates.

[44] The convergence of two subduction zones in the Molucca Passage has been well established since *Silver and Moore* [1978]. The Sangihe subduction zone on the west dips westward and consumes Molucca Sea plate (MS) beneath SU. The Halmahera subduction zone on the east dips eastward and consumes MS beneath PS. In the northern Molucca Passage, the two forearcs have already collided to form the Talaud-Mayu Ridge, so the MS plate is no longer present at the surface

at these latitudes. But there are two active volcanic arcs and two Benioff zones, and there is still the potential for great thrusting earthquakes on each side. To represent this in the global plate model, I use two coincident subduction boundaries (SU/MS and MS/PS) instead of a single SU-PS collisional boundary. That is, the MS plate is topologically and kinematically present in the northern Molucca Passage, although it has no surface area there. In the Molucca Sea, these boundaries diverge because the SU/MS boundary is transformed northwest to a SU\MS boundary with opposite subduction polarity at the North Sulawesi Trench. The remainder of the MS boundary is based on the Sula block outline drawn by *Rangin et al.* [1999], including the Palu fault in Sulawesi and the Hamilton thrust between Sulawesi and the North Banda Sea. The SU-MS Euler pole at (2.1°N, 126.2°E, 3.4°/Ma) is from Table 2 of the same paper (where it is labeled “SUL/SU”).

[45] The presence of an independent Banda Sea (BS) plate has long been suspected because if this region were firmly fixed to SU (or EU) it would be a geometric impossibility for the Banda volcanic arc to curve around to a northwest trend at Banda Api. *Rangin et al.* [1999] defined boundaries for this plate and computed the BS-SU Euler vector as (6.93°S, 118.85°E, 2.671°/Ma) based on GEODYSSSEA velocities at 5 sites. Under western Sulawesi, a few earthquakes deeper than 70 km suggest the development of a subduction zone, although there are no active volcanoes. Further south on the SU-BS boundary, motion would be predicted to become sinistral with only minor compression. The northeastern boundary of the BS plate is also an active or recently-active subduction zone, with clear forearc ridge, forearc basin, and volcanic arc.

[46] The Timor plate (TI) was discovered in geodetic results by *Genrich et al.* [1996]. This portion of the Sunda-Banda forearc and volcanic arc has apparently been broken loose from SU by the collision with the continent of Australia on the AU plate, and now moves with a velocity closer to that of AU than to SU. The Flores and Wetar thrusts on the north margin are young [*Silver et al.*, 1983, 1986], and have not yet developed Benioff zones of intermediate-depth earthquakes.

Rangin et al. [1999] proposed an outline of this plate, which I adopt in the central and eastern parts. (However, *Genrich et al.* [1996] showed that Sumba is more likely to be part of SU.) To obtain an Euler pole for TI-SU, I fit the GEODYSSSEA velocity vectors at ENDE, KAPA, and LIRA together with the azimuths of 9 TI-SU seismic slip vectors from *Genrich et al.* [1996], and obtain (11.1°S, 110.6°E, 2.09°/Ma). This implies a TI-AU pole of (14.1°S, 129.5°E, 1.74°/Ma). Although somewhat different from the “northern Australia-southern Banda block” pole of *Genrich et al.* [1996], it is consistent with their observation of predominantly sinistral slip on the former subduction boundary to the south of TI; the predicted rates are about 20 mm/a.

[47] In the Aru Trough, which appears to be bounded by stable AU on the east, there are many earthquakes whose Harvard CMT mechanisms imply extension directed WNW-ESE. The plate immediately west of the Trough might be either TI or BS, because both the TI-AU and BS-AU poles lie SSW of this lineation and predict the correct sense of relative motion. It is noticeable that in this sector of the Seram arc to the west there are no earthquakes with thrusting mechanisms. Probably a geologically recent change in the absolute velocity of BS (caused by the progressive accretion of TI onto AU) has resulted in reversal of dip-slip on this part of the boundary.

[48] In Irian Jaya to the northeast, the major source of neotectonic information is the GPS geodetic study of *Puntodewo et al.* [1994]. Their results were surprising, because in contrast to previous models they indicated no measurable sinistral slip on the E-W-trending Sorong fault in Birds Head, and no thrusting (but sinistral slip) across the steep southern front of the Highlands thrust belt in the Maoke Mountains. Stations SORO and BIAK are moving at velocities closer to those of the adjacent PS and PA plates than to the velocity of AU. This requires an additional small plate in northern Irian Jaya; following *Rangin et al.* [1999] I refer to this as the Birds Head (BH) plate. I use the velocities of SORO and BIAK relative to the NNR reference frame of *Argus and Gordon* [1991] to calculate the BH-AU Euler pole as (55.5°S, 152.0°E, 1.05°/Ma).

BH/PS and BH/CL relative velocities are then convergent and are taken up offshore in the Manokwari Trough (22 mm/a toward 026°) and New Guinea Trench (32 mm/a toward 003°), respectively. A proposed BH-SU transform boundary in the northwest corner of BH is drawn along a line of earthquakes which is parallel to the model BH-SU velocity; these events have appropriate dextral mechanisms if the WNW-ESE-striking nodal plane is the fault plane. This boundary is suggested to pass through the strait (Selat Morotai) between Halmahera and Morotai, where there is a discontinuity in volcanic arcs and focal mechanisms as well as topography.

[49] The primary new feature in Figure 6 is the proposed Moake plate southeast of BH and north of stable AU. The E-W-trending onshore Highlands thrust belt connects westward to the onshore and offshore Tarera-Aiduna fault zone that connects to the Banda arc. It is seismically active, with 24 CMT events and total moment of 1×10^{20} N m [Puntodewo *et al.*, 1994] and a predominance of sinistral mechanisms. The relative geodetic velocity WME-TIMI suggests sinistral slip at 13 ± 8 mm/a [Puntodewo *et al.*, 1994], although this rate could be either raised or lowered by consideration of elastic strain changes. I suggest that this additional plate south of the BH plate and north of stable AU be called the Maoke (MO) plate after the Maoke Mountains, which are its most prominent feature. The eastern boundary of MO is the NW-SE-trending Mamberambo thrust belt, to the northeast of which I propose an expanded Woodlark plate (discussed below). To estimate MO plate motion, I observe that the MO-AU boundary is well fit by a small circle about (14.6° S, 136.4° E). The geodetic velocity mentioned above gives a very rough rate of $0.64 \pm 0.4^\circ$ /Ma for this MO-AU pole.

[50] The southern boundary of BH (and the northwestern boundary of MO) is controversial. Considering seismic moment sums and focal mechanisms, Puntodewo *et al.* [1994] suggest that a possible sinistral boundary is the Birds Neck fault through Teluk Berau (the bay between Birds Head and Birds Neck), which connects eastward to the Yapen fault. Alternatively, Rangin *et al.* [1999] defined BH as ending at the NE-trending sinistral Tarera and

Paniai faults that lie southeast of Cenderwasih Bay. Each group of authors acknowledges the others' model as an alternative. A choice cannot be made on the basis of geodesy, because the relative velocity BIAK-WAME is 83 mm/a toward 253° , and this azimuth is intermediate between the mean azimuths of the two fault systems. The Birds Neck-Yapen fault boundary has had more seismic moment in earthquakes with strike-slip character (B-axis more vertical than P or T) during the time window of the CMT catalog: 3×10^{20} N m in 19 events, versus 7×10^{18} N m in 6 events. However, this difference could be eliminated by one future $m_w = 7.6$ event on the Tarera or Paniai fault. To me, the decisive observation is that the Seram Trough has numerous thrusting events between longitudes 130° and 132° E. This requires the Trough to be part of a BS/BH boundary which would be convergent (70 mm/a toward 78°), and not part of a BS-MO boundary which would be divergent (9 ± 8 mm/a toward 244°). Therefore, I adopt the BH-MO boundary along the Tarera and Paniai faults where a plate boundary was proposed by Rangin *et al.* [1999]. Whether the BH plate should also be divided into two by a slow-moving sinistral boundary at the Birds Neck-Yapen fault line is a question for future geodetic investigations.

5.8. Caroline Plate (CL)

[51] The Caroline plate was proposed as a distinct neotectonic plate by Weissel and Anderson [1978] based on a combination of seafloor morphology, seismicity, gravity data, and seismic reflection profiles. It lies north of New Guinea (Figure 7) and encompasses the West Caroline Basin and East Caroline Basin (which formed by North-South spreading in mid-Tertiary time), and the inactive north-south-trending Eauripik Rise which separates them. (The Caroline plate does not include either the Caroline Islands or the Caroline Ridge.) Its boundary with the Birds Head (BH) and Woodlark (WL) plates to the south is the New Guinea Trench, in which CL subducts southward. Its boundary with the Philippine Sea (PS) plate to the west has two segments. The southern segment is the Ayu Trough, which formerly spread at rates on the order of 8 mm/a from about 25–2 Ma, but may spread

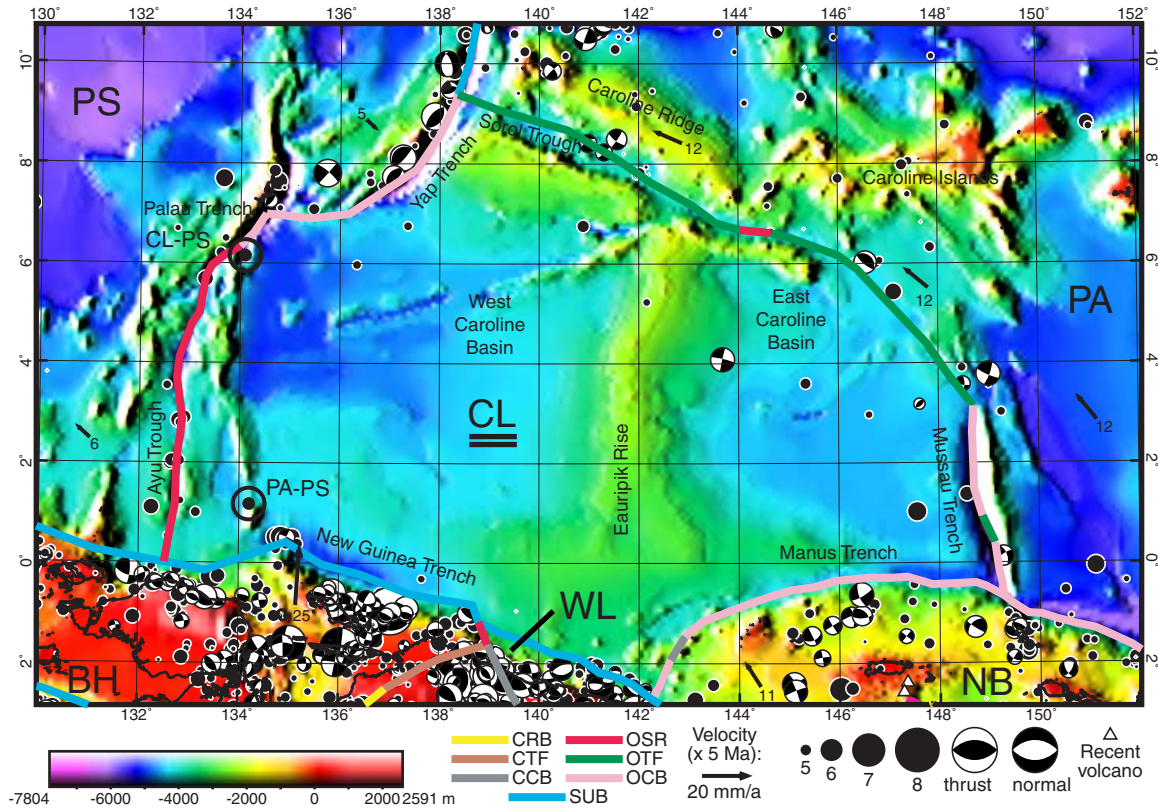


Figure 7. Boundaries (heavy colored lines) of the Caroline (CL) plate. Surrounding plates include Philippine Sea (PS), Birds Head (BH), Woodlark (WL), North Bismarck (NB) and Pacific (PA). Conventions as in Figure 2. Oblique Mercator projection with great circle passing E-W through (141°E, 4°N).

more slowly now [Fujiwara *et al.*, 1995]. The northern segment is composed of the Palau Trench and southern Yap Trench, which are associated with thrusting earthquakes on high-angle reverse faults [Ranken *et al.*, 1984]. (The Palau and southern Yap Trench boundaries do not appear to be true subduction zones, as they have no low-angle thrust events or active volcanoes, and their forearcs are anomalously narrow.) The CL-PS pole must lie near the division between these segments. The CL boundary with the Pacific plate (PA) to the northeast varies in style according to boundary azimuth [Weissel and Anderson, 1978]: sinistral transtension in the Sorol Trough on the north, sinistral transpression in the northeast, and eastward underthrusting of CL beneath PA in the Mussau Trench on the east. (The Mussau Trench boundary also lacks active volcanoes and deep earthquakes, and is not considered a subduction zone, although it may become one in the future.) The southeastern boundary of the Caroline plate is here interpreted to be

the Manus Trench (also known as West Melanesian Trench). Based on principal stress directions inferred from Harvard moment tensors, this appears to be a convergent boundary with N-S shortening, but it lacks active volcanoes and deep earthquakes and so is not currently a subduction zone.

[52] Although the Caroline plate is clearly a terrane with a history distinct from that of the adjacent Pacific plate, it has been lumped with the Pacific in previous 14-plate neotectonic models. This is because seismicity along their common boundary is sparse, and their relative velocities are not large [McCaffrey, 1996b]. *Circum-Pacific Map Project* [1986] equivocated on this point by using the map symbols for intraplate faults along the CL-PA boundary. The Euler pole adopted here for CL-PA rotation (10.13°S, 134.43°E, 0.309°/Ma) is from Table 4 of Seno *et al.* [1993], who used seismic slip vectors around PS to determine its current motion, and then determined CL motion from the CL-PS pole (noted

previously) and a few CL-PA slip vectors. With this pole, relative velocities are predicted to be as much as 11 mm/a on the CL-PA boundary, and up to 7 mm/a on the PS-CL boundary. If the PS-PA pole position of *Seno et al.* [1993] is correct, then a distinct Caroline (neotectonic) plate is required to explain continuing extension in the Ayu Trough.

5.9. Mariana Plate (MA)

[53] Evidence for seafloor spreading in the Mariana Trough (west of the Mariana volcanic arc) was noted by *Karig* [1971] and by *Anderson* [1975]. Deep Sea Drilling Project Leg 60 investigated a profile at 18°N. The spreading rate there was estimated to be between 30 mm/a [from magnetic lineations, *Bibee et al.*, 1980] and 43 mm/a [from age of basal sediments, *Hussong and Uyeda*, 1981], both assuming a rift-normal spreading direction of N60°E. Therefore, a “Mariana plate” (Figure 8) lying between the Mariana Trench and the Mariana Trough was indicated on the tectonic map by *Circum-Pacific Map Project* [1986]; this map also shows that a former spreading ridge west of the Izu volcanic arc (north of 25°N) is presently inactive, or perhaps active at low rates [*Seno et al.*, 1993]. *Eguchi* [1984] and *Otsuki et al.* [1990] suggested that back-arc spreading is limited to latitudes between the points where two buoyant ridges on the Pacific plate are subducting (Caroline Ridge and Ogasawara Plateau). At 21°N, *Otsuki et al.* [1990] interpreted a half-spreading-rate of 10 mm/a from the western half of a magnetic profile by *Yamazaki et al.* [1988]; the same rate was given by *Yamazaki et al.* [1993]. *Martinez et al.* [1995] and *Baker et al.* [1996] made detailed studies of the north end of the Mariana Trough (N of 22°N) and emphasized a complex and heterogeneous extension which is not simple seafloor spreading. *Martinez et al.* [2000] used sidescan sonar and geophysical methods to map the fine structure of the southern end of the Trough; they found it has many characteristics of a fast spreading ridge, but is complicated by cross-faults accommodating trench-parallel extension on the eastern (Mariana plate) side of the Trough. Their Figure 1 also indicates two apparent transform offsets in the spreading ridge, at 15.7°N and 17.6°N, with azi-

muths of N70°E. Preliminary geodetic velocities from the GPS network WING were reported by *Kato et al.* [1998]: Guam is moving 50 ± 7 mm/a toward $N96 \pm 8^\circ E$ with respect to the *Seno et al.* [1993] model of Philippine Sea plate motion. Recently, *Ishihara et al.* [2001] reported marine magnetics showing spreading rates of approximately 50–56 mm/a at 13–14°N, and 30–34 mm/a at 16–17°N.

[54] The differences in character and apparent opening velocity between the north and south ends of the Mariana Trough suggest that it may not be symmetrical about an E-W axis, but instead is opening more rapidly in the south, with the Mariana plate rotating about a northern Euler pole with respect to the Philippine Sea (PS) plate. Under this hypothesis, net spreading in the southern Trough would be oblique, and therefore greater than the Trough width measured orthogonal to its strike. If the data cited above are required to fit a single MA-PS pole, it would be located near (25.4°N, 141.4°E) with rate of about 2.11°/Ma. This solution fits each of the known spreading rates (to within 2–8 mm/a) and compromises between the apparent spreading directions given by the apparent transform offsets and by the single GPS velocity at Guam (with errors of 2° and 21°, respectively). The predicted direction of spreading at the Guam GPS site would be significantly different from the observed two-year geodetic trend. This may be evidence for the hypothesized extension within the Mariana arc [*McCaffrey*, 1996a; *Martinez et al.*, 2000]. However, it may also be a transient velocity which only represents one part of the seismic cycle on the adjacent southern part of the Mariana Trench. Based on the rule stated earlier, I prefer not to introduce additional plates (or orogens) based on a single anomalous geodetic velocity, unless supported by seismicity and topographic lineaments.

[55] The shape of the proposed MA plate is taken primarily from Figure 1 of *Martinez et al.* [2000]. However, they did not indicate how or where this plate ends in the North. The MA-PS boundary, which according to plate theory must be connected to other plate boundaries, is here suggested

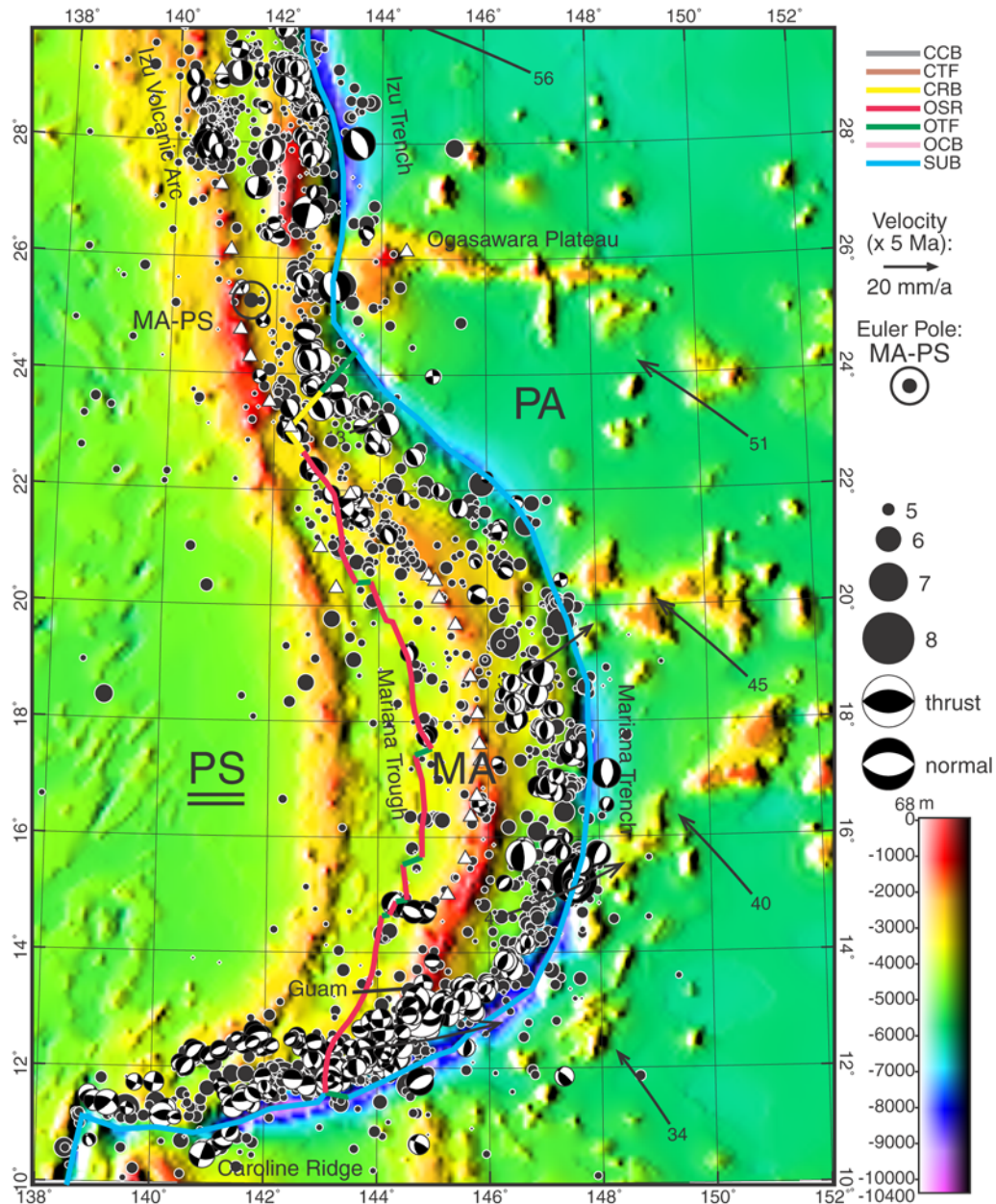


Figure 8. Boundaries (heavy colored lines) of the Mariana (MA) plate, lying between the Philippine Sea (PS) and Pacific (PA) plates. Conventions as in Figure 2. Transverse Mercator projection on meridian 145°E.

to cut perpendicularly across the arc near 24°N (where the backarc basin ends) and connect to the MA/PA boundary in the Mariana Trench. The position of the suggested cross-arc boundary (which may be an over-simplification of a zone of deformation) relative to the MA-PS pole computed above would then imply that this NE-trending boundary should be a site of sinistral transtension within the arc. Harvard CMT solu-

tions include a group of shallow earthquakes at this latitude which may mark the plate boundary. The most concentrated group of events showing arc-parallel extension (by either strike-slip or normal faulting) is found near 23.8°N (although it cannot be ruled out that these events might have occurred in the subducting Pacific plate). Also, *Wessel et al.* [1994] documented swarms of minor normal faults which accommodate trench-parallel

extension within the arc near 22°N. Since their survey did not extend to 24°N, the possibility of more intense transverse faulting at that latitude remains open.

[56] Back-arc extension is also occurring in the Izu extensional zone west of the Izu Trench. *Seno et al.* [1993] discuss the evidence and conclude that the rates are probably in the range of 1–2.5 mm/a. As this is well below the threshold for plate differentiation used in this paper (~8 mm/a in the Pacific basin), the Izu arc is here considered to be part of the Philippine Sea plate.

5.10. North Bismarck Plate (NB), South Bismarck Plate (SB), and Manus Plate (MN)

[57] A schematic comparison of 8 alternative kinematic models for this area was presented by *Tregoning et al.* [1998]. *Johnson and Molnar* [1972] proposed two small plates in the Bismarck Sea: “North Bismarck” (NB) and “South Bismarck” (SB), separated by a straight sinistral transform boundary. *Curtis* [1973] drew a curved boundary, and called the northern one the “Manus plate” and the southern one the “New Britain plate”, but these names were not generally accepted (and now the term “Manus plate” is used in a different way). *Hamilton* [1979] drew a more complex boundary between NB and SB with both sinistral transform and spreading segments; this was supported by the seismicity study of *Johnson* [1979] and the mapping of seafloor spreading anomalies by *Taylor* [1979].

[58] Some authors have considered the present relative motion between NB and Pacific (PA) to be uncertain or insignificant, and have merged these two in neotectonic models. However, this approximation is not compatible with recognition of a separate Caroline (CL) plate. Where the CL-PA boundary in the Mussau Trench meets the CL-NB and NB-PA boundaries in the Manus Trench (also known as West Melanesian Trench), it is the Manus Trench whose trend continues smoothly through the triple-junction, as if NB-CL and NB-PA relative velocities were at least as large as CL-

PA velocities. Second, the Harvard CMT catalog records about 10 $m > 6$ earthquakes in 25 years which appear to be associated with active NB-CL and NB-PA boundaries. Finally, *Tregoning et al.* [1998] report that stations MANU and KAVI in the NB plate have velocities of 5 and 8 mm/a (respectively) north-northwestward with respect to PA, while the baseline between them is stable at -0.1 ± 6.0 mm/a. They did not consider this definitive proof of a separate NB plate because this motion exceeds their 95%-confidence limits but does not exceed their 99%-confidence limits. However, the geodetic velocities of these two stations with respect to the *Seno et al.* [1993] model of CL is ~14 mm/a toward 336°, which exceeds the threshold used in this model for discrimination of plates in the Pacific basin. I use these two geodetic velocities to estimate a NB-PA Euler pole of (4°S, 139°E, 0.33°/Ma).

[59] The existence of the SB plate has never been controversial. Its southern boundary is the North-dipping subduction zone at the New Britain Trench. Its eastern boundary (with NB) is from *B. Taylor et al.* [1995], and is expected to have sinistral strike-slip motion. The eastern half of the northern boundary of SB (also with NB) in the Manus Basin is from *Martinez and Taylor* [1996]. The western half of the northern boundary lies along the spreading Western Ridge mapped by *Auzende et al.* [2000], and then along a prominent alignment of large strike-slip earthquakes with uniform sinistral mechanisms from the Harvard CMT catalog. The southwestern boundary of SB (with the Woodlark plate of the New Guinea region) is along the Ramu-Markham thrust fault on the southwest flank of the Finisterre Range [*Tregoning et al.*, 1998] where the New Britain volcanic arc is colliding with the northern margin of New Guinea. The motion of the South Bismarck plate with respect to its neighbors is well determined by a combination of seafloor spreading anomalies in Manus Basin [*Taylor*, 1979; *Martinez and Taylor*, 1996], paleomagnetic rotation rates observed in the Finisterre Range [*Weiler and Coe*, 2000], and GPS geodesy [*Tregoning et al.*, 1998, 1999]. I use the PA-SB pole at (10.61°S, 147.01°E) from *Tregoning et al.* [1999] in Table 1.

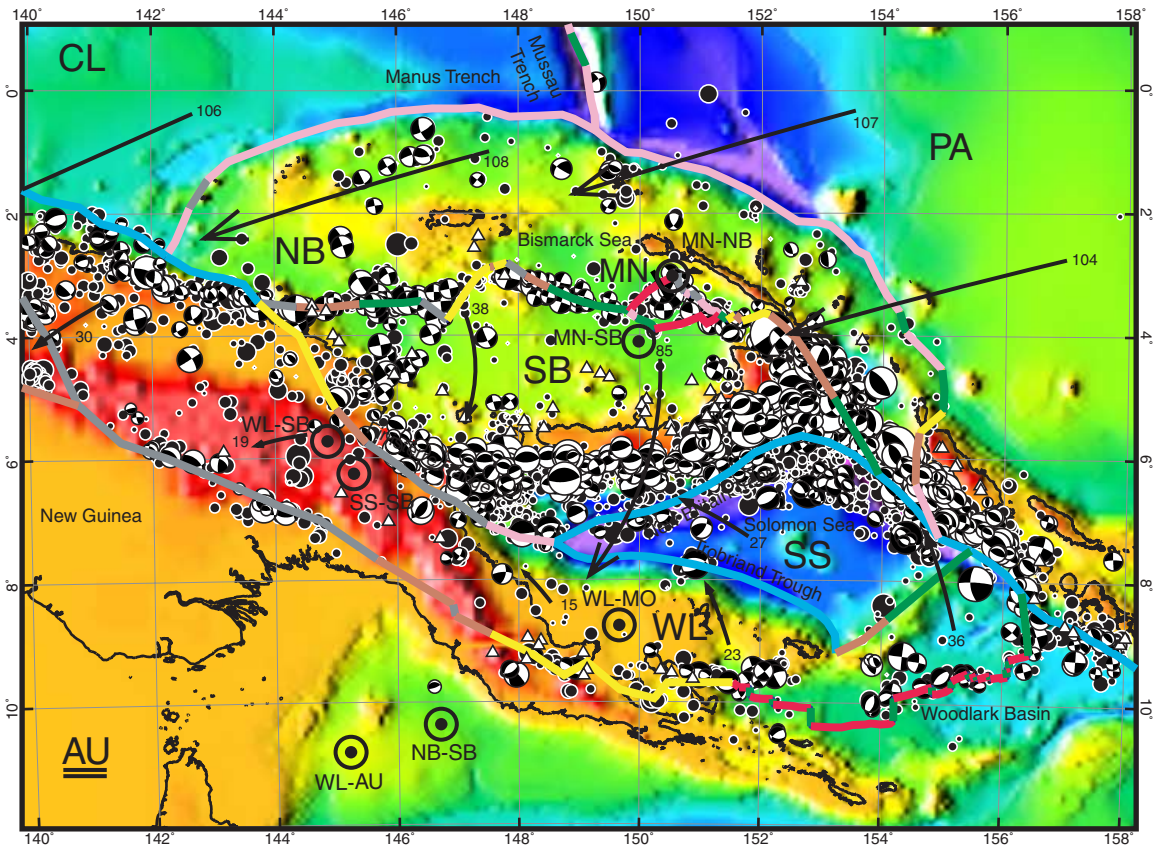


Figure 9. Boundaries (heavy colored lines) of the North Bismarck (NB), Manus (MN), South Bismarck (SB), Solomon Sea (SS) and Woodlark (WL) plates. Surrounding plates include Australia (AU), Caroline (CL), and Pacific (PA). Conventions as in Figure 2. Oblique Mercator projection with great circle passing E-W through (149°E, 5.5°S).

[60] The small (100-km-wide) “Manus microplate” (MN) is from the detailed bathymetric and magnetic study of *Martinez and Taylor* [1996] in the Manus Basin. (Note that their “Pacific plate” is here interpreted as NB, while their “Bismarck plate” is here interpreted as SB.) Locally the sinistral transtensional NB-SB boundary divides into the Manus Spreading Center on the northwest and the Southern Rifts on the southeast, isolating a microplate of very young oceanic crust which rotates relatively counterclockwise. The very small size of this plate means that inaccurate epicenters determined from teleseisms are not sufficient to outline it; I have interpreted the boundaries of this plate from the bathymetry and seafloor magnetization data of *Martinez and Taylor* [1996]. They located the MN-NB pole at the northeast end of the Manus Spreading Center (3.03°S, 150.53°E), and used the map of Brunhes epoch magnetization to determine its rotation rate

as 51°/Ma (which is probably the fastest relative rotation in the world).

5.11. Solomon Sea Plate (SS) and Woodlark Plate (WL)

[61] *Johnson and Molnar* [1972] first defined a Solomon Sea (SS) plate, outlined by seismicity, to explain slip vectors in the northwestern part of the South Solomon Trench which are not parallel to Australia-Pacific (AU-PA) slip directions seen in the southeastern part of the same trench. On the north, the Solomon Sea plate subducts beneath the South Bismarck plate (and, very locally, beneath North Bismarck and Pacific plates) at the New Britain and Solomon Trenches (Figure 9).

[62] Opinions have shifted concerning the southwestern boundary of the Solomon Sea plate, which some early authors placed in the vicinity of the Owen Stanley Range in the Papuan Peninsula, and

most later authors place offshore in the Trobriand Trough. (See the comparison of 8 published models in *Tregoning et al.* [1998].) *Johnson and Molnar* [1972] could obtain only one focal mechanism in the Owen Stanley Range, which showed a combination of normal and strike-slip strain, and they assumed that this constrained the SS-AU boundary. *Curtis* [1973] found only one (other) mechanism, which was strike-slip, and drew a SS-AU plate boundary on land along the center of the range, and inferred that it should be sinistral and transtensional. *Hamilton* [1979] proposed another plate boundary north of the Papuan Peninsula in the Trobriand Trough, with slow subduction of SS plate to the southwest. To avoid a Z-shaped SS-AU boundary with serious kinematic difficulties, he invoked two zones of distributed deformation and an additional “Woodlark plate” (WL; named for Woodlark Island). The first Plate Tectonic Map of the Circum-Pacific Region [*Circum-Pacific Map Project*, 1981] did not take a position on this controversy, leaving the southwest boundary of the Solomon Sea plate unmarked. However, in the 1986 edition, the Trobriand Trough was shown as an active subduction zone. *Lock et al.* [1987] and *Honza et al.* [1987] also argued for subduction at the Trobriand Trough on the basis of seismic reflection profiles, and seismicity and arc-type volcanism, respectively. I accept the Trobriand Trough as the southwestern boundary of SS, but follow *Hamilton* [1979] in considering that the overriding plate is WL rather than AU.

[63] *B. Taylor et al.* [1995], *Goodliffe et al.* [1997], and *Taylor et al.* [1999] interpret this SS\WL boundary along the Trobriand Trough as connecting to a northeast-trending transform fault on the northwest margin of the Woodlark Rise, which connects back to the South Solomon Trench, closing the SS plate outline. This is supported by a lineament of small earthquakes recorded in the ISC catalog; unfortunately, there are no Harvard CMT mechanisms to confirm the sense of slip (which is expected to be sinistral). The Solomon Sea plate apparently contains no islands, so its velocity cannot be determined by geodesy. It is apparently not in contact with any spreading center, so its velocity cannot be determined by marine mag-

netics. Because the Trobriand Trough subduction zone (SS\WL) has only 7 volcanoes and a few intermediate-depth earthquakes, it is probably much more slow-moving than the nearby New Britain Trench; *Tregoning et al.* [1998] estimate its convergence rate as 6–20 mm/a. For this compilation, I estimate the Euler poles of SS from the transform fault azimuth of 050° (giving the direction of SS-WL relative velocity) and a median SS\WL convergence rate of 13 mm/a.

[64] Seafloor spreading in the Woodlark Basin had been abundantly documented. *Milsom* [1970] was one of the first to propose spreading; *Curtis* [1973] suggested 5 transform faults along this spreading center on the basis of seismicity. A second survey of the marine magnetics by *Weissel et al.* [1982] led them to revise these transforms, and infer a westward-propagating rift with a current pole of spreading located 15–20° to the west. *B. Taylor et al.* [1995] reported a third high-resolution survey and inferred Brunhes-epoch spreading rates as increasing from 36 mm/a (west end) to 67 mm/a (east end). However, *Goodliffe et al.* [1997] found evidence in sidescan and multibeam bathymetry that spreading shifted its direction by 8–22° counterclockwise at 0.08 Ma, synchronously, and without evidence of propagation. This leads to doubt [e.g., *Tregoning et al.*, 1998] whether the Brunhes-era rates would still apply to the present. Therefore, I have adopted the geodetic Euler pole of *Tregoning et al.* [1998] for WL-AU motion which is found in their Table 5: (10.8°S, 145.2°E, 1.86°/Ma).

[65] I believe that the Woodlark plate extends further northwest than *Hamilton* [1979] originally proposed, into central New Guinea, and possibly as far as the Mamberambo thrust belt in Irian Jaya (Figures 7 and 9). The WL-AU pole position cited above would imply that the sense of relative motion along the WL-AU boundary should change gradually from spreading in the Woodlark Basin and D’Entrecasteaux Islands, to sinistral extension in the Papuan Peninsula, and then to sinistral transpression in the Owen Stanley Range of central Papua New Guinea (and further northwest). All of these predictions are supported by moment

tensors from the Harvard CMT catalog. A cursory look at shallow seismicity within the area of the proposed WL plate (e.g., Bismarck Range area) might suggest that it is undergoing internal deformation as an “orogen”. However, it is important to realize that this is a region of both shallow and intermediate-depth seismicity within the volume of the doubly-subducted SS plate, which is being strongly bent in a mode analogous to the deformation of the Molucca Sea plate (MS) in the Molucca Passage (SU/MS\BH). Hypocenters determined teleseismically will not always have the precision in depth which we would like in order to determine which of the two plates contained the event.

5.12. New Hebrides (NH), Conway Reef (CR), Balmoral Reef (BR), and Futuna (FT) Plates(?) in the New Hebrides-Fiji Orogen

[66] The North Fiji Basin (formerly known as the Fiji Plateau) is large region of young oceanic crust (<12 Ma) formed by backarc spreading between the diverging New Hebrides and Tonga subduction zones [Auzende *et al.*, 1995a]. Most of the region lacks islands to permit geodetic measurements of relative velocity. (The only GPS velocities available are in the New Hebrides volcanic arc [Calmant *et al.*, 1995; F. Taylor *et al.*, 1995], where elastic strain changes probably affect the results.) Magnetic lineations are complex and difficult to identify. Most ridges do not produce earthquakes large enough to appear in teleseismic catalogs [Bird *et al.*, 2002]. The water depths above spreading centers frequently differ from global averages by a kilometer or more, so water depth is not a good guide to crustal age. Nevertheless, authors since Chase [1971] have attempted to divide the region into small plates. Pelletier *et al.* [1998] sketched a plate tectonic map, although they did not complete all boundaries or compute Euler poles. There is general acceptance of four regions which have significantly higher strain rates around their margins than in their interiors (plate criterion 1 of this paper). I will describe each briefly, referring to them by names (Figure 10) which are assigned here for the first time (because of the absence of clear precedents in the literature). I will then discuss

some reasons to doubt that these “plates” move coherently within the velocity tolerance (8 mm/a) that is used here to divide plate-like behavior (plate criterion 2 of this paper) from orogens.

[67] The New Hebrides plate (NH) corresponds roughly to “block M” of Chase [1971]. I interpret it to include the New Hebrides volcanic arc and the western North Fiji Basin. Its boundaries are the New Hebrides Trench on the south and southwest, the Hazel Holme Ridge-South Pandora Ridge on the north, the N160° Ridge (named by Auzende *et al.* [1995a] for its azimuth) on the northeast, and the Central Spreading Ridge on the southeast. At its NE corner, NH moves 16 mm/a southward with respect to PA by spreading on the South Pandora Ridge [Lagabrielle *et al.*, 1996]. Southward velocity components with respect to PA are also suggested by GPS velocities at Efate and Tana in the New Hebrides [Calmant *et al.*, 1995], although these components are 34–38 mm/a, and probably not applicable over the same timescale. This southward component explains the thrusting earthquakes in the southernmost part of the New Hebrides Trench (172–174°E), which could not occur if NH were a part of PA. The southern part of NH also moves at least 20 mm/a westward with respect to PA, because the combined spreading rates of the Central Spreading Ridge and West Fiji Ridge are approximately 100 mm/a [Auzende *et al.*, 1994, 1995b], exceeding the relative velocity AU-PA at this latitude (80 mm/a). These constraints suggest a PA-NH Euler pole of approximately (12°S, 164°E, 1.0°/Ma), which would be consistent with the interpretations of Pelletier *et al.* [1993] and Schellart *et al.* [2002] that spreading rates on the Hazel Holme Ridge decrease westward.

[68] Note that some authors would divide NH into two or more plates. Louat and Pelletier [1995] inferred high relative velocities between the New Hebrides arc and the western North Fiji Basin, although Maillet *et al.* [1995] found no evidence of this in the region of their study. Also, the eastward GPS velocity (with respect to PA) at Santo and some thrusting earthquakes occurring locally along the east margin of the New Hebrides arc lead F. Taylor *et al.*, 1995 to interpret that the New Hebrides arc is

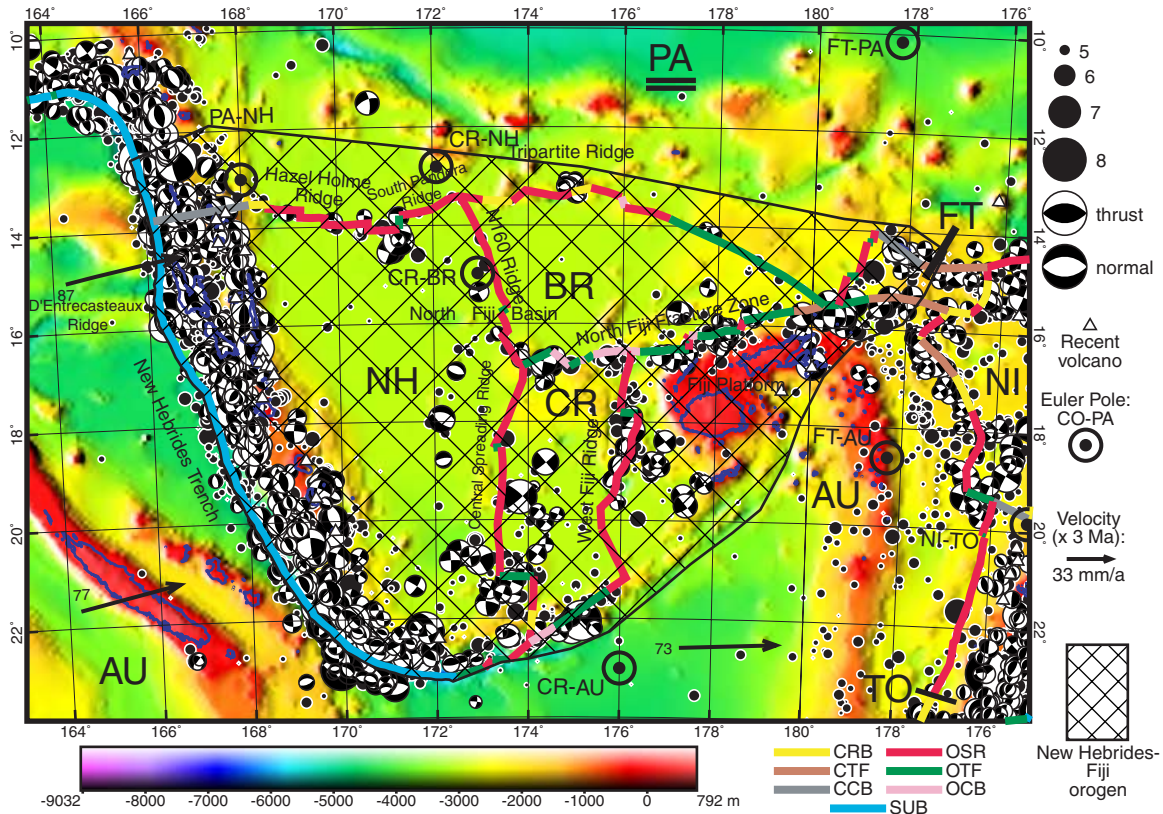


Figure 10. Boundaries (heavy colored lines) of the New Hebrides (NH), Balmoral Reef (BR), Conway Reef (CR), and Futuna (FT) plates. All are included in the New Hebrides-Fiji orogen because of evidence that they may be deforming rapidly. Surrounding plates are Australia (AU), Tonga (TO), Niuafo'ou (NI), and Pacific (PA). Conventions as in Figure 2, except coastlines are blue. Oblique Mercator projection on great circle passing E-W through (17°S, 174°E).

locally being indented by the D'Entrecasteaux Ridge, although neither trench nor arc morphology shows this indentation clearly. Finally, earthquakes in the Harvard CMT catalog, seen in Figure 10, suggest that the southeast corner of this plate may be fractured by two or more sinistral faults trending WSW-ENE. Another suggestion of such complications is that the spreading rate on the southernmost segment of the Central Spreading Ridge is only 50 mm/a, compared with 80 mm/a in the longest central segment [Pelletier *et al.*, 1998].

[69] The Conway Reef plate (CR) corresponds roughly to “block A” of Chase [1971]. It lies between two spreading centers [Auzende *et al.*, 1994, 1995a, 1995b; Pelletier *et al.*, 1998]: the Central Spreading Ridge on the west (border with NH), and the West Fiji Ridge on the east (border with the Fiji Platform, usually interpreted as a

northeast projection of AU). Because spreading rates on the Central Spreading Ridge increase southward from 50 to 80 mm/a, while spreading rates on the West Fiji Ridge decrease southward from 50 to 20 mm/a [Auzende *et al.*, 1994, 1995a, 1995b; Pelletier *et al.*, 1998], this CR plate is rotating counterclockwise with respect to all of its neighbors. Its northern boundary with BR is the North Fiji Fracture Zone, and its southern boundary with AU is a belt of large sinistral earthquakes on trend with the termination of the New Hebrides Trench. These constraints suggest a CR-AU Euler pole of approximately (23°S, 176°E, 4.4°/Ma). Adding AU-PA relative rotation from NUVEL-1A, the CR-PA pole would be approximately (13°S, 175°E, 3.6°/Ma).

[70] The Balmoral Reef plate (BR) corresponds roughly to “block P” of Chase [1971]. It is spreading away from PA at the Tripartite Ridge

at rates of 15 mm/a [Lagabrielle *et al.*, 1996; Pelletier *et al.*, 1998; Schellart *et al.*, 2002] on its northern margin. It also spreads away from NH at the N160° Ridge at rates which appear to increase southward to 40–50 mm/a [Auzende *et al.*, 1995a] or perhaps less [Pelletier *et al.*, 1998]. It has sinistral transform and pull-apart basin boundaries with CR and AU along the North Fiji Fracture Zone. Using the AU-PA velocity (83 mm/a toward 087°) from NUVEL-1A, and the 086° trend of transform segments in the NFFZ [Auzende *et al.*, 1995a], I constructed a velocity vector diagram for BR-NH-CR-AU-PA, which shows that these constraints are incompatible. The Tripartite Ridge spreading rate is in direct conflict with North Fiji Fracture Zone azimuth and AU-PA velocity from NUVEL-1A (under the assumption that the Fiji Platform is part of AU). I believe a more realistic estimate should take into account the many magnitude-6+ earthquakes within the CR and northeastern AU “plates”, all of which have strike-slip mechanisms showing N-S shortening and E-W extension. If these regions are shortening in the N-S direction by 16 mm/a, then the permitted southward component of BR-PA motion can be increased by the same amount. Furthermore, if there is 16 mm/a of distributed E-W extension within CR and the Fiji Platform (to balance the N-S shortening in a strike-slip regime), then the E-W velocity component of NH-PA should be 16 mm/a more westward than estimated above. This relaxation of rigid plate assumptions allows a solution in which BR-PA velocity is 22 mm/a toward 132°, and the PA-NH Euler pole is adjusted to (13°S, 168°E, 2.7°/Ma), which is just at the western termination of the Hazel Holme Ridge.

[71] The Futuna plate (FT) is a discovery of Pelletier *et al.* [2001], who describe the 200-km-long Futuna Ridge spreading center which trends North and runs in en-echelon fashion from the northeast corner of the Fiji Platform to a point northwest of the Îles de Horne (Fortuna and Alofi islands). They estimated its spreading rate very roughly as 30–60 mm/a. Regardless of whether the lithosphere west of Futuna Ridge is part of PA (as interpreted here) or part of BR, the lithosphere east of Futuna Ridge is moving rapidly eastward with

respect to PA. It might even be a northward projection of AU (eastward velocity 86 mm/a with respect to PA) if the Futuna Ridge is the eastern boundary of BR. However, an E-W alignment (with convexity to the North, and gradual rotation of nodal planes) of sinistral strike-slip earthquakes from the Harvard CMT catalog appears to separate FT from AU; I interpret this as small-circle transform boundary indicating that the FT-AU Euler pole is approximately (18.6°S, 178.3°W, 5.6°/Ma). The northeast boundary of the FT plate is probably at the southwestern slope of the uplifted crustal block which supports the Îles de Horne; here there is a concentration of thrusting and sinistral earthquake mechanisms which suggest an oblique convergent boundary.

[72] In addition to the local problems described above, there are some general reasons to doubt that this four-plate model is definitive, or that it meets the standards of precise velocity prediction (within 8 mm/a) attempted in other parts of this global model. (1) Many spreading rates have been determined solely from anomaly 1 (or J); therefore, the redundancy typical of marine magnetics is lacking, and the chances of error are increased. (This may be the only part of the world where marine magnetics researchers quote spreading rates to the nearest cm/a rather than the nearest mm/a.) (2) All authors agree that interpretation of magnetics and topography in this region is difficult, and many postulate multiple tectonic stages since 12 Ma (e.g., 4 stages according to Pelletier *et al.* [1993]). Alternately, this should be viewed as evidence that the data do not have the internal consistency or redundancy that is expected where plates are (approximately) rigid. (3) Many earthquakes in the Harvard CMT catalog do not lie on the proposed plate boundaries (Figure 10). Some of these are as large as moment magnitude 7.1 (2000.02.25), and therefore exceed the empirical corner magnitude for oceanic transform earthquakes at these relative velocities [Bird *et al.*, 2002], suggesting that some of these large earthquakes may represent new fractures rather than sliding on established plate boundaries.

[73] For all these reasons, I overlay this set of 4 small plates with the additional designation of a

“New Hebrides-Fiji orogen” (Figure 10). This signifies both low precision of the plate model, and also suspected internal deformation of some “plates” on the order of 16 mm/a (exceeding the 8 mm/a threshold).

5.13. Tonga Plate (TO), Kermadec Plate (KE), and Niufo’ou Plate (NI)

[74] Back-arc spreading in the Lau-Havre trough to the west of the Tonga-Kermadec volcanic arc was first recognized by *Karig* [1970]. *Pelletier and Louat* [1989] referred to the region between the Tonga-Kermadec trench and this back-arc spreading center as the “Tonga-Kermadec plate” (even though it may be deforming) in recognition of the fact that its velocity is significantly different from that of either adjacent plate, Australia or Pacific. Recently, the region between the Australia and Pacific plates was divided into at least two small plates, Niufo’ou (NI) and Tonga (TO), by *Zellmer and Taylor* [2001]. They compiled high-resolution bathymetry and magnetics, seismicity, and geodesy and used these to demonstrate an active Fonualei Rift and Spreading Center between NI and TO (Figure 11).

[75] Of the various solutions presented by *Zellmer and Taylor* [2001], I use solution 2b, which incorporates geodetic velocities and seismic slip vectors as well as seafloor magnetics and bathymetry, and satisfies a local closure requirement. I have digitized the AU-NI and NI-TO plate boundaries north of 24°S from their Figure 6. The TO-PA boundary is the Tonga trench, which at its north end bends westward and makes a gradual transition to a transform boundary [*Wright et al.*, 1986].

[76] The south end of the NI plate is at about 19–20°S, and the TO plate is then in contact with AU across the East Lau spreading center. Further to the south, back-arc spreading continues in the Havre trough, the Whakatane graben [*Lamarche et al.*, 2000], and into the Taupo volcanic zone on North Island of New Zealand. The AU-TO pole of *Zellmer and Taylor* [2001] is not compatible with this spreading, and so (as they note) an additional small plate is required. I call this the Kermadec (KE) plate, after the island chain along its center.

The extension direction in the onshore Taupo volcanic zone in North Island, New Zealand was measured geodetically by *Darby and Meertens* [1995] as $124 \pm 13^\circ$. Extension decreases to the south across North Island, until near Wellington the main tectonic activity is right-lateral slip on arc-parallel faults. This suggests that the AU-KE pole lies very close, and slightly west of the southernmost extensional zone in North Island. I have estimated it very roughly as (40°S, 175°E). The southern boundary of the KE plate is unclear, but probably lies beneath Cook Strait, since it is known to be a region of discontinuity between the faults of North Island and those of South Island. The KE-PA boundary is the Hikurangi-Kermadec trench.

[77] The two problems left unresolved are the location of the KE-TO boundary (which is probably short) and the relative rotation rate for the AU-KE pole. I assume that the KE-TO boundary is located in the complex deformed region at 23–25°S which overlies the subducting aseismic Louisville Ridge on the Pacific plate [*Pelletier et al.*, 1998]. *Wright* [1993] concludes that the Havre Trough is rifting, not spreading, so that the extension cannot yet be measured directly using linear magnetic anomalies. My suggested rate of 1.8°/Ma for the AU-KE pole is based solely on the geodetically measured spreading rate in North Island of 8 ± 4 mm/a [*Darby and Meertens*, 1995]; it is highly uncertain both because of the geodetic uncertainty and because of the unfortunate “leverage” when the rate is measured so close to the inferred pole. (AU-KE spreading rates at the north end of the KE plate would be expected to be about 7 times as large, or 56 ± 28 mm/a.) Additional GPS data from the Kermadec Islands would be very useful to improve this estimate.

5.14. Rivera Plate (RI)

[78] The Rivera plate is the region east of the East Pacific Rise (or Pacific-Rivera Rise), north of the Rivera transform fault, and southwest of the Middle America trench. *DeMets and Traylen* [2000] made a new magnetic-anomaly map of the region from 1400 crossing points, and computed Rivera

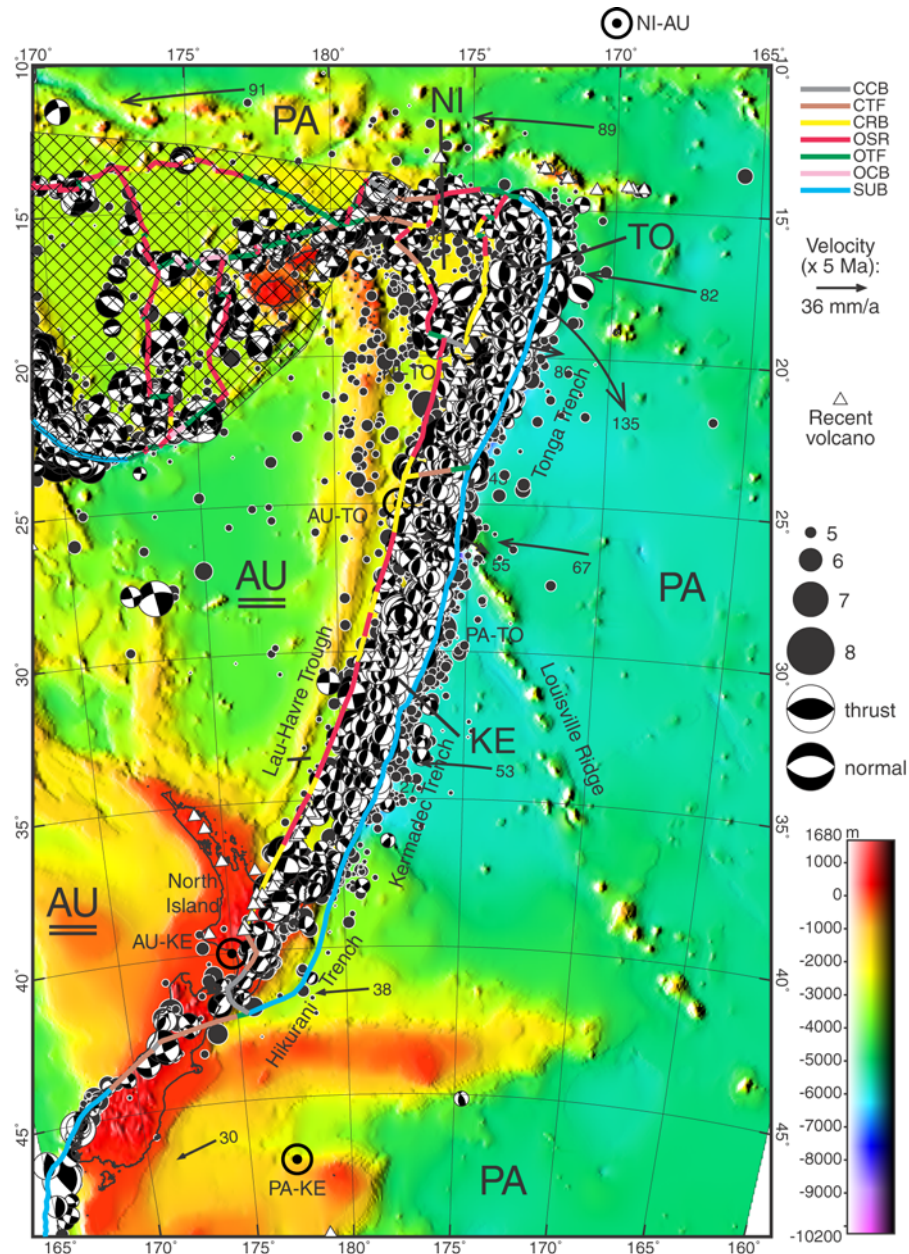


Figure 11. Boundaries (heavy colored lines) of the Tonga plate (TO), Kermadec plate (KE), and Niufo’ou plate (NI). Surrounding large plates are Australia (AU) and Pacific (PA). Cross-hatched region is the New Hebrides-Fiji orogen (see Figure 10). Conventions as in Figure 2. Transverse Mercator projection on meridian 177.5°W.

plate motion and strain using 14 PA-RI finite rotations since 9.9 Ma. The Euler pole which I show in Table 1 is obtained by dividing their chron-1 finite rotation by its age of 0.78 Ma. The same study clarifies that the Rivera transform fault is currently the southern limit of the plate, although there was a period between 7.2 and 2.2 Ma when the southern part of the plate was deforming. In the north, however, they confirm the results of *Lons-*

dale [1995] and *DeMets and Wilson* [1997] that the former northernmost part of the RI plate has transferred and bonded to NA since about 3.6–1.5 Ma. Therefore, I have digitized the present RI-NA plate boundary (Figure 12) from Figure 7 of *DeMets and Wilson* [1997]. In the east, the RI-CO boundary is clearly sinistral, but its exact location is unclear [*DeMets and Wilson*, 1997]; I have digitized this boundary from the most seismic lineament in their

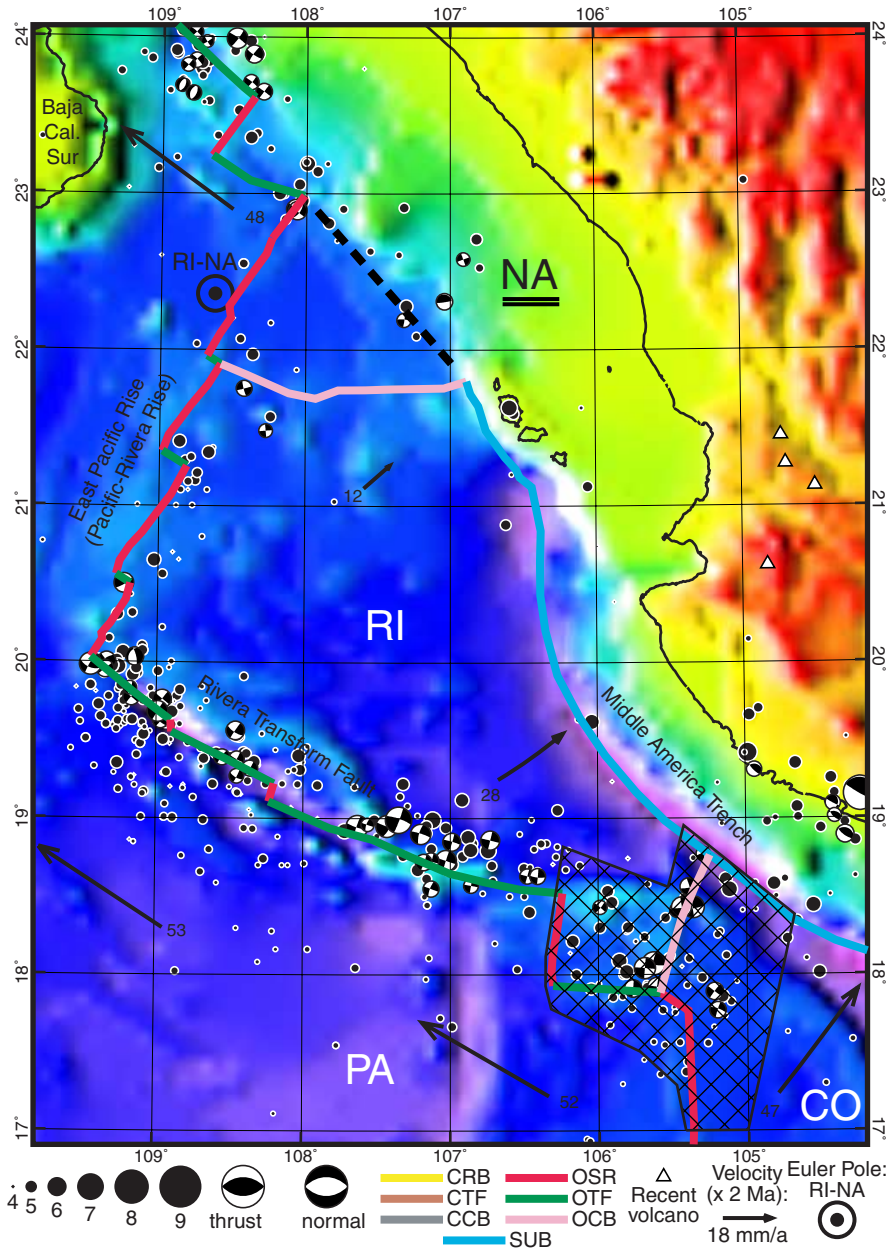


Figure 12. Boundaries (heavy colored lines) of the Rivera (RI) plate, surrounded by North America (NA), Pacific (PA), and Cocos (CO) plates. Cross-hatched area is the Rivera-Cocos orogen. Dashed black line shows former RI-NA boundary. Other conventions as in Figure 2. At the large scale of this map, errors in hypocenter and centroid locations are not negligible.

Figure 8, and then overlay a “Rivera-Cocos orogen” based on their Figure 9.

5.15. “Microplates” on the East Pacific Rise: Galapagos (GP), Easter (EA), Juan Fernandez (JZ)

[79] The term “microplate” has not been precisely defined, but in practice is used most often for a

plate of ~100–500 km dimensions which appears spontaneously in the center of an ocean spreading system, and rotates rapidly with respect to its neighboring plates. Their recognition is relatively recent because it follows on the concepts of propagating rifts and non-transform offsets. *Schouten et al.* [1993] gave one possible idealized model of microplate kinematics.

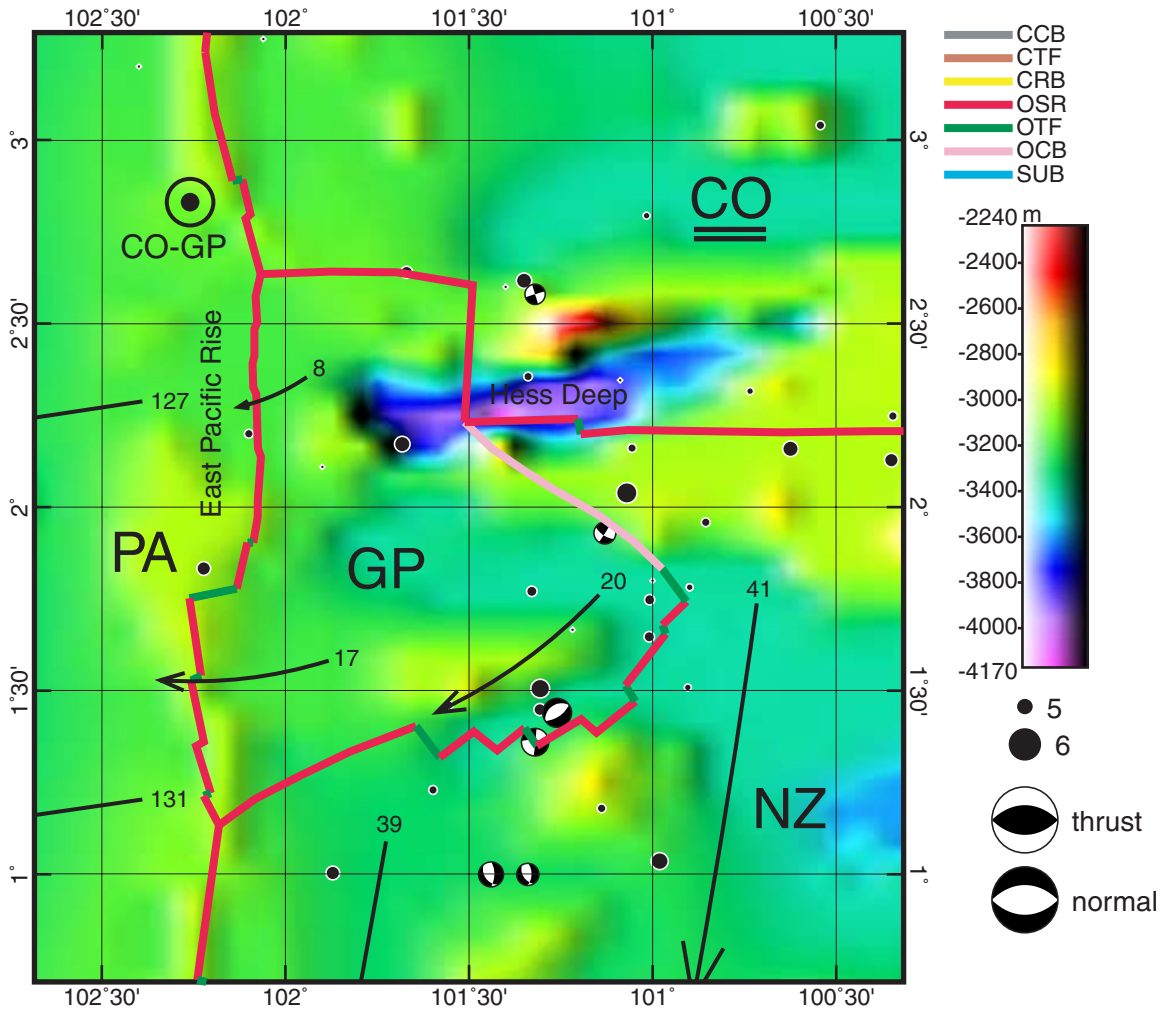


Figure 13. Boundaries (heavy colored lines) of the Galapagos (GP) plate, surrounded by Pacific (PA), Cocos (CO), and Nazca (NZ) plates. Conventions as in Figure 2. At the large scale of this map, errors in hypocenter and centroid locations are not negligible, and the limited resolution of topographic model ETOPO5 is apparent. High-resolution bathymetry may be seen in *Lonsdale* [1988].

[80] *Lonsdale* [1988] discovered a microplate of ~ 120 km width at 2°N on the East Pacific Rise, in the region that had been previously expected to hold a triple junction between the Pacific (PA), Cocos (CO), and Nazca (NZ) plates (Figure 13). Following a long-standing but unfortunate tradition in marine geology, he named it “Galapagos” (GP) for the nearest land (although the Galapagos Islands are about 1100 km to the east). He mapped the regional bathymetry with high-resolution Sea-Beam and Deep Tow equipment and outlined the boundaries of GP on this basis; there are also a few (imprecise) teleseismic determinations of epicenters which lend support to the model. Assuming that spreading is orthogonal and symmetrical, he

developed velocity triangles for the triple junctions, and used these to estimate an Euler pole of (2.5°N , 99°W , $6^\circ/\text{Ma}$) for NZ-GP. *Lonsdale et al.* [1992] conducted a second survey to complete the GP-CO boundary, by mapping a young spreading ridge which forms a RRR triple-junction (CO-PA-GP) at $2^\circ 40'\text{N}$. *Schouten et al.* [1993] reinterpreted the kinematics by requiring the Euler poles for GP with respect to its neighbors to lie on the boundaries of GP, but as this was an idealized model I have not adopted their suggested poles.

[81] The Easter plate is a small (550×410 km) oceanic plate lying in a bifurcation of the East Pacific Rise at $22\text{--}27^\circ\text{S}$ between PA to the west

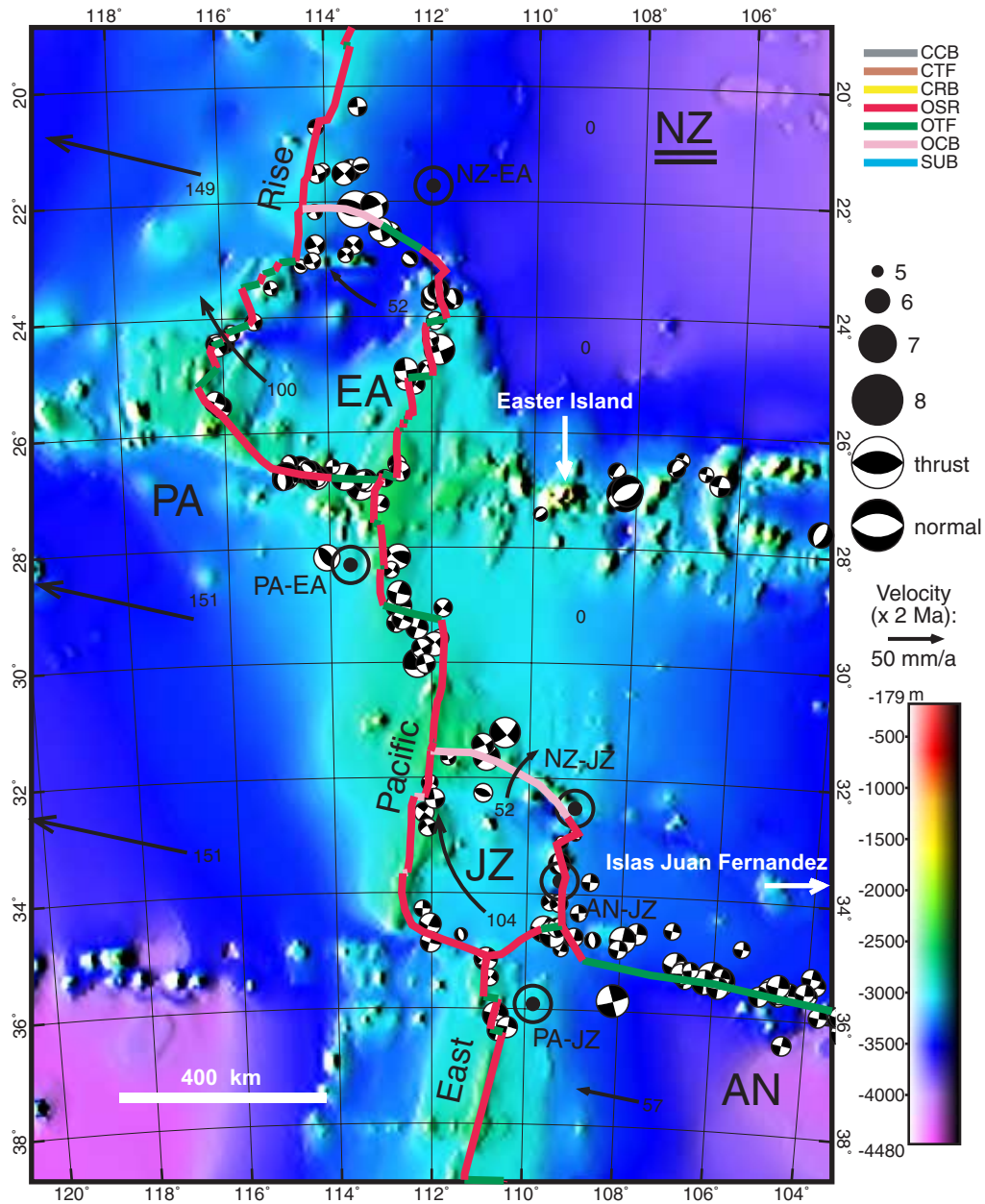


Figure 14. Plate boundaries (heavy colored lines) of the Easter (EA) and Juan Fernandez (JZ) plates. Surrounding plates are Pacific (PA), Antarctica (AN), and Nazca (NZ). Conventions as in Figure 2. Transverse Mercator projection on meridian 112°W.

and NZ to the east (Figure 14). (It was named for, but does not include, Easter Island, which is now located in the Nazca plate.) The plate was proposed by *Herron* [1972] based on magnetic anomalies and seismicity, and also by *Forsyth* [1972] based on divergent slip vectors. *Engeln and Stein* [1984] used seismicity, slip vectors, bathymetry, and magnetic anomalies to define most boundaries of this plate and to determine its Euler poles with respect

to adjacent plates. I adopt the pole solution which they based on all spreading rates and slip vectors (but without making an assumption of orthogonal spreading). *Naar and Hey* [1991] surveyed the Easter plate region with high-resolution sonar (SeaBeam and SeaMARC), revised its boundaries, and reconstructed its evolution. Although they found kinematic problems in the past which require some plate deformation, they observe that currently

the majority of the plate is behaving as a rigid body. I take the plate boundaries shown in Figure 14 from their Figure 3.

[82] The Juan Fernandez plate is another small (410×270 km) oceanic plate lying in a bifurcation of the East Pacific Rise at $32\text{--}35^\circ\text{S}$, bordered by PA to the west, NZ to the northeast, and Antarctica plate (AN) to the southeast. Its existence was also proposed independently by *Herron* [1972] and *Forsyth* [1972]. The name (based on islands 2800 km to the east) was proposed by *Craig et al.* [1983] who mapped the bathymetry of the eastern and western spreading ridges. *Anderson-Fontana et al.* [1986] combined bathymetry, magnetic anomalies, seismicity, and slip vectors to outline the plate and define its Euler vectors with respect to neighboring plates. I adopt their solution which used all slip vectors and spreading rates based on magnetic anomaly 2, and determined the NZ-JZ pole as (32.51°S , 109.05°W , $22.49^\circ/\text{Ma}$). The JZ-PA pole shown in Table 1 is then slightly different from the one quoted by *Anderson-Fontana et al.* [1986] because the newer NZ-PA pole of NUVEL-1A is slightly different from theirs. *Larson et al.* [1992] collected magnetic profiles and high-resolution sonar images (GLORIA and Hydrosweep) of the plate and slightly revised its boundaries; I digitized the plate boundaries shown in Figure 14 from their Figure 1.

[83] *Larson et al.* [1992] and *Searle et al.* [1993] compared the kinematics of each of these microplates to an idealized “roller bearing” model (with at least two Euler poles located on the microplate boundary, at the tips of propagating rifts) and claimed a good match in all cases, implying that internal deformation of these plates has been small. However, in Table 1 I give preference to the data-based Euler poles that were cited above.

[84] *Hey et al.* [1995] and *Martinez et al.* [1997] studied the part of the East Pacific Rise between the Easter and Juan Fernandez plates, where they interpret cyclical contrary propagation and failure of two overlapping spreading centers (OSCs) at $28.5^\circ\text{--}29.5^\circ\text{S}$, without formation of an additional microplate. The present model PB2002 cannot represent this level of detail, because (1) it involves

locally nonrigid behavior, and (2) OSCs of small size may be found within larger OSCs [*Martinez et al.*, 1997], suggesting possible nested levels of complexity. In this case, as in others, the non-transform offset is represented in the plate-boundary curves of PB2002 by an idealized equivalent transform in the same general location.

5.16. Panama Plate (PM) and North Andes Plate (ND)

[85] The easternmost part of Central America (Costa Rica and Panama) is bracketed between the sinuous E-W-trending North Panama deformed belt and the South Panama deformed belt (both primarily offshore, and both seismically active). *Kellogg et al.* [1985] referred to this region as the “Panama block” and inferred that it is moving northward relative to the Caribbean plate (CA) and eastward relative to the South America plate (SA). To the east, in Columbia, Ecuador and Venezuela, the northernmost segment of the Andes is divided into a Western Cordillera and an Eastern Cordillera (including the Merida Andes), both of which are seismically active. *Kellogg et al.* [1985] referred to this wedge as the “North Andes block” and inferred from geologic and seismicity data that it moves about 10 mm/a toward 055° with respect to SA, or about $17\text{--}19$ mm/a northwestward with respect to CA. A different block-kinematic model was presented by *Dewey and Pindell* [1985], based on estimated displacements since 9 Ma. In this model the “Cordillera Central block” moved about 275 km northeastward with respect to SA, while the “Maracaibo block” moved even further northward due to 105 km of sinistral slip on the Santa Marta-Bucaramanga fault. However, such block models were rather fragile with respect to small changes in assumptions, as shown by the revision of *Dewey and Pindell* [1986]: the motion of the Cordillera Central block was changed to 150 km ESE with respect to South America (almost orthogonal to the previous model).

[86] A very important new source of constraining data in the region is the Central And South America (CASA) geodetic study, which has involved benchmarks in 5 countries and on offshore islands representing the Cocos (CO), Nazca (NZ) and CA

plates. Some have been occupied since 1988 [e.g., *Frey Mueller et al.*, 1993; *Kellogg et al.*, 1995, 1996; *Trenkamp et al.*, 1996]. This project has quantified the relative velocities of the Panama plate (PA) and North Andes plate (ND), basically confirming the concepts of *Kellogg et al.* [1985]. Meanwhile, the proposal that ND (and/or the Maracaibo block) converges with CA has been confirmed by the discovery of a high-seismic-velocity slab of subducted Caribbean lithosphere which dips 17° toward 150° down to a depth of 275 km [*van der Hilst and Mann*, 1994]. *Perez et al.* [1997] studied the Benioff zone of seismicity within this slab, and showed that it terminates eastward near Curacao-Aruba. This discovery of subduction proves that CA does not extend (on the surface) south of the South Caribbean deformed belt.

[87] The southern boundary of PM is complex because it changes character eastward from sinistral subduction to sinistral strike-slip. The thrust front in 83°W – 80.5°W (including the CO-NZ-PM triple-junction at the Panama Fracture Zone) has been mapped by *Moore and Sender* [1995]. From 80°W – 78.8°W the main plate boundary appears to be the sinistral South Panama fault zone [*Westbrook et al.*, 1995]. A relay of faults (Rio Flores and Azuero-Soná) provides a connection in the middle zone [*Kolarsky and Mann*, 1995]. (Of course, if the situation is one of strain partitioning it may be an oversimplification to select a single plate boundary fault at each longitude.) The collisional boundary between PM and ND is near the Panama-Colombia border, and has been described by *Mann and Kolarsky* [1995]; I select the Pirre thrust as the principal strand (because it is associated with a small patch of earthquakes deeper than 70 km), although other thrusts which share the shortening occur up to 100 km east and west. On the north side of PM, the subduction boundary with CA is the frontal thrust of the North Panama deformed belt [*Kellogg and Vega*, 1995; *Mann and Kolarsky*, 1995], which is interpreted as crossing western Costa Rica on a westward trend to meet the Middle America Trench in a CA-CO-PM triple junction. The motion of PM is best defined with respect to Isla San Andres on CA; it is northward at 11 mm/a without apparent relative

rotation [*Kellogg and Vega*, 1995]. Therefore I estimate the PM-CA pole very roughly as lying 90° away: (172°W , 0°N , $0.10^\circ/\text{Ma}$).

[88] Beginning in the south, the boundary between the North Andes plate (ND) and SA is the Dolores Guayaquil megathrust [*Collet et al.*, 2002] which is apparently reactivated in an oblique dextral-normal sense. To the northeast, it follows the East Andean Frontal fault system along the Eastern Cordillera to the Merida Andes. This fault system is zone of partitioned slip [*Audemard and Audemard*, 2002] on subparallel and/or en-echelon dextral and thrust faults, including the Pallafanga, Algecira, Gualcaramo, Yopal, and Bocono faults [*Taboada et al.*, 2000; *Audemard and Audemard*, 2002]. Based on the extent of the subducted CA slab, *Perez et al.* [1997] have interpreted the present CA-ND-SA triple-junction as lying at the intersection of the Bocano fault (ND-SA), San Sebastian-El Pilar fault (CA-SA), and an unnamed but seismically active dextral fault trending NW (ND-CA). (This would explain why the former Leeward Antilles subduction zone is now seismically quiescent east of Curacao.) The northern boundary of ND is the subduction zone, discussed previously, in which it overthrusts CA; this extends westward to the Gulf of Darien where the CA-PM-ND triple junction is located. As defined here, the ND plate includes the Maracaibo block, and the southwest and north boundaries of that block (Santa Marta-Bucaramanga and Oca-Ancon faults, respectively) are not considered plate boundaries. I suggest that these conjugate strike-slip faults may be secondary faults of lesser slip which formed in response to the confining left step of the ND-SA boundary where the Eastern Cordillera meets the Merida Andes. (If Maracaibo were to be separated from ND as a separate plate, then the region of the Bonaire block to the north of Maracaibo would necessarily become an additional plate as well.) Geodetic results from the CASA project [*Trenkamp et al.*, 1996] have defined the motion of ND with respect to SA as including a 7–8 mm/a dextral component and a 4–5 mm/a compressive component on their common boundary (implying resultant 9 mm/a toward 076°). This is broadly consistent with geologic estimates from the Merida Andes [*Audemard*

and Audemard, 2002] where post-Late Miocene dextral and shortening strains are comparable. I assume no relative rotation of ND with respect to SA and estimate their Euler pole very roughly as (179°W , 75°N , $0.08^{\circ}/\text{Ma}$).

5.17. Altiplano (AP) Plate and Two Adjacent Orogens

[89] Shallow seismicity ($z < 70$ km, $m > 4.4$) from the ISC and CMT catalogs divides into two belts in the latitudes between 3°S (south end of the ND plate) and 35°S . (South of 35°S , there is relatively uncomplicated subduction of NZ or AN beneath SA.) The western belt of seismicity lies over the trench and continental slope and is clearly associated with subduction. The eastern belt generally follows the eastern slope of the Andes, occasionally spreading into the pampas. This double seismicity belt is too broad (up to 900 km) to be described as a simple subduction zone, but alternatively could be described by some combination of small plates and orogens. Here I consider a probable “Altiplano plate” (AP; Figure 15), flanked on both North and South by orogens.

[90] In the last decade, velocities in the central Andes have been measured using GPS geodesy by at least 3 groups: South America-Nazca Plate Project (SNAPP) [Norabuena *et al.*, 1998], Central Andes GPS Project (CAP) [Kendrick *et al.*, 1999; Bevis *et al.*, 1999, 2001], and South American Geodynamic Activities (SAGA) [Klotz *et al.*, 1999]. The latitude range of good coverage of the central Andes only extends from 12°S to 28°S . The SNAPP campaign had stations well placed to test the concept and determine the motion of any Altiplano plate. However, there are several serious difficulties in using these velocities directly as estimates of plate velocity: uncertainty about the South American reference frame [Bevis *et al.*, 1999], overprinting of slow plate movements by sudden earthquake displacements [Klotz *et al.*, 1999], and elastic smoothing of velocities over decadal timescales which might be plate-like on geologic timescales [Norabuena *et al.*, 1998; Liu *et al.*, 2000].

[91] Norabuena *et al.* [1998] saw no sign of sudden earthquake displacements in their data, and modeled it taking elastic smoothing into account; they found that in their south segment the shortening velocity in the eastern Andes (including, but not limited to the AP-SA boundary) is about 12 ± 4 mm/a. Then, Bevis *et al.* [1999] suggested that their SA reference frame might be faulty by as much as 9 mm/a, and that convergence is less. But they independently found convergence of 9 mm/a between two of the CAP stations in the southern AP plate and South America.

[92] Lamb [2000] performed more sophisticated modeling of geodetic data, by comparing and then combining it with geologic strains and paleomagnetic rotations in multiple inversions for regional strain rates and velocities. He found no major discrepancies between data sets, and concluded that neither elastic strain accumulation nor the possible reference-frame bias in SNAPP data is a serious problem. In the area of the proposed AP plate, he found low strain rates (e.g., $1\%/ \text{Ma}$) that contrast with much higher strain rates (e.g., $18\%/ \text{Ma}$) in the eastern thrust belt along the proposed AP-SA boundary. I use the velocities at 8 internal (southwestern) nodes from his combined inversion (experiment 3) to define the AP-SA pole by least squares as (2°S , 77°W , $0.4^{\circ}/\text{Ma}$). The velocity of the AP block with respect to South America averages about 15 mm/a toward $\text{N}59^{\circ}\text{E}$.

[93] Two recent reviews of geodetic data by Bevis *et al.* [2001] and Kendrick *et al.* [2001] confirm the concept of an Altiplano plate extending from the Peru-Chile trench to the eastern thrust belt, whose internal strains are probably elastic and related to the subduction earthquake cycle on the NZ\AP boundary; however, they favor a lower AP-SA rate of about 7 mm/a.

[94] There are a number of compelling reasons to designate the parts of the Andes north and south of AP as orogens: (1) If these flanking regions were rigid parts of SA, then there would necessarily be transform or transtensional boundaries between AP and SA to both the northwest and south of AP; but, no sign of such boundaries is seen in the seismicity or geology. (2) If AP were moving east with

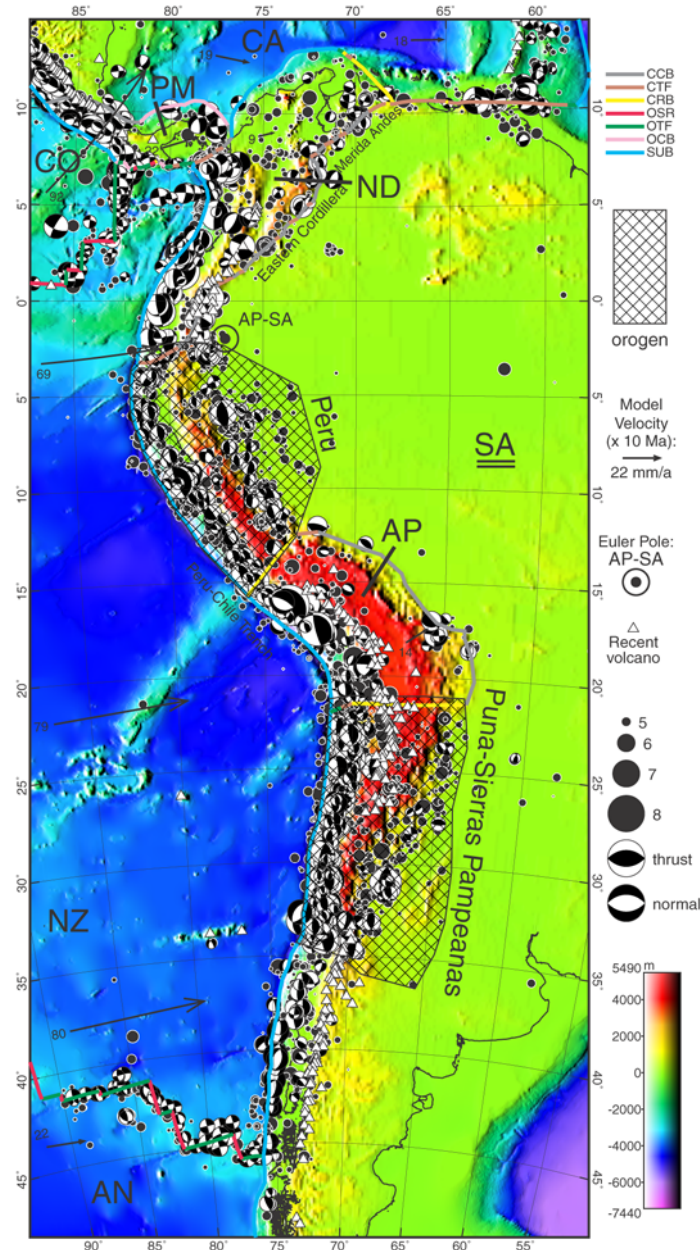


Figure 15. Boundaries (heavy colored lines) of the Panama (PM), North Andes (ND), and Altiplano (AP) plates. Surrounding plates are Antarctica (AN), South America (SA), Caribbean (CA), Cocos (CO), and Nazca (NZ). Cross-hatched areas are the Peru and Puna-Sierras Pampeanas orogens. Conventions as in Figure 2. Transverse Mercator projection on meridian 72.5°W.

respect to SA but adjacent parts of SA were rigid, then the Peru-Chile trench should develop two kinks or tear-fault offsets, but this has not occurred. Apparently the velocity of the central Andes with respect to SA has no major discontinuities as a function of latitude. (3) As mentioned, the seismicity in these flanking regions extends too far inland to be described by normal subduction pro-

cesses. (4) These flanking regions are sites of near-horizontal subduction of Nazca plate [Gutscher *et al.*, 2000], which has eliminated the asthenospheric wedge normally found above subducted slabs and shut off these portions of the Andean volcanic arc. Horizontal subduction is associated with strong horizontal compressive stress in the overriding plate and distributed orogeny, even as much as

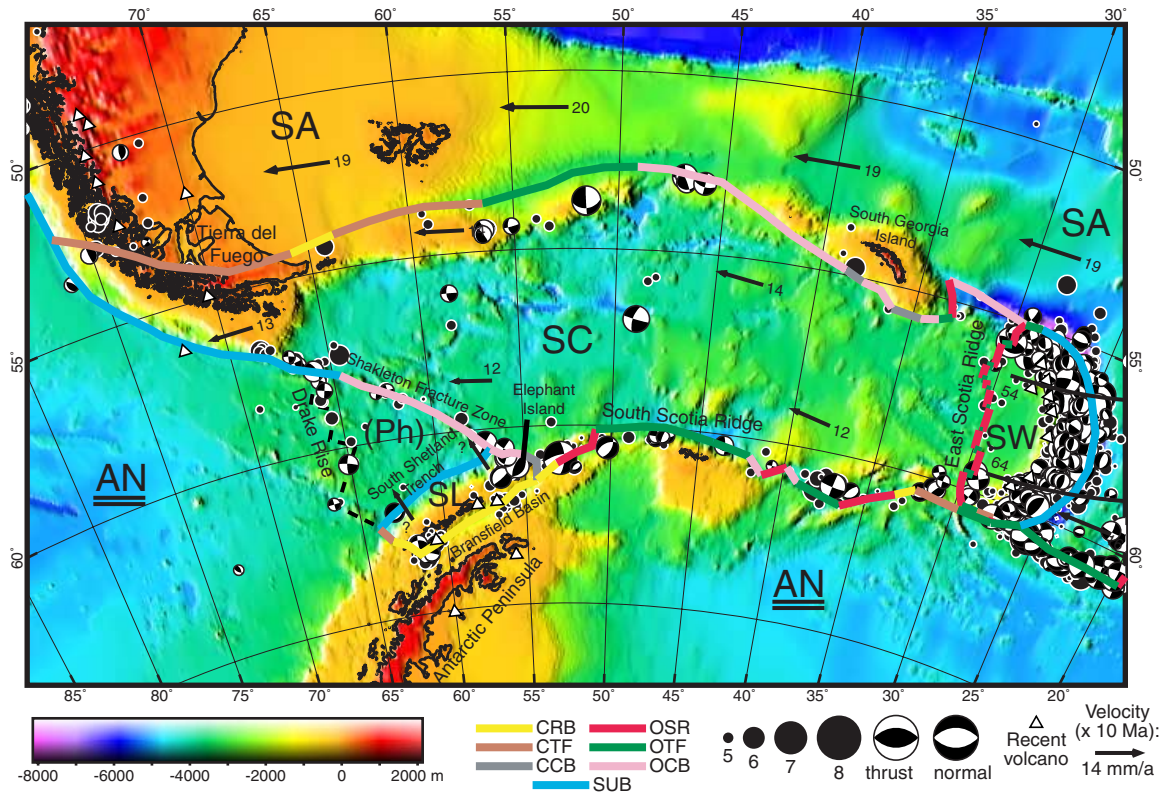


Figure 16. Boundaries (heavy colored lines) of the Shetland (SL), Scotia (SC), and Sandwich (SW) plates. Surrounding plates are Antarctica (AN) and South America (SA). The former Phoenix plate [(Ph); dashed black line] has now merged with AN. Other conventions as in Figure 2. Oblique Mercator projection with great circle passing E-W through (52°W, 58°S).

1600 km from the trench. This is well established by an actualistic example in the Sierras Pampeanas [Allmendinger *et al.*, 1983] and a late Cretaceous-early Tertiary example in North America [Bird, 1988, 1998]. Therefore, I have designated a “Peru orogen” to the north of AP and a “Puna-Sierras Pampeanas orogen” to the south (Figure 15).

5.18. Shetland Plate (SL), Scotia Plate (SC), and Sandwich Plate (SW)

[95] There is an extensive literature about the complex region lying between the South America (SA) and Antarctica (AN) plates, and it will not be possible to review it all here. This part of model PB2002 (Figure 16) is mainly taken from the work of Pelayo and Wiens [1989], who relocated earthquakes and determined focal mechanisms and used them to solve for Euler vectors of two of these three small plates.

[96] Prior to 4 Ma, there was also a small Phoenix (or Drake) oceanic plate lying between Tierra del Fuego and the Antarctic Peninsula [Pelayo and Wiens, 1989; Klepeis and Lawver, 1996]. It spread southeastward with respect to the oceanic part of the Antarctica plate at the Drake Rise (or Aulk Ridge) and also subducted southeastward beneath the continental part of the Antarctica plate at the South Shetland Trench. Back-arc spreading developed in the Bransfield Basin southeast of the South Shetland Islands volcanic arc, causing a small Shetland (SL) plate to separate from AN. When the Phoenix plate later became welded to the Antarctica plate along the Drake Rise and Hero Fracture Zone, the Shetland plate apparently continued to move slowly northwestward with respect to the surrounding Antarctica plate [Barker and Dalziel, 1983]. Lawver *et al.* [1996] described bathymetric evidence for continued dike intrusion and normal faulting in the Bransfield Basin.

[97] Recently, *Gonzalez-Casado et al.* [2000] documented two neotectonic fault trends (both SW-NE and NW-SE) and a mixture of normal and reverse slip senses in the South Shetland Islands arc, and used these to argue that the South Shetland Trench is permanently locked. However, they did not invalidate the previous seismic evidence of *Pelayo and Wiens* [1989], who located approximately 34 moderate ($5 < m_b < 6.5$) earthquakes with predominantly dip-slip mechanisms which they attribute to continued activity of the South Shetland outer rise, South Shetland Trench, and Bransfield Basin extensional zone. Also, there are three active volcanoes in the South Shetland arc. My interpretation is that the observations of *Gonzalez-Casado et al.* can also be explained by a model in which the trench remains active, but intermittently locks and unlocks during seismic cycles, causing temporal reversals of stress sense in some parts of the adjacent island arc.

[98] In the two editions of the Plate Tectonic Map of the Circum-Pacific Region [*Circum-Pacific Mapping Project*, 1981, 1986] the Shetland Islands arc is shown as a westward projection of the larger Scotia plate. (In the earlier edition, this implies a hypothetical spreading center west of Elephant Island. In the later edition, the South Scotia Ridge fault is drawn with greater curvature to eliminate the need for this.) However, there are a number of earthquakes in the region of intersection between the Shackleton fracture zone and the South Scotia Ridge which cast doubt on the stability of this possible region of connection. Also, *Klepeis and Lawver* [1996] argue for the formation of a new dextral transpressive fault linking the South Scotia Ridge and Shackleton fracture zone, which would sever any previous connection between the Shetland and Scotia plates. Therefore, Shetland is presently a distinct plate; unfortunately, its motion is very poorly constrained. So that the correct sense of motion may be seen in plots derived from this model, I have assigned a nominal SL-PA pole (in Table 1) which is derived by assuming a SL-AN pole at 90° distance along the long axis of the SL plate (at 174°W , 13°S), with SL-AN relative velocity of 10 mm/a. However, neither location nor rate is based on quantitative data.

[99] The mid-sized Scotia plate (SC) largely coincides with the Scotia Sea, and is bounded by SA on the north and AN on the south and west (except, locally, by SL). To the east, the small Sandwich (SW) plate is a volcanic arc/forearc block separated from SC by the East Scotia Ridge spreading center, and separated from SA by the South Sandwich Trench. I digitized the shape of the East Scotia Ridge from Figure 2 of *Livermore et al.* [1997] and Figure 1 of *Leat et al.* [2000].

[100] *Pelayo and Wiens* [1989] inverted seismic slip vectors from the whole region and spreading rates from the East Scotia Ridge [*Barker*, 1972; *Barker and Hill*, 1981], using known SA-AN motion from NUVEL-1 as a constraint, to obtain Euler poles for SC and SW with respect to neighboring plates. I adopt these Euler poles; specifically, I use the better-constrained SC-AN pole to determine the SC-PA pole in Table 1.

[101] Because of the small scales and distorted projections of most published plate maps in this region, I digitized all plate boundaries in the region relative to the digital bathymetric data set ETOPO5 [*Anonymous*, 1988], using published sources [*Pelayo and Wiens*, 1989; *Klepeis*, 1994; *Klepeis and Lawver*, 1996; *Maldonado et al.*, 1998] as general guidance to indicate which topographic lineaments are active plate boundaries. I interpret the SA-SC boundary as passing south of South Georgia Island because there is higher seismicity there, including a magnitude 5.9 event (1965.09.26, ISC catalog), because I interpret the steep submarine slope east of the island as a detachment fault surface, and because extensional faulting is more mechanically plausible than thrusting in the vicinity of the extensional SC-SW spreading center.

5.19. Aegean Sea Plate (AS) and Anatolia Plate (AT)

[102] The recognition of discrete plates between Africa and Eurasia began with the wide-ranging study of *McKenzie* [1972], who combined historical and instrumental seismicity, focal mechanisms, geology, and topography to propose that Anatolia is extruded westward to escape the collision of Arabia with Eurasia. He also proposed a separate

Aegean block which travels southwestward with respect to Eurasia, diverging from the Anatolia plate and overriding the Africa plate at the Aegean Trench. (This arcuate depression, lying south of Crete, is also known in different regions as the Hellenic Trough, Strabo Trough, Trough of Rhodes, and Pliny Trench.) *Jackson* [1992] and *Westaway* [1994] supported and developed the model by showing that the major faults in the region have estimated slip rates which are compatible with rigid-plate kinematics.

[103] When GPS geodesy became available, it was a high priority to test McKenzie's model, and a very extensive literature developed. The predicted westward motion and counterclockwise rotation of Anatolia were quickly apparent. Based on preliminary results, some [e.g., *Le Pichon et al.*, 1995; *Reilinger et al.*, 1997] were inclined to simplify the model by merging the Aegean Sea and Anatolia plates into one (but allowing some internal deformation); but others [e.g., *Papazachos*, 1998] maintained that the motions of the Aegean Sea and Anatolia are distinct.

[104] A very valuable summary of 10 years of GPS results from 189 stations in the region was published by a consortium of 28 authors writing as *McClusky et al.* [2000]. This compilation clearly shows that geodesy agrees with historical seismicity in defining two regions of low strain rate outlined by belts of deformation: an Aegean Sea plate, and an Anatolia plate (Figure 17). These authors derived Euler vectors for AT-EU (30.7°N, 32.6°E, 1.2°/Ma) and AT-AS (38.0°N, 19.6°E, 1.2°/Ma); I have adopted their solutions and converted the AT and AS rotation rates to the Pacific-plate reference frame for Table 1. The selection of plate boundaries is straightforward in the north and east (North Anatolian fault and East Anatolian fault).

[105] In the south, it is unclear whether the subduction plate boundaries (AS/AF and AT/AF) should be drawn at the Aegean Trench, or south of the Mediterranean Ridge. *Masche et al.* [1999] described the Mediterranean Ridge as a complex region of many folds, faults, and mud diapirs with low overall relief, and suggested that it should be considered a part of the European accretionary

prism (that is, belonging to the AS and AT plates, rather than to AF). I do not accept this interpretation, for several reasons: (1) No other subduction forearc in the world is 500 km wide; 200–250 km is more typical, and this is the distance from the Aegean volcanoes to the Aegean Trench. (2) Most forearcs maintain a consistent (or at least monotonic) slope down from the coast to the trench; it would be exceptional for a forearc to include a trench. (3) Seismicity decreases by an order of magnitude going southward across the Aegean Trench. The events under the Mediterranean Rise are mostly of strike-slip or normal character (according to the CMT catalog), and the only two events which have thrust mechanisms show NW-SE shortening, which is orthogonal to the expected plate convergence. Instead, I interpret the Mediterranean Ridge as a flexural outer rise created in the Africa plate as it approaches the subduction zone at the Aegean Trench. The flexure and tilting of this lithosphere has disrupted sedimentary layers which include weak evaporites, and the result has been complex but shallow-rooted gravity tectonics.

[106] The western and eastern boundaries of the Aegean Sea plate present additional difficulties, because topography, geology, and seismicity all indicate activity of multiple en-echelon grabens. This is not rigid-plate behavior (except perhaps at a very fine scale), so I have drawn very approximate boundaries through the centers of the apparent regions of maximum strain rate, and then designated these boundary regions as extensions of the Alps orogen.

5.20. Somalia Plate (SO)

[107] The East Africa rift appears to be a slowly spreading plate boundary, based on topography, seismicity, and volcanism (Figure 18). *McKenzie et al.* [1970] were probably the first to use the name "Somalian plate" and computed net AF-SO separation since 20 Ma to be up to 65 km in the NW-SE direction. However, some global inversion studies of plate motions [*Minster and Jordan*, 1978; *DeMets et al.*, 1990] considered this possible boundary and rejected it because the inferred motion was unreasonable (i.e., convergent, or right-lateral, respectively). *Jestin et al.* [1994] re-

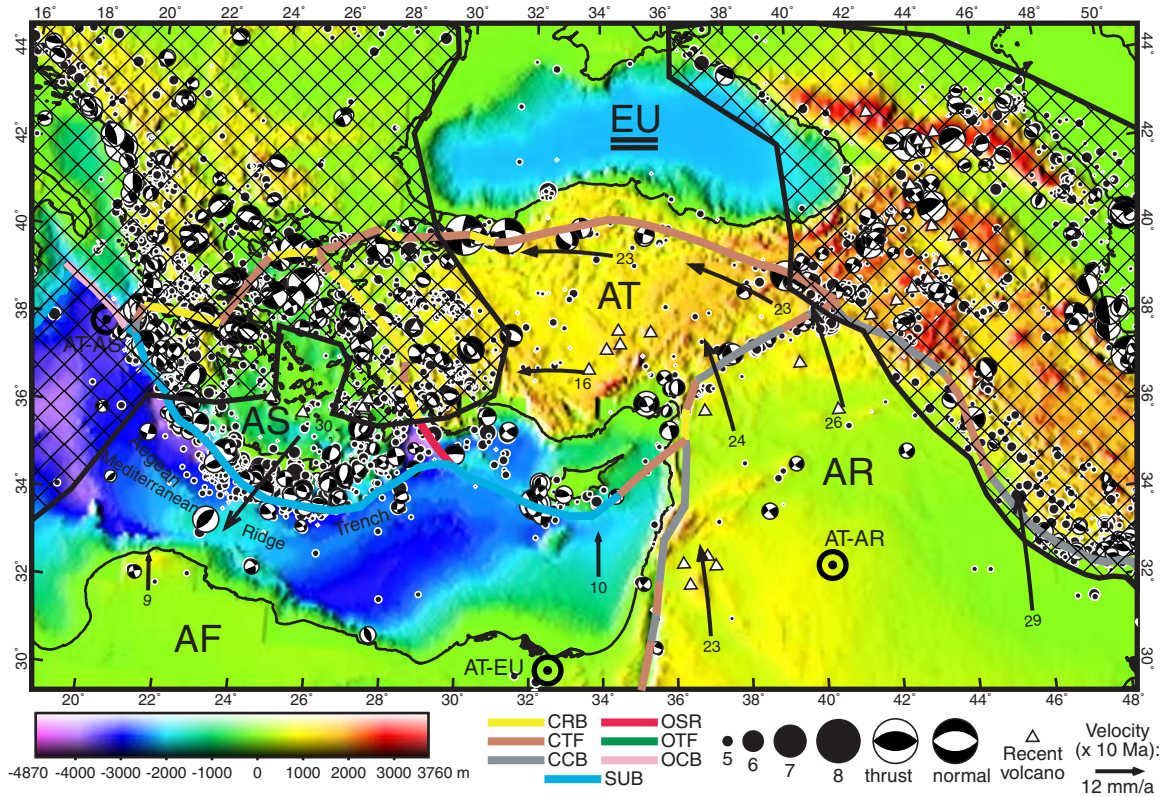


Figure 17. Boundaries (heavy colored lines) of the Aegean Sea (AS) and Anatolia (AT) plates, which are surrounded by the Africa (AF), Arabia (AR), and Eurasia (EU) plates. The two cross-hatched regions are the Alps and Persia-Tibet-Burma orogens in the west and east, respectively. Conventions as in Figure 2. Oblique Mercator projection with great circle passing E-W through (33.5°E, 38°N).

visited the problem, added additional data, and conducted the inversion using an L1 norm (least absolute value of errors) instead of an L2 norm (least squared errors). They found that incorporation of a Somalia plate (SO) lying east of the East Africa rift improves the fit to data, and located Euler poles by Monte Carlo methods. *Chu and Gordon* [1999] added additional data on Southwest Indian Ridge spreading rates and azimuths since chron 2A, and found that SO and AF motions are distinct with high confidence. Their chron 2A pole for AF-SO (which they refer to as Nubia-Somalia) is (27.3°S, 36.2°E, 0.089°/Ma), which implies separation at 6 mm/a at the north end of the AF-SO boundary, and neotectonic compression at 1–2 mm/a at the southern end of the boundary.

[108] The geometry of the AR-SO-IN triple junction was recently revised by *Fournier et al.* [2001], which I incorporate. In defining the AF-SO boundary, the first challenge is to choose between the

west and east branches of the East Africa rift system. (Future studies supported by new geodetic data may define an additional Victoria plate between them, but *Jestin et al.* [1994] were not able to constrain its motion in trial solutions.) I have drawn the boundary along the western rift (Malawi and Tanganyika rifts) because of its higher seismicity in the ISC and CMT catalogs. The connection to the Southwest Indian Ridge was studied by both *Chu and Gordon* [1999] and *Lemaux et al.* [2002]. The former study offered a choice of discrete or diffuse boundary models; the latter study showed that AF-SO deformation has been strongly concentrated at or near the Andrew Bain Fracture Zone since 11 Ma.

5.21. Capricorn Plate?

[109] It has been known at least since *DeMets et al.* [1994] that there are fast and significant relative motions between the India plate and the Australia

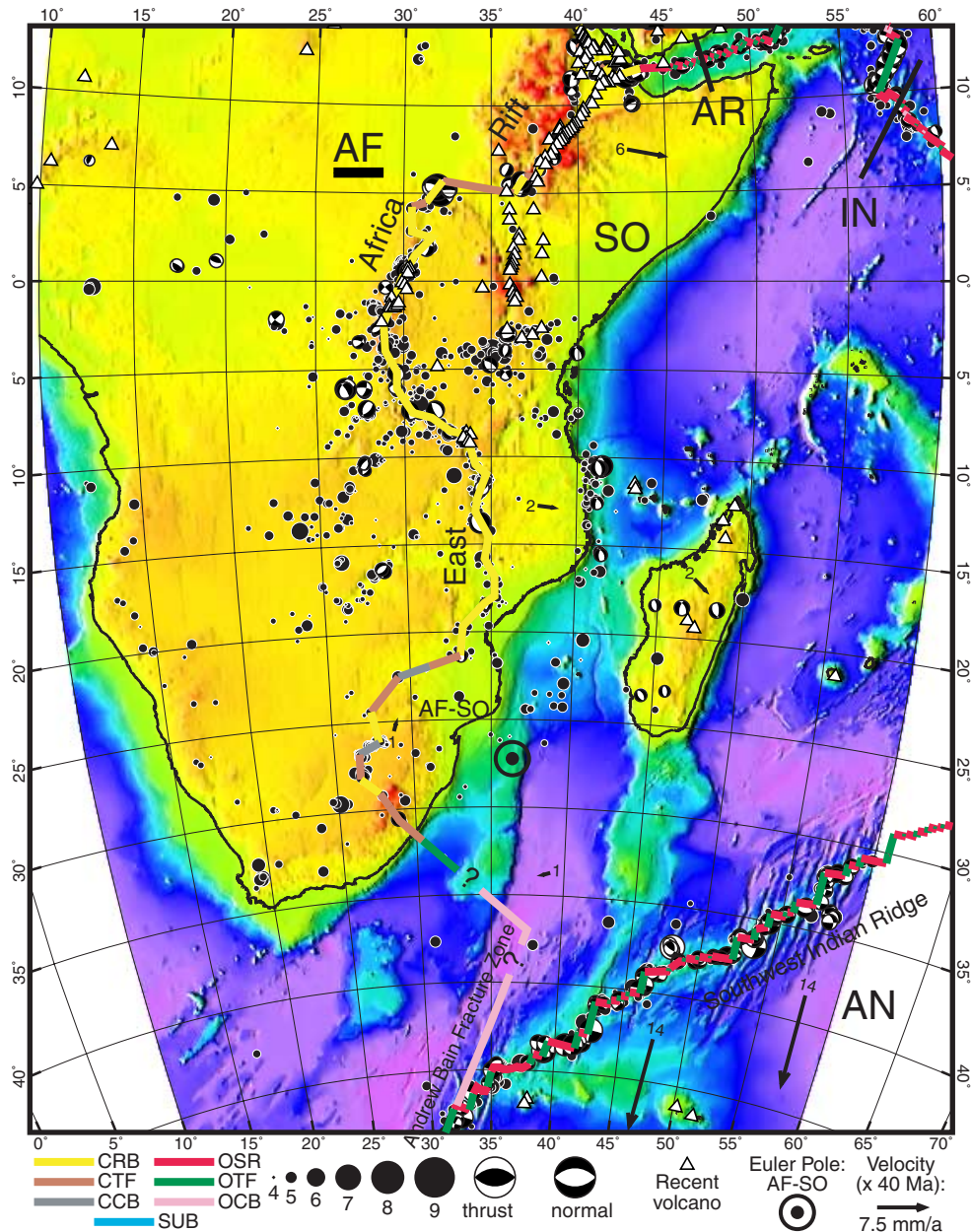


Figure 18. Western boundaries (heavy colored lines) of the Somalia (SO) plate, surrounded by Africa (AF), Antarctica (AN), India (IN), and Arabia (AR). Conventions as in Figure 2. Southernmost part of AF-SO boundary is from *Lemaux et al.* [2002], but portions in 22°–42°S are conjectural. Transverse Mercator projection on meridian 35°E.

plate (which had once been considered to be a single Indo-Australian plate). Because the present model PB2002 is built on the framework of NUVEL-1A, that division has been incorporated. In addition, *Royer and Gordon* [1997] have shown, with high confidence, that the Australia plate (AU) is not rigid. To describe its deformation, they propose an additional Capricorn plate, and a dif-

fuse plate boundary (Capricorn-Australia), across which there is a relative rotation, such that Capricorn and AU diverge by 1.2 ± 2.2 mm/a (95%-confidence limits) in the southwest part of their boundary, and converge by 2.1 ± 2.4 mm/a in the northeast part of their boundary. While accepting their calculations, I have not incorporated a Capricorn plate in PB2002 because: (1) The relative

velocities stated above do not differ from zero with 95% confidence. (2) Even at their upper limits, the relative velocities still fall below the thresholds used in this paper (2–8 mm/a, depending on context) for internal relative velocities which require recognition (either by new plate boundaries, or by an orogen). (3) Because there are no islands on the proposed Capricorn plate, there is little chance that new geodetic results will become available to define the relative motion more precisely. (4) Because the entire proposed Capricorn-AU boundary is diffuse, the model of a separate Capricorn plate cannot be tested by geologic study of any individual fault, or by teleseismic study of any individual earthquake. That is, the model has modest predictive power outside the realm of the marine magnetic and regional seismicity data sets that were used to create it.

6. Topology

[110] Euler’s formula for a solid bounded by polygons is: $faces + vertices = edges + 2$. (All italicized words represent integer counts.) I propose a conjecture: a similar formula appears to describe global plate models on planets that have at least one junction between plate boundaries: $plates + junctions = boundaries + 2$. If all the junctions are triple-junctions, and if there are no isolated “island” plates whose boundaries close on themselves, then an additional constraint is: $junctions = (2/3) boundaries$, which can be justified by the observation that each plate has an equal number of boundaries and junctions around its perimeter, but each boundary is shared by two plates while each junction is shared by three plates. For such a planet, $junctions = 2 \times (plates - 2)$, and $boundaries = 3 \times (plates - 2)$.

[111] Model PB2002 has 52 plates, each with a unique two-letter identifier (Figure 1, Table 1). Together they exactly cover the Earth, with no gaps or overlaps. There are 100 triple-junction points. Each of these triple-junctions can be uniquely identified by listing the 3 plates in counterclockwise order, beginning with the plate whose identifier has alphabetical priority (example: “AF-EU-NA” for the Africa-Eurasia-North America

triple junction near the Azores). There are no quadruple or higher-order junctions in this model.

[112] A plate boundary is a continuous simply-connected curve on the surface of the Earth which everywhere separates the same two different plates, and either (1) begins at a junction and ends at a junction, or (2) closes on itself in an isolated loop. There are 150 plate boundaries in model PB2002, and all are of type 1. Although some plate boundaries can be identified by specifying the pair of plates involved, such identifiers are ambiguous in other cases. (There are 2 AN-SA boundaries, 2 AN-SC, 2 AU-PA, 2 NA-PA, 2 NB-SB, 2 NZ-PA, 2 NZ-SA, 2 PA-PS, and 2 SC-AN boundaries.) The largest plates naturally have the most neighbors: Pacific 23; Australia 18; Eurasia 11; Antarctica 10. At the other extreme, 6 small plates have only 2 neighbors each (Manus, Juan de Fuca, Altiplano, Mariana, Easter, Shetland). The Shetland plate comes closest to being an “island” plate (type 2) because it is almost surrounded by the Antarctica plate, but it also has a short boundary with the Scotia plate.

[113] The 13 “orogens” are represented by simply-connected closed outline curves. They should be considered as an overlay layer, because they enclose areas already defined as parts of plates, and their presence does not affect plate topology. Their purpose is to give warning of probable non-rigid behavior and horizontal velocities significantly different from those that would be computed from Euler poles. Even if distributed deformation only occurs on one side of a plate boundary, the relative velocities predicted along that boundary from Euler poles will be incorrect (typically, too high). To make this explicit, the orogens defined here intentionally overlap adjacent plate boundaries by a nominal amount (about 10 km).

7. Cumulative-Number/Area Distribution

[114] The increase in the number of plates from previous models RM2, NUVEL-1, and PB1999 to the present model PB2002 (from 14 to 52) begs the question [e.g., Anderson, 2002], how many more small plates remain to be defined in the future? There are certain to be some, as precision of geo-

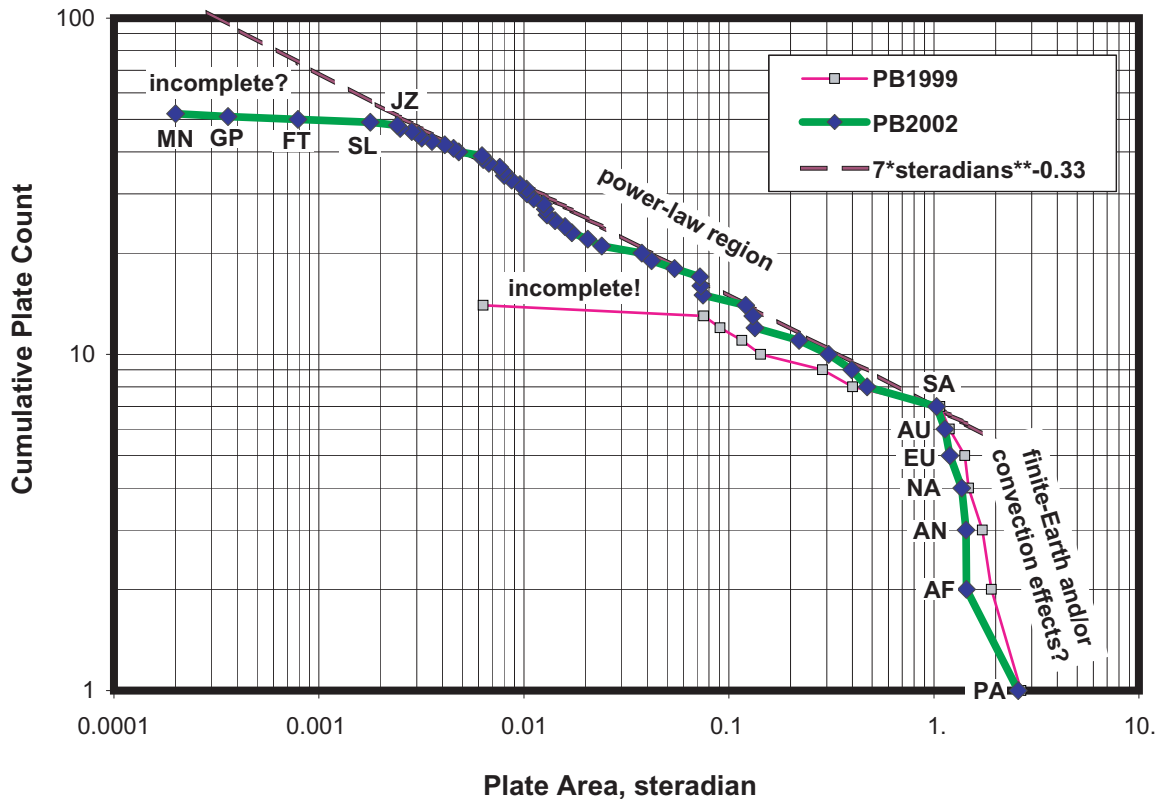


Figure 19. Number of plates exceeding a given area, plotted as a function of area. Curve PB2002 is for the present model, and curve PB1999 is for the previous 14-plate model of *Bird et al.* [2002]. The relatively steady slope of the PB2002 curve for plate areas between 0.002 and 1 steradian suggests a power law relationship between the number of plates and their minimum size. Just as flattening of the PB1999 curve was an artifact of model incompleteness, flattening of the PB2002 curve at 0.002 probably indicates that there are many more small plates below this size not recognized in the model. Very large plates are limited in their area because of the finite area of the Earth, and perhaps also by mantle convection tractions.

detic velocities will increase, earthquake catalogs will get longer, and geologic and paleoseismological knowledge will accumulate. Philosophically, it is interesting to speculate whether the plates would even be countable, if we had access to perfect knowledge of the Earth?

[115] As one approach to an answer, I have computed the areas of the plates in PB2002, sorted them in order of area, and created a cumulative-number vs. area diagram (Figure 19). When plotted with logarithmic scales, this shows that plates of areas between 0.002 and 1 steradian (from JZ to SA) occur in numbers that roughly obey a power law: (cumulative count) $\cong 7$ (steradians)^{-1/3}.

[116] The flattening of the PB1999 distribution at 0.07 steradian (size of CO) is now seen to be an

artifact of incompleteness of that model. In a similar way, the flattening of the PB2002 curve at 0.002 steradian (size of SL) probably indicates incompleteness of the present model for plates smaller than SL. If the same power law were to apply for all smaller sizes, then hypothetically there would be about 100 plates larger than 0.00032 steradian (13,000 km² or 114 × 114 km). The total area needed to define another 48 plates ranging from this size up to the size of JZ (where model PB2002 appears to become complete) would be only about 0.039 steradian (about the size of EA), which could be taken from large plates like EU and NA without materially affecting their areas. The places where additional very small plates are most likely to be recognized is within the “orogens” defined here, which have total area of 0.937 steradian (compara-

ble to SA; 7.5% of Earth). For example, *Avouac and Tapponnier* [1993] proposed small Tibet and Tarim plates within the “Persia-Tibet-Burma orogen” of this paper. On a finer scale, *Bird and Rosenstock* [1984] suggested 22 very small plates within the southern California part of the “Gorda-California-Nevada orogen” of this paper.

[117] Given this strong suggestion that plates may be “fractal” in some loose sense, it may be important to develop more precise definitions in the future about what ratio of relative boundary velocities to internal deformation velocities is needed to qualify a region as a “plate,” and whether this minimum ratio should be a function of plate size. It might also be prudent to communicate this evolving understanding to students in elementary Earth science classes, rather than asking them to memorize a list of plate names which is potentially unbounded.

[118] Plates larger than 1 steradian (size of SA) are much less common than they would be under an extrapolation of the same power law. Mathematically this must be the case because the total area of all plates is fixed at 4π steradian. The physical reason why there is a soft limit at the size of AF (with one exception: PA) may be that mantle convection exerts significant tractions on larger plates that tend to break them up. The plate width at which this soft limit occurs is about one Earth radius, and this may give a clue to the planform of convective cells in the mantle and their interaction with plates. For example, this characteristic size seems more consistent with whole mantle convection than with layered convection which does not cross the transition zone.

8. Digital Data Formats

[119] Plate boundary curves and the curves which outline orogens are approximated by sequences of discrete points. The intention is that adjacent points should be connected by short arcs of great circles. However, since no arc between adjacent points is longer than 111 km (1°), it will not cause significant additional error if maps derived from this data set show the points as connected by straight lines, regardless of the map projection.

[120] Each point is given as a (longitude, latitude) pair, with coordinates in units of decimal degrees. Latitude is positive in the northern hemisphere and negative in the southern hemisphere. Longitude is generally positive to the east of the Greenwich meridian, and negative to the west, but some points in the western hemisphere are represented with positive longitudes in the range $180\text{--}360^\circ\text{E}$. All coordinates are given with 6 significant digits, so that round-off error in positions does not exceed ± 60 m; however, accuracy never equals precision.

[121] In most of the digital files presenting model PB2002, sequences of points are grouped into “segments”, whose ends are indicated by a marker record, “*** end of line segment ***”. Preceding the list of sequential points is a title record for the segment; in these records, the essential information is contained in the first 2–8 bytes, and notations following byte 27 (if any) are to give attribution to the source of the information or opinion.

[122] File PB2002_boundaries.dig contains the plate boundary curves in the most compact form, and should be used to add plate boundaries to maps. (Digital files are available as auxiliary material in the HTML version of this article.) It contains 6,048 points grouped into 229 segments. The title record for each segment has 5 bytes, in which the first two bytes give the identifier of the plate on the left (as one travels along the segment, looking down from outside the Earth) and bytes 4–5 give the identifier of the plate on the right. In byte 3, the symbol “/” indicates that the right-hand plate subducts under the left-hand plate, while symbol “\” indicates the opposite polarity of subduction. All non-subducting plate boundary segments have a hyphen “-” in byte 3. The number of segments exceeds the number of plate boundaries for several reasons: (1) because a single plate boundary may include both subduction and non-subduction segments, which require different titles; (2) because different parts of a single plate boundary may be credited to different sources; (3) for convenience in digitizing long plate boundaries which did not fit onto a single map.

[123] For some applications it is necessary to represent plates by closed outlines. They include

Table 2. Data for Each Plate Boundary Step in File PB2002_steps.dat

Bytes	Contain (all fields are right-justified)
1–4	Sequence number (for tying to seismic catalogs).
6	Continuity? “:” appears if this step connects to previous step, in same segment.
7–11	Plate-boundary identifier (from PB2002_boundaries.dig; example: “AF-AN”).
13–20	Longitude of initial point, degrees East, with precision 0.001°.
22–28	Latitude of initial point, degrees North, with precision 0.001°.
30–37	Longitude of final point, degrees East, with precision 0.001°.
39–45	Latitude of final point, degrees North, with precision 0.001°.
47–51	Length of step, km, with precision 0.1 km
53–55	Azimuth of step at center point, degrees clockwise from North, with precision 1°.
57–61	Velocity of left plate with respect to right plate, mm/a, precision 0.1 mm/a.
63–65	Azimuth of velocity (above), degrees clockwise from North, precision 1°.
67–72	Divergent component of relative velocity (convergence negative), pr. 0.1 mm/a.
74–79	Right-lateral component of relative velocity, mm/a, precision 0.1 mm/a.
81–86	Elevation (bathymetry negative), from ETOPO5, m, precision 1 m.
88–90	Age of seafloor, from <i>Mueller et al.</i> (1997), Ma, precision 1 Ma. >180 = unknown.
92	Continuity? “:” appears if step class = class of previous step <i>and</i> “:” is in byte 6.
93–95	Step class: CCB, CTF, CRB, OSR, OTF, OCB, or SUB (see text).
96	Orogen? “*” appears if midpoint of step lies in any orogen.

computing the areas of plates, determining which plate a given point lies within, and mapping plates as regions of contrasting color. For such applications, file PB2002_plates.dig is provided. It contains 52 segments, each titled with the two-letter identifier of a plate. Each segment is a closed curve outlining that plate in the counterclockwise direction (as seen from outside the Earth). The last point in the segment is identical to the first point. Because each plate boundary necessarily appears twice in this file, it is about twice as large as the first.

[124] File PB2002_orogens.dig contains 13 segments which give the outlines of the orogens. Each outline is digitized in the counterclockwise direction, as seen from outside the Earth. The format is the same as in the file above, except that orogens are given spelled-out names (e.g., “Alps”, “Persia-Tibet-Burma”) to help prevent confusion between orogens and plates.

[125] For studies of seismicity and geochemical cycles it is useful to know how much plate boundary is of spreading, transform, or subduction class, and how fast these boundaries slip. But a single class cannot always be specified for an entire plate boundary curve, or even for an entire plate boundary segment, because the class may change repeatedly with local changes in the azimuth of the

boundary. A similar problem arises with computed relative velocities, which change smoothly in both magnitude and azimuth along every boundary. Therefore, file PB2002_steps.dat presents detailed information for each “digitization step”. (A digitization step is the short great circle arc between adjacent digitized plate boundary points.) There are 5,819 steps in model PB2002, with mean length of 44.7 km and length range from 1 km to 109 km. Table 2 details the information which is computed at the midpoint of every step.

[126] The 7 classes of plate boundary step contained in this file are defined as follows. Subduction zones (SUB) are plate boundary steps with a convergent (component of) velocity and a Benioff zone of intermediate to deep earthquakes and/or a parallel volcanic arc with Quaternary activity. (These criteria exclude the Alps, Zagros, Pamirs, Himalaya, Tien Shan, and Taiwan.) The designation of Benioff zones and/or volcanic arcs with the title symbols “/” or “\” was manual, with the intention that small gaps in a Benioff zone or volcanic arc should not cause unrealistic high-frequency changes in the interpreted step character. Because so many subduction zones lie along continental margins, or contain thickened arc crust which may be considered to have some “continental” character, subduction zones are not divided into continental and oceanic types.

Table 3. Collective Properties of Plate Boundaries by Class

Class	Total Length, km	Mean Velocity, mm/a	Area production, m ² /s
Continental Convergent Boundary	23,003 (8.8%)	26.2	-0.013616 (-12.6%)
Continental Transform Fault	26,132 (10.0%)	24.7	-0.000599 (-0.5%)
Continental Rift Boundary	27,472 (10.5%)	17.6	+0.011502 (+10.7%)
Oceanic Spreading Ridge	67,338 (25.8%)	46.6	+0.095348 (+88.4%)
Oceanic Transform Fault	47,783 (18.3%)	40.5	+0.001022 (+1.0%)
Oceanic Convergent Boundary	17,449 (6.7%)	17.6	-0.007141 (-6.7%)
Subduction Zone	51,310 (19.7%)	62.3	-0.086516 (-80.1%)
Totals	260,487 (100%)	39.6	0.10787 - 0.10787 = 0

[127] Other plate boundaries are classified into one of 6 types according to whether they are oceanic or continental, and whether their relative velocity is divergent, strike-slip, or convergent. Oceanic plate boundary steps are those lying entirely: (1) within seafloor whose age is known from linear magnetic anomalies to be less than 180 Ma [Mueller *et al.*, 1997]; and/or (2) at water depths exceeding 2000 m (ETOPO5 [Anonymous, 1988]). Continental plate boundary steps are any that are not oceanic. (Thus, transitional steps are considered continental.) Boundary steps are considered strike-slip if the computed relative velocity (based on the Euler poles of Table 1) has an azimuth within $\pm 20^\circ$ of the azimuth of the plate boundary step. (This tolerance is intended to allow for random local errors in plate boundary azimuth, as well as systematic errors in model velocity azimuth caused by errors in Euler pole positions.) Combining these two tests yields the 6 non-subduction types: oceanic spreading ridge (OSR), oceanic transform fault (OTF), oceanic convergent boundary (OCB), continental rift boundary (CRB), continental transform fault (CTF), and continental convergent boundary (CCB). Table 3 gives summary statistics concerning the 7 classes. The plate boundaries shown in the figures of this paper are color-coded in a consistent way according to these 7 classes: CCB, gray; CTF, brown; CRB, yellow; OSR, red; OTF, green; OCB, magenta; SUB, blue.

[128] One notable result is that the ratio of Earth's surface area ($5.10 \times 10^{14} \text{ m}^2$) to the total rate of lithosphere creation ($0.10787 \text{ m}^2/\text{s}$) is a scale time of only 150 Ma. The overall rate of lithosphere creation and destruction is larger than in previous plate models because of the recognition of back-arc

spreading in the vicinity of many subduction zones.

Acknowledgments

[129] A constructive and extremely detailed review by Brian Taylor contributed greatly to this model. Research was supported by the U.S. Geological Survey (USGS), Department of the Interior, under USGS award number 01HQGR0021. The views and conclusions contained in this document are those of the author and should not be interpreted as necessarily representing the official policies, either express or implied, of the U.S. Government.

References

- Allmendinger, R. W., V. A. Ramos, T. E. Jordan, M. Palma, and B. L. Isacks, Paleogeography and Andean structural geometry, northwest Argentina, *Tectonics*, 2, 1–16, 1983.
- Anderson, D. L., How many plates?, *Geology*, 30, 411–414, 2002.
- Anderson, R. N., Heat flow in the Mariana marginal basin, *J. Geophys. Res.*, 80, 4043–4048, 1975.
- Anderson-Fontana, S., J. F. Engeln, P. Lundgren, R. L. Larson, and S. Stein, Tectonics and evolution of the Juan Fernandez microplate at the Pacific-Nazca-Antarctic plate junction, *J. Geophys. Res.*, 91, 2005–2018, 1986.
- Anonymous, Digital Relief of the Earth, *Data Announcement* [CD-ROM], 88-MGG-02, Natl. Geophys. Data Cent., Boulder, Colo., 1988.
- Argus, D. F., and R. G. Gordon, No-net-rotation model of current plate velocities incorporating plate motion model NUVEL-1, *Geophys. Res. Lett.*, 18, 2039–2042, 1991.
- Audemard, F. E., and F. A. Audemard, Structure of the Merida Andes, Venezuela: Relations with the South America-Caribbean geodynamic interaction, *Tectonophysics*, 345, 299–327, 2002.
- Auzende, J.-M., B. Pelletier, and Y. Lafoy, Twin active spreading ridges in the North Fiji Basin (southwest Pacific), *Geology*, 22, 63–66, 1994.
- Auzende, J.-M., B. Pelletier, and J.-P. Eissen, The North Fiji Basin: Geology, structure, and geodynamic evolution, in *Back-arc Basins: Tectonics and Magmatism*, edited by B. Taylor, pp. 139–175, Plenum Press, New York, 1995a.

- Auzende, J.-M., R. N. Hey, B. Pelletier, D. Rouland, Y. Lafoy, E. Gracia, and P. Huchon, Propagating rift west of the Fiji Archipelago (North Fiji Basin, SW Pacific), *J. Geophys. Res.*, *100*, 17,823–17,835, 1995b.
- Auzende, J.-M., J.-I. Ishibashi, Y. Beaudoin, J.-L. Charlou, J. Delteil, J.-P. Donval, Y. Fouquet, B. Ildefonse, H. Kimura, Y. Nishio, J. Radford-Knoery, and E. Ruellan, Extensive magmatic and hydrothermal activity documented in Manus Basin, *Eos Trans. AGU*, *81*, 449–456, 2000.
- Avouac, J.-P., and P. Tapponnier, Kinematic model of active deformation in central Asia, *Geophys. Res. Lett.*, *20*, 895–898, 1993.
- Baker, N., P. Fryer, F. Martinez, and T. Yamazaki, Rifting history of the northern Mariana Trough: SeaMARC II and seismic reflection surveys, *J. Geophys. Res.*, *101*, 11,427–11,455, 1996.
- Barker, P. F., A spreading centre in the east Scotia Sea, *Earth Planet. Sci. Lett.*, *15*, 123–132, 1972.
- Barker, P. F., and I. W. D. Dalziel, Progress in geodynamics in the Scotia Arc region, in *Geodynamics of the Easter Pacific Region: Caribbean and Scotia Arcs*, *Geodyn. Ser.*, vol. 9, edited by R. Cabre, pp. 137–170, AGU, Washington, D. C., 1983.
- Barker, P. F., and I. A. Hill, Back arc extension in the Scotia Sea, *Philos. Trans. R. Soc. London Ser. A*, *300*, 249–262, 1981.
- Benpei, L., Z. Zhengguo, and L. Xiang, Terrane accretion and continent collision between Sino-Korean plate and South China plate during Hercynian-Indosinian orogeny, paper presented at the International Tectonostratigraphic Terrane Conference, 4, 58, Nonjing, China, 1998.
- Bevis, M., E. C. Kendrick, R. Smalley Jr., T. Herring, J. Godoy, and F. Galban, Crustal motion north and south of the Arica deflection; comparing recent geodetic results from the Central Andes, *Geochem. Geophys. Geosyst.*, *1*, paper number 1999GC000011, 1999.
- Bevis, M., E. Kendrick, R. Smalley Jr., B. Brooks, R. Allmendinger, and B. Isacks, On the strength of interplate coupling and the rate of back arc convergence in the Central Andes: An analysis of the interseismic velocity field, *Geochem. Geophys. Geosyst.*, *2*, paper number 2001GC000198, 2001.
- Bibee, L. D., G. G. Shor, and R. S. Lu, Inter-arc spreading in the Mariana Trough, *Mar. Geol.*, *35*, 183–197, 1980.
- Bird, P., Formation of the Rocky Mountains, western United States: A continuum computer model, *Science*, *239*, 1501–1507, 1988.
- Bird, P., Kinematic history of the Laramide orogeny in latitudes 35° to 49° degrees North, western United States, *Tectonics*, *17*, 780–801, 1998.
- Bird, P., and R. W. Rosenstock, Kinematics of present crust and mantle flow in southern California, *Geol. Soc. Am. Bull.*, *95*, 946–957, 1984.
- Bird, P., Y. Y. Kagan, and D. D. Jackson, Plate tectonics and earthquake potential of spreading ridges and oceanic transform faults, in *Plate Boundary Zones*, *Geophys. Monogr. Ser.*, vol. 30, edited by S. Stein and J. T. Freymueller, 203–218, AGU, Washington, D. C., 2002.
- Calais, E., O. Lesne, J. Deverchere, V. San'kov, A. Lukhnev, A. Miroshnitchenko, V. Buddo, K. Levi, V. Zalutzky, and Y. Baskhiev, Crustal deformation in the Baikal rift from GPS measurements, *Geophys. Res. Lett.*, *25*, 4003–4006, 1998.
- Calmant, S., P. Lebellegard, F. Taylor, M. Bevis, D. Maillard, J. Recy, and J. Bonneau, Geodetic measurements of convergence across the New Hebrides subduction zone, *Geophys. Res. Lett.*, *22*, 2573–2576, 1995.
- Chamote-Rooke, N., and X. Le Pichon, GPS determined eastward Sundaland motion with respect to Eurasia confirmed by earthquake slip vectors at Sunda and Philippine Trenches, *Earth Planet. Sci. Lett.*, *173*, 439–455, 1999.
- Chapman, M. E., and S. C. Solomon, North American-Eurasian plate boundary in northeast Asia, *J. Geophys. Res.*, *81*, 921–930, 1976.
- Chase, C. G., Tectonic history of the Fiji Plateau, *Geol. Soc. Am. Bull.*, *82*, 3087–3110, 1971.
- Chu, D., and R. G. Gordon, Evidence for motion between Nubia and Somalia along the Southwest Indian ridge, *Nature*, *398*, 64–67, 1999.
- Circum-Pacific Map Project, *Plate-Tectonic Map of the Circum-Pacific Region*, edited by M. T. Halbouty et al., 5 sheets at 1:10,000,000, *Am. Assoc. Petrol. Geol.*, Tulsa, Okla., 1981.
- Circum-Pacific Map Project, *Plate-Tectonic Map of the Circum-Pacific Region*, edited by M. T. Halbouty et al., 5 sheets at 1:10,000,000 and 1 sheet at 1:20,000,000, *Amer. Assoc. Petr. Geol.*, Tulsa, Okla., 1986.
- Collot, J.-Y., P. Charvis, M.-A. Gutscher, and S. Operto, Exploring the Ecuador-Colombia active margin and interplate seismogenic zone, *Eos Trans. AGU*, *83*, 185–190, 2002.
- Cook, D. B., K. Fujita, and C. A. McMullen, Present-day plate interactions in northeast Asia; North America, Eurasian, and Okhotsk plates, *J. Geodyn.*, *6*, 33–51, 1986.
- Craig, H., K.-R. Kim, and J. Franchetau, Active ridge crest mapping on the Juan Fernandez micro-plate: The use of Sea Beam-controlled hydrothermal plume surveys (abstract), *Eos Trans. AGU*, *64*, 45, 1983.
- Curry, J. R., D. G. Moore, L. A. Lawver, F. J. Emmel, R. W. Raitt, M. Henry, and R. Kieckhefer, Tectonics of the Andaman Sea and Burma, in *Geological and Geophysical Investigations of Continental Margins*, edited by J. Watkins, L. Montadert, and P. Dickerson, *AAPG Mem.*, *29*, 189–198, 1979.
- Curry, J. R., F. J. Emmel, D. G. Moore, and R. W. Raitt, Structure, tectonics, and geological history of the northeastern Indian Ocean, in *The Indian Ocean, The Ocean Basins and Margins*, vol. 6, edited by A. E. M. Nairn and F. G. Stehli, pp. 399–450, Plenum, New York, 1982.
- Curtis, J. W., Plate tectonics and the Papua-New Guinea-Solomon Islands region, *J. Geol. Soc. Australia*, *20*, 21–36, 1973.
- Darby, D. J., and C. M. Meertens, Terrestrial and GPS measurements of deformation across the Taupo back arc and Hikurangi forearc regions in New Zealand, *J. Geophys. Res.*, *100*, 8221–8232, 1995.
- DeMets, C., A test of present-day plate geometries for north-eastern Asia and Japan, *J. Geophys. Res.*, *97*, 17,627–17,635, 1992.

- DeMets, C., and S. Traylen, Motion of the Rivera plate since 10 Ma relative to the Pacific and North American plates and the mantle, *Tectonophysics*, *318*, 119–159, 2000.
- DeMets, C., and D. S. Wilson, Relative motions of the Pacific, Rivera, North America, and Cocos plates since 0.78 Ma, *J. Geophys. Res.*, *102*, 2789–2807, 1997.
- DeMets, C., R. G. Gordon, D. F. Argus, and S. Stein, Current plate motions, *Geophys. J. Int.*, *101*, 425–478, 1990.
- DeMets, C., R. G. Gordon, D. F. Argus, and S. Stein, Effect of recent revisions to the geomagnetic reversal time scale on estimate of current plate motions, *Geophys. Res. Lett.*, *21*, 2191–2194, 1994.
- Dewey, J. F., and J. L. Pindell, Neogene block tectonics of eastern Turkey and northern South America: Continental applications of the finite difference method, *Tectonics*, *4*, 71–83, 1985.
- Dewey, J. F., and J. L. Pindell, Reply to comment by Amos Salvador on “Neogene block tectonics of eastern Turkey and northern South America: Continental applications of the finite difference method,” *Tectonics*, *5*, 703–705, 1986.
- Eguchi, T., Seismotectonics around the Mariana Trough, *Tectonophysics*, *102*, 33–52, 1984.
- Engeln, J. F., and S. Stein, Tectonics of the Easter plate, *Earth Planet. Sci. Lett.*, *68*, 259–270, 1984.
- Fabbri, O., and M. Fournier, Extension in the southern Ryukyu arc (Japan): Link with oblique subduction and back arc rifting, *Tectonics*, *18*, 486–497, 1999.
- Fitch, T. J., Plate convergence, transcurrent faults and internal deformation adjacent to southeast Asia and the western Pacific, *J. Geophys. Res.*, *77*, 4432–4460, 1972.
- Forsyth, D. W., Mechanisms of earthquakes and plate motions in the east Pacific, *Earth Planet. Sci. Lett.*, *17*, 189–193, 1972.
- Fournier, M., P. Patriat, and S. Leroy, Reappraisal of the Arabia-India-Somalia triple junction kinematics, *Earth Planet. Sci. Lett.*, *189*, 103–114, 2001.
- Freymueller, J. T., J. N. Kellogg, and V. Vega, Plate motions in the north Andean region, *J. Geophys. Res.*, *98*, 21,853–21,863, 1993.
- Fujiwara, T., K. Tamaki, H. Fujimoto, T. Ishii, N. Seama, H. Toh, K. Koizumi, C. Ishigari, J. Segawa, and K. Kobayashi, Morphological studies of the Ayu Trough, Philippine Sea-Caroline plate boundary, *Geophys. Res. Lett.*, *22*, 109–112, 1995.
- Genrich, J. F., Y. Bock, R. McCaffrey, E. Calais, C. W. Stevens, and C. Subarya, Accretion of the southern Banda arc to the Australia plate margin determined by Global Positioning System measurements, *Tectonics*, *15*, 288–295, 1996.
- Giardini, D., G. Grunthal, K. Shedlock, and P. Zhang, *Global Seismic Hazard Map*, 1:35,000,000, Global Seismic Hazard Assessment Program, UN/International Decade of Natural Disaster Reduction, International Lithosphere Program, 1999. (Available at <http://seismo.ethz.ch/GSHAP>)
- Gonzalez-Casado, J. M., J. L. Giner-Robles, and J. Lopez-Martinez, Bransfield basin, Antarctic Peninsula: Not a normal basaltic basin, *Geology*, *28*, 1043–1046, 2000.
- Goodliffe, A. M., B. Taylor, F. Martinez, R. Hey, K. Maeda, and K. Ohno, Synchronous reorientation of the Woodlark Basin Spreading Center, *Earth Planet. Sci. Lett.*, *146*, 233–242, 1997.
- Gordon, R. G., Present plate motions and plate boundaries, in *Global Earth Physics: A Handbook of Physical Constants, Reference Shelf Ser.*, vol. 1, edited by T. J. Ahrens, pp. 66–87, AGU, Washington, D. C., 1995.
- Gutscher, M.-A., W. Spakman, J. Bijwaard, and E. R. Engdahl, Geodynamics of flat subduction: Seismicity and tomographic constraints from the Andean margin, *Tectonics*, *19*, 814–833, 2000.
- Haines, A. J., and W. E. Holt, A procedure for obtaining the complete horizontal motions within zones of distributed deformation from the inversion of strain rate data, *J. Geophys. Res.*, *98*, 12,025–12,082, 1993.
- Hamilton, W., Tectonics of the Indonesian region, *U.S. Geol. Surv. Prof. Pap.*, *1078*, 1979.
- Heki, K., S. Miyazaki, H. Takahashi, M. Kasahara, F. Kimata, S. Miura, N. F. Vasilenko, A. Ivaschenko, and K.-D. An, The Amurian plate motion and current plate kinematics in eastern Asia, *J. Geophys. Res.*, *104*, 29,147–29,155, 1999.
- Herron, E. M., Two small crustal plates in the South Pacific near Easter Island, *Nature*, *240*, 35–37, 1972.
- Hey, R. N., P. D. Johnson, F. Martinez, J. Korenaga, M. L. Somers, Q. J. Huggett, T. P. LeBas, R. I. Rusby, and D. F. Naars, Plate boundary reorganization at a large-offset, rapidly propagating rift, *Nature*, *378*, 167–170, 1995.
- Holt, W. E., J. F. Ni, T. C. Wallace, and A. J. Haines, The active tectonics of the eastern Himalayan syntaxis and surrounding regions, *J. Geophys. Res.*, *96*, 14,595–14,632, 1991.
- Holt, W. E., N. Chamot-Rooke, X. Le Pichon, A. J. Haines, B. Shen-Tu, and J. Ren, Velocity field in Asia inferred from Quaternary fault slip rates and global positioning system observations, *J. Geophys. Res.*, *105*, 19,185–19,209, 2000.
- Honza, E., H. L. Davies, J. B. Keene, and D. L. Tiffin, Plate boundaries and evolution of the Solomon Sea region, *Geo Mar. Lett.*, *7*, 161–168, 1987.
- Hu, J.-C., S.-B. Yu, J. Angelier, and H.-T. Chu, Active deformation of Taiwan from GPS measurements and numerical simulations, *J. Geophys. Res.*, *106*, 2265–2280, 2001.
- Hussong, D. M., and S. Uyeda, Tectonic process and history of the Mariana Arc: A synthesis of the results of Deep Sea Drilling Project Leg 60, *Init. Rep. Deep Sea Drill. Project*, *60*, 909–929, 1981.
- Ishihara, T., R. J. Stern, P. Fryer, S. Bloomer, and N. C. Becker, Seafloor spreading in the southern Mariana Trough inferred from 3-component magnetometer data, *Eos Trans. AGU*, *82*, Fall Meet. Suppl., F1202, 2001.
- Jackson, J., Partitioning of strike-slip and convergent motion between Eurasia and Arabia in eastern Turkey and the Caucasus, *J. Geophys. Res.*, *97*, 12,471–12,479, 1992.
- Jackson, J., J. Haines, and W. Holt, The accommodation of Arabia-Eurasia plate convergence in Iran, *J. Geophys. Res.*, *100*, 15,205–15,220, 1995.
- Jestin, F., P. Huchon, and J. M. Gaulier, The Somalia plate and the East African Rift system: Present-day kinematics, *Geophys. J. Int.*, *116*, 637–654, 1994.

- Johnson, R. W., Geotectonics and volcanism in Papua New Guinea: A review of the late Cainozoic, *BMR J. Aust. Geol. Geophys.*, *4*, 181–207, 1979.
- Johnson, T., and P. Molnar, Focal mechanisms and plate tectonics of the southwest Pacific, *J. Geophys. Res.*, *77*, 5000–5032, 1972.
- Karig, D. E., Ridges and basins of the Tonga-Kermadec arc system, *J. Geophys. Res.*, *75*, 239–254, 1970.
- Karig, D. E., Structural history of the Mariana island arc system, *Geol. Soc. Am. Bull.*, *82*, 323–334, 1971.
- Kato, T., Y. Kotake, S. Nakao, J. Beavan, K. Hirahara, M. Okada, M. Hoshiba, O. Kamigaichi, R. B. Feir, P. H. Park, M. Gerasimenko, and M. Kasahara, Initial results from WING, the continuous GPS network in the Western Pacific area, *Geophys. Res. Lett.*, *25*, 369–372, 1998.
- Kellogg, J. N., I. J. Ogujiofor, and D. R. Kansakar, Cenozoic tectonics of the Panama and North Andes blocks, *Mem. Congr. Latinoam. Geol.*, *6*, 40–59, 1985.
- Kellogg, J. N., V. Vega, T. C. Stallings, and C. L. V. Aiken, Tectonic development of Panama, Costa Rica, and the Columbian Andes: Constraints from Global Positioning System geodetic studies and gravity, in *Geologic and Tectonic Development of the Caribbean Plate Boundary in Southern Central America*, edited by P. Mann, *Geol. Soc. Am. Spec. Pap.*, *295*, 75–86, 1995.
- Kellogg, J. N., R. Trenkamp, and J. T. Freymueller, Transect of the southern Caribbean plate boundary: 8 years of CASA GPS results, *Eos Trans. AGU*, *77*(46), Fall Meet. Suppl., F142, 1996.
- Kendrick, E. C., M. Bevis, R. F. Smalley Jr., O. Cifuentes, and F. Galban, Current rates of convergence across the Central Andes: Estimates from continuous GPS observations, *Geophys. Res. Lett.*, *26*, 541–544, 1999.
- Kendrick, E. C., M. Bevis, R. F. Smalley Jr., and B. Brooks, An integrated crustal velocity analysis for the Central Andes, *Geochem. Geophys. Geosyst.*, *2*, paper number 2001GC000191, 2001.
- Klepeis, K. A., The Magallanes and Deseado fault zones: Major segments of the South America-Scotia transform plate boundary in southernmost South America, Tierra del Fuego, *J. Geophys. Res.*, *99*, 22,001–22,014, 1994.
- Klepeis, K. A., and L. A. Lawver, Tectonics of the Antarctic-Scotia plate boundary near Elephant and Clarence Islands, West Antarctica, *J. Geophys. Res.*, *101*, 20,211–20,231, 1996.
- Klotz, J., D. Angermann, G. Michel, R. Porth, C. Reigber, J. Reinking, J. Viramonte, R. Perdomo, V. Rios, S. Barrientos, R. Barriga, and O. Cifuentes, GPS-derived deformation of the central Andes including the 1995 Antofagasta $M_w = 8.0$ earthquake, *Pure Appl. Geophys.*, *154*, 709–730, 1999.
- Kolarsky, R. A., and P. Mann, Structure and neotectonics of an oblique-subduction margin, southwestern Panama, in *Geologic and Tectonic Development of the Caribbean Plate Boundary in Southern Central America*, edited by P. Mann, *Geol. Soc. Am. Spec. Pap.*, *295*, 131–158, 1995.
- Kreemer, C., J. Haines, W. E. Holt, G. Blewitt, and D. Lavallee, On the determination of a global strain rate model, *Earth Planets Space*, *52*, 765–770, 2000.
- Lagabrielle, Y., et al., Active oceanic spreading in the northern North Fiji Basin: Results of the NOFI cruise of R/V L'Atalante (Newstarmer Project), *Mar. Geophys. Res.*, *18*, 225–247, 1996.
- Lallemant, S. E., C.-S. Liu, and Y. Font, A tear fault boundary between the Taiwan orogen and the Ryukyu subduction zone, *Tectonophysics*, *274*, 171–190, 1997a.
- Lallemant, S. E., and C.-S. Liu, Swath bathymetry reveals active arc-continent collision near Taiwan, *Eos Trans. AGU*, *78*, 173–175, 1997b.
- Lamarche, G., J. M. Bull, P. M. Barnes, S. K. Taylor, and J. Horgan, Constraining fault growth rates and fault evolution in New Zealand, *Eos Trans. AGU*, *81*, 481–486, 2000.
- Lamb, S., Active deformation in the Bolivian Andes, South America, *J. Geophys. Res.*, *105*, 25,627–25,653, 2000.
- Lander, A. V., B. G. Bukchin, A. V. Kiryushin, and D. V. Droznin, The tectonic environment and source parameters of the Khailino, Koryakiya earthquake of March 8, 1991: Does a Beringia plate exist?, *Comput. Seismol. Geodyn.*, *3*, 80–96, 1996.
- Larson, R. L., R. C. Searle, M. C. Kleinrock, H. Schouten, R. T. Bird, D. F. Naar, R. I. Rusby, E. E. Hooft, and H. Lasthiotakis, Roller-bearing tectonic evolution of the Juan Fernandez microplate, *Nature*, *356*, 571–576, 1992.
- Lawver, L. A., B. J. Sloan, D. H. N. Barker, M. Ghidella, R. P. Von Herzen, R. A. Keller, G. P. Klinkhammer, and C. S. Chin, Distributed, active extension in Bransfield basin, Antarctic Peninsula: Evidence from multibeam bathymetry, *GSA Today*, *6*, 1–17, 1996.
- Le Pichon, X., N. Chamot-Rooke, and S. Lallemant, Geodetic determinations of the kinematics of central Greece with respect to Europe: Implications for eastern Mediterranean tectonics, *J. Geophys. Res.*, *100*, 12,675–12,690, 1995.
- Leat, P. T., R. A. Livermore, I. L. Millar, and J. A. Pearce, Magma supply in back-arc spreading centre segment E2, East Scotia Ridge, *J. Petrol.*, *41*, 845–866, 2000.
- Lemaux, J., II, R. G. Gordon, and J.-Y. Royer, Location of Nubia-Somalia boundary along the Southwest Indian ridge, *Geology*, *30*, 339–342, 2002.
- Letouzey, J., and M. Kimura, Okinawa Trough genesis: Structure and evolution of a backarc basin developed in a continent, *Mar. Petrol. Geol.*, *2*, 111–130, 1985.
- Liu, C.-S., S. E. Lallemant, S.-J. Lin, P. Schnurle, and D. L. Reed, Forearc structure of the Ryukyu subduction-Taiwan collision zone from seismic reflection studies east of Taiwan, *Eos Trans. AGU*, *78*(46), Fall Meet. Suppl., F718, 1997.
- Liu, M., Y. Yang, S. Stein, Y. Zhu, and J. Engeln, Crustal shortening in the Andes: Why do GPS rates differ from geological rates?, *Geophys. Res. Lett.*, *27*, 3005–3008, 2000.
- Livermore, R., A. Cunningham, L. Vanneste, and R. Larter, Subduction influence of magma supply at the East Scotia Ridge, *Earth Planet. Sci. Lett.*, *150*, 261–275, 1997.
- Lock, J., H. L. Davies, D. L. Tiffin, F. Murakami, and K. Kisimoto, The Trobriand subduction system in the western Solomon Sea, *Geo Mar. Lett.*, *7*, 129–134, 1987.
- Lonsdale, P., Structural pattern of the Galapagos microplate and evolution of the Galapagos triple junctions, *J. Geophys. Res.*, *93*, 13,551–13,574, 1988.

- Lonsdale, P., Segmentation and disruption of the East Pacific Rise in the mouth of the Gulf of California, *Mar. Geophys. Res.*, *17*, 323–359, 1995.
- Lonsdale, P., N. Blum, and H. Puchelt, The RRR triple junction at the southern end of the Pacific-Cocos East Pacific Rise, *Earth Planet. Sci. Lett.*, *109*, 73–85, 1992.
- Louat, R., and B. Pelletier, Seismotectonics and present-day relative plate motions in the New Hebrides-North Fiji Basin region, *Tectonophysics*, *167*, 41–55, 1995.
- Maillet, P., E. Ruellan, M. Gerard, A. Person, H. Bellon, J. Cotten, J.-L. Joron, S. Nakada, and R. C. Price, Tectonics, magmatism, and evolution of the New Hebrides backarc troughs (southwest Pacific), in *Backarc Basins: Tectonics and Magmatism*, edited by B. Taylor, pp. 177–235, Plenum, New York, 1995.
- Maldonado, A., et al., Small ocean basin development along the Scotia-Antarctica plate boundary and in the northern Weddell Sea, *Tectonophysics*, *296*, 371–402, 1998.
- Mann, P., and R. A. Kolarsky, East Panama deformed belt: Structure, age, and neotectonic significance, in *Geologic and Tectonic Development of the Caribbean Plate Boundary in Southern Central America*, edited by P. Mann, *Geol. Soc. Am. Spec. Pap.*, *295*, 111–130, 1995.
- Martinez, F., and B. Taylor, Fast backarc spreading, rifting, and microplate rotation, between transform faults in the Manus Basin, Bismarck Sea, *Mar. Geophys. Res.*, *18*, 203–224, 1996.
- Martinez, F., P. Fryer, N. A. Baker, and T. Yamazaki, Evolution of backarc rifting: Mariana Trough, 20–24N, *J. Geophys. Res.*, *100*, 3807–3827, 1995.
- Martinez, F., R. N. Hey, and P. D. Johnson, The East ridge system 28.5–32°S East Pacific rise: Implications for overlapping spreading center development, *Earth Planet. Sci. Lett.*, *151*, 13–31, 1997.
- Martinez, F., P. Fryer, and N. Becker, Geophysical characteristics of the southern Mariana Trough, 11°50'N–13°40'N, *J. Geophys. Res.*, *105*, 16,591–16,607, 2000.
- Masce, J., C. Huguen, J. Benkhelil, N. Chamot-Rooke, E. Chaumillon, J. P. Foucher, R. Gribouard, A. Kopf, G. Lamarche, A. Volkonskaia, J. Woodside, and T. Zitter, Images may show start of European-African plate collision, *Eos Trans. AGU*, *80*, 421–436, 1999.
- Massell, C. M., F. Coffin, P. Mann, S. Mosher, C. Frohlich, C. S. Duncan, G. Karner, D. Ramsay, and J.-F. Lebrun, Neotectonics of the Macquarie Ridge Complex, Australia-Pacific plate boundary, *J. Geophys. Res.*, *105*, 13,457–13,480, 2000.
- Maung, H., Transcurrent movements in the Burma-Andaman Sea region, *Geology*, *15*, 911–912, 1987.
- McCaffrey, R., Slip vectors and stretching of the Sumatran fore arc, *Geology*, *19*, 881–884, 1991.
- McCaffrey, R., Oblique plate convergence, slip vectors, and forearc deformation, *J. Geophys. Res.*, *97*, 8905–8915, 1992.
- McCaffrey, R., Estimates of modern arc-parallel strain rates in fore arcs, *Geology*, *24*, 27–30, 1996a.
- McCaffrey, R., Slip partitioning at convergent plate boundaries of SE Asia, in *Tectonic Evolution of Southeast Asia*, edited by R. Hall and D. Blundell, *Geol. Soc. Spec. Publ.*, *106*, 3–18, 1996b.
- McClusky, S., et al., Global Positioning System constraints on plate kinematics and dynamics in the eastern Mediterranean and Caucasus, *J. Geophys. Res.*, *105*, 5695–5719, 2000.
- McKenzie, D. P., Active tectonics of the Mediterranean region, *Geophys. J. R. Astron. Soc.*, *30*, 109–185, 1972.
- McKenzie, D. P., D. Davies, and P. Molnar, Plate tectonics of the Red Sea and East Africa, *Nature*, *226*, 243–248, 1970.
- Miki, M., Two-phase opening model for the Okinawa Trough inferred from paleomagnetic study of the Ryukyu arc, *J. Geophys. Res.*, *100*, 8169–8184, 1995.
- Milsom, J. S., Woodlark basin, a minor center of sea-floor spreading in Melanesia, *J. Geophys. Res.*, *75*, 7335, 1970.
- Minster, J. B., and T. H. Jordan, Present-day plate motions, *J. Geophys. Res.*, *83*, 5331–5354, 1978.
- Miyazaki, S., K. Heki, Y. Hatanaka, T. Sagiya, and H. Tsuji, Determination of the Euler vector between the Amurian and the Eurasian plates with GPS data, paper presented at 86th Meeting of the Geodetic Society of Japan, Geod. Soc. of Jpn., Kochi, 1996.
- Moore, G. F., and K. L. Sender, Fracture zone collision along the South Panama margin, in *Geologic and Tectonic Development of the Caribbean Plate Boundary in Southern Central America*, edited by P. Mann, *Geol. Soc. Am. Spec. Pap.*, *295*, 201–212, 1995.
- Morgan, W. J., Rises, trenches, great faults, and crustal blocks, *J. Geophys. Res.*, *73*, 1959–1982, 1968.
- Mueller, D., W. R. Roest, J.-Y. Royer, L. M. Gahagan, and J. G. Sclater, Digital isochrons of the world's ocean floor, *J. Geophys. Res.*, *102*, 3211–3214, 1997.
- Mukhopadhyay, M., Seismotectonics of subduction and back-arc rifting under the Andaman Sea, *Tectonophysics*, *108*, 229–239, 1984.
- Mukhopadhyay, M., and S. Dasgupta, Deep structure and tectonics of the Burmese arc: Constraints from earthquake and gravity data, *Tectonophysics*, *149*, 299–322, 1988.
- Naar, D. F., and R. N. Hey, Tectonic evolution of the Easter microplate, *J. Geophys. Res.*, *96*, 7961–7993, 1991.
- Norabuena, E., L. Leffler-Griffin, A. Mao, T. Dixon, S. Stein, I. S. Sacks, L. Ocola, and M. Ellis, Space geodetic observations of Nazca-South America convergence across the central Andes, *Science*, *279*, 358–362, 1998.
- Otsuki, K., K. Heki, and T. Yamazaki, New data which supports the “laws of convergence rate of plates” proposed by Otsuki, *Tectonophysics*, *172*, 365–368, 1990.
- Pacheco, J. F., and L. R. Sykes, Seismic moment catalog of large shallow earthquakes, *Bull. Seismol. Soc. Am.*, *82*, 1306–1349, 1992.
- Papazachos, C. B., Seismological and GPS evidence for the Aegean-Anatolia interaction, *Geophys. Res. Lett.*, *26*, 2653–2656, 1998.
- Park, J.-O., H. Tokuyama, M. Shinohara, K. Suyehiro, and A. Taira, Seismic record of tectonic evolution and backarc rifting in the southern Ryukyu island arc system, *Tectonophysics*, *294*, 21–42, 1998.

- Pelayo, A. M., and D. A. Wiens, Seismotectonics and relative plate motions in the Scotia Sea region, *J. Geophys. Res.*, *94*, 7293–7320, 1989.
- Pelletier, B., and R. Louat, Seismotectonics and present-day relative plate motions in the Tonga-Lau and Kermadec-Havre region, *Tectonophysics*, *165*, 237–250, 1989.
- Pelletier, B., Y. Lafoy, and F. Missegue, Morphostructure and magnetic fabric of the northwestern North Fiji Basin, *Geophys. Res. Lett.*, *20*, 1151–1154, 1993.
- Pelletier, B., S. Calmant, and R. Pillet, Current tectonics of the Tonga-New Hebrides region, *Earth Planet. Sci. Lett.*, *164*, 263–276, 1998.
- Pelletier, B., Y. Lagabriele, M. Benoit, G. Cabioch, S. Calmant, E. Garel, C. Guivel, and J. Perrier, Newly discovered active spreading centers along the North Fiji transform zone (Pacific-Australia plates boundary): Preliminary results of the R/V L'Atalante ALAUF1 cruise (February–March 2000), *RIDGE Events*, *11*, 7–9, 2001.
- Peltzer, G., and P. Tapponnier, Formation and evolution of strike-slip faults, rifts, and basins during the India-Asia collision: An experimental approach, *J. Geophys. Res.*, *93*, 15,085–15,117, 1988.
- Perez, O. J., M. A. Jaimes, and E. Garciacaro, Microseismicity evidence for subduction of the Caribbean plate beneath the South American plate in northwestern Venezuela, *J. Geophys. Res.*, *102*, 17,875–17,882, 1997.
- Puntodewo, S. S. O., R. McCaffrey, E. Calais, Y. Bock, J. Rais, C. Subarya, R. Poewariardi, C. Stevens, J. Genrich, Fauzi, P. Zwick, and S. Wdowinski, GPS measurements of crustal deformation within the Pacific-Australia plate boundary zone in Irian Jaya, *Tectonophysics*, *237*, 141–153, 1994.
- Rangin, C., X. Le Pichon, S. Mazzotti, M. Pubellier, N. Chamot-Rooke, M. Aurelio, A. Walpersdorf, and R. Quebral, Plate convergence measured by GPS across the Sundaland/Philippine Sea plate deformed boundary: The Philippines and eastern Indonesia, *Geophys. J. Int.*, *139*, 296–316, 1999.
- Ranken, B., R. K. Cardwell, and D. E. Karig, Kinematics of the Philippine Sea plate, *Tectonics*, *3*, 555–575, 1984.
- Reilinger, R. E., S. C. McClusky, M. B. Oral, R. W. King, M. N. Toksoz, A. A. Barka, I. Kinik, O. Lenk, and I. Sanli, Global Positioning System measurements of present-day crustal movements in the Arabia-Africa-Eurasia plate collision zone, *J. Geophys. Res.*, *102*, 9983–10000, 1997.
- Royer, J.-Y., and R. G. Gordon, The motion and boundary between the Capricorn and Australian plates, *Science*, *277*, 1268–1274, 1997.
- Savostin, L. A., A. I. Verzhbitskaya, and B. V. Baranov, Holocene plate tectonics of the Sea of Okhotsk region, *Dokl. Acad. Sci. USSR, Earth Sci. Ser., Engl. Trans.*, *266*, 62–65, 1982.
- Savostin, L. A., L. Zonenshain, and B. V. Baranov, Geology and plate tectonics of the Sea of Okhotsk, *Geodynamics of the Western Pacific-Indonesian Region*, *Geodyn. Ser.*, vol. 11, edited by T. W. C. Hilde and S. Uyeda, pp. 189–221, AGU, Washington, D. C., 1983.
- Schellart, W. P., G. S. Lister, and M. W. Jessell, Analogue modeling of arc and backarc deformation in the New Hebrides arc and North Fiji Basin, *Geology*, *30*, 311–314, 2002.
- Schouten, H., K. D. Klitgord, and D. G. Gallo, Edge-driven microplate kinematics, *J. Geophys. Res.*, *98*, 6689–6701, 1993.
- Searle, R. C., R. T. Bird, R. I. Rusby, and D. F. Naar, The development of two oceanic microplates: Easter and Juan Fernandez microplates, East Pacific Rise, *J. Geol. Soc. London*, *150*, 965–976, 1993.
- Seno, T., S. Stein, and A. E. Gripp, A model for the motion of the Philippine Sea plate consistent with NUVEL-1 and geological data, *J. Geophys. Res.*, *98*, 17,941–17,948, 1993.
- Seno, T., T. Sakurai, and S. Stein, Can the Okhotsk plate be discriminated from the North American plate?, *J. Geophys. Res.*, *101*, 11,305–11,316, 1996.
- Sibuet, J.-C., et al., Backarc extension in the Okinawa Trough, *J. Geophys. Res.*, *92*, 14,041–14,063, 1987.
- Sibuet, J.-C., S.-K. Hsu, C.-T. Shyu, and C.-S. Liu, Structural and kinematic evolutions of the Okinawa Trough backarc basin, in *Backarc Basins: Tectonics and Magmatism*, edited by B. Taylor, pp. 343–379, Plenum, New York, 1995.
- Silver, E. A., and J. C. Moore, The Molucca Sea collision zone, Indonesia, *J. Geophys. Res.*, *83*, 1681–1691, 1978.
- Silver, E. A., D. Reed, R. McCaffrey, and Y. Joyodiwiryo, Back arc thrusting in the eastern Sunda arc, Indonesia: A consequence of arc-continent collision, *J. Geophys. Res.*, *88*, 7429–7448, 1983.
- Silver, E. A., N. A. Breen, and H. Prasetyo, Multibeam study of the Flores backarc thrust belt, Indonesia, *J. Geophys. Res.*, *91*, 3489–3500, 1986.
- Simkin, T., and L. Siebert, *Volcanoes of the World*, Smithsonian Inst., Washington, D. C., 1995.
- Stoddard, P. R., On the relation between transform fault resistance and plate motion, *J. Geophys. Res.*, *97*, 17,637–17,650, 1992.
- Taboada, A., L. A. Rivera, A. Fuenzalida, A. Cisternas, J. Philip, J. Bijwaard, J. Olaya, and C. Rivera, Geodynamics of the northern Andes: Subductions and intracontinental deformation (Columbia), *Tectonics*, *19*, 787–813, 2000.
- Takahashi, H., et al., Velocity field of around the Sea of Okhotsk and Sea of Japan regions determined from a new continuous GPS network data, *Geophys. Res. Lett.*, *26*, 2533–2536, 1999.
- Taylor, B., Bismarck Sea: Evolution of a back-arc basin, *Geology*, *7*, 171–174, 1979.
- Taylor, B., A. Goodliffe, F. Martinez, and R. Hey, Continental rifting and initial sea-floor spreading in the Woodlark basin, *Nature*, *374*, 534–537, 1995.
- Taylor, B., A. M. Goodliffe, and F. Martinez, How continents break up: Insights from Papua New Guinea, *J. Geophys. Res.*, *104*, 7497–7512, 1999.
- Taylor, F. W., M. G. Bevis, B. E. Schutz, D. Kuang, J. Recy, S. Calmant, D. Charley, M. Regnier, B. Perin, M. Jackson, and C. Reichfield, Geodetic measurements of convergence at the New Hebrides island arc indicate arc fragmentation caused by an impinging aseismic ridge, *Geology*, *23*, 1011–1014, 1995.

- Tregoning, P., et al., Estimation of current plate motions in Papua New Guinea from Global Positioning System observations, *J. Geophys. Res.*, *103*, 12,181–12,203, 1998.
- Tregoning, P., R. J. Jackson, H. McQueen, K. Lambeck, C. Stevens, R. P. Little, R. Curley, and R. Rosa, Motion of the South Bismarck plate, Papua New Guinea, *Geophys. Res. Lett.*, *26*, 3517–3520, 1999.
- Trenkamp, R., J. N. Kellogg, and J. T. Freymueller, Transect of Nazca-South America plate boundary in Ecuador and Colombia: 8 years of CASA GPS results (abstract), *Eos Trans. AGU*, *77*(46), Fall Meet. Suppl., F142, 1996.
- van der Hilst, R., and P. Mann, Tectonic implications of tomographic images of subducted lithosphere beneath northwestern South America, *Geology*, *22*, 451–454, 1994.
- Weber, J. C., T. H. Dixon, C. DeMets, W. B. Ambeh, P. Jansma, G. Mattioli, J. Saleh, G. Sella, R. Bilham, and O. Perez, GPS estimate of relative motion between the Caribbean and South American plates, and geologic implications for Trinidad and Venezuela, *Geology*, *29*, 75–78, 2001.
- Wei, D., and T. Seno, Determination of the Amurian plate motion, in *Mantle Dynamics and Plate Interactions in East Asia*, *Geodyn. Series*, vol. 27, edited by M. F. J. Flower et al., pp. 337–346, AGU, Washington, D. C., 1998.
- Weiler, P. D., and R. S. Coe, Rotations in the actively colliding Finisterre Arc Terrane; paleomagnetic constraints on Plio-Pleistocene evolution of the South Bismarck Microplate, northeastern Papua New Guinea, *Tectonophysics*, *316*, 297–325, 2000.
- Weissel, J. K., and R. Anderson, Is there a Caroline plate?, *Earth Planet. Sci. Lett.*, *41*, 143–158, 1978.
- Weissel, J. K., B. Taylor, and G. D. Karner, The opening of the Woodlark basin, subduction of the Woodlark spreading system, and the evolution of Northern Melanesia since mid-Pliocene time, *Tectonophysics*, *87*, 253–277, 1982.
- Wessel, J. K., P. Fryer, P. Wessel, and B. Taylor, Extension in the northern Mariana inner forearc, *J. Geophys. Res.*, *99*, 15,181–15,203, 1994.
- Westaway, R., Present-day kinematics of the Middle East and eastern Mediterranean, *J. Geophys. Res.*, *99*, 12,071–12,090, 1994.
- Westbrook, G. K., N. C. Hardy, and R. P. Heath, Structure and tectonics of the Panama-Nazca plate boundary, in *Geologic and Tectonic Development of the Caribbean Plate Boundary in Southern Central America*, edited by P. Mann, *Geol. Soc. Am. Spec. Pap.*, *295*, 91–110, 1995.
- Wilson, D. S., Tectonic history of the Juan de Fuca Ridge over the last 40 million years, *J. Geophys. Res.*, *93*, 11,863–11,876, 1988.
- Wright, I. C., Pre-spread rifting and heterogeneous volcanism in the southern Havre Trough back-arc basin, *Mar. Geol.*, *113*, 179–200, 1993.
- Wright, D. J., W. W. Sager, and T. Hilde, Plate boundary structures and processes at the northern terminus of the Tonga trench (abstract), *Eos Trans. AGU*, *67*, 1238, 1986.
- Yamazaki, T., F. Murakami, E. Saito, and M. Yuasa, Opening of the northern Mariana Trough (abstract), paper presented at Tectonics of Eastern Asia and Western Pacific Continental Margin, 1988 DELP Tokyo International Symposium 6th Japan-U.S.S.R. Geotectonic Symposium, 25–26, 1988.
- Yamazaki, T., F. Murakami, and E. Saito, Mode of seafloor spreading in the northern Mariana Trough, *Tectonophysics*, *221*, 207–222, 1993.
- Zellmer, K. E., and B. Taylor, A three-plate kinematic model for Lau Basin opening, *Geochem. Geophys. Geosyst.*, *2*, paper number 2000GC000106, 2001.
- Zoback, M. L., First- and second-order patterns of stress in the lithosphere: The World Stress Map project, *J. Geophys. Res.*, *97*, 11,703–11,728, 1992.